Aus dem Labor für Molekulare Neurobiologie der
Neurologischen Klinik
der Heinrich-Heine-Universität Düsseldorf

Axonal Regeneration, Reconnection, and Functional Recovery following a Complete Spinal Cord Transection in Adult Rats and a Combinatorial Treatment of Stem Cell Transplantation and a Mechanical Microconnector System

Inaugural - Dissertation

zur Erlangung des Doktorgrades
der Mathematisch-Naturwissenschaftlichen Fakultät
der Heinrich-Heine-Universität Düsseldorf

vorgelegt von

Jennifer Illgen

aus Berlin

Düsseldorf, März 2019

aus dem Labor für Molekulare Neurobiologie der Neurologischen Klinik

der Heinrich-Heine-Universität Düsseldorf

Gedruckt mit der Genehmigung der
Mathematisch-Naturwissenschaftlichen Fakultät der

Heinrich-Heine-Universität Düsseldorf

Berichterstatter:

1. Prof. Dr. Hans Werner Müller

2. Prof. Dr. Dieter Willbold

Tag der mündlichen Prüfung: 28.05.2019

It always feels impossible until it’s done.

- Nelson Mandela -

Zusammenfassung

Eine Schädigung des Rückenmarks führt meist zu einer permanenten Lähmung. Der Grund dafür ist die Limitation der spontanen Axonregeneration, die durch die Bildung der Glianarbe und einer erhöhten Freisetzung inhibitorischer Moleküle an der Läsionsstelle vermindert wird. Diese multifaktorielle und multiphasische Pathophysiologie der Rückenmarksschädigung und die Tatsache, dass es bisher keinen therapeutischen Ansatz gibt, der eine langanhaltende Verbesserung hervorruft, führt zu der Annahme, dass eine Kombination verschiedener Therapien erforderlich ist, um eine effektive Wirkung zu zeigen. In einer vorherigen Studie unseres Labors wurde, nach einer Totaltransektion (TX) des Rückenmarks, ein mechanisches Mikrokonnektorsystem (mMS), das in Zusammenarbeit mit der Technischen Universität Hamburg-Harburg und der BG Trauma-Klinik in Hamburg entwickelt wurde, in die Läsionsstelle implantiert. Diese Implantation führte zur Wiederherstellung der Gewebekontinuität und zusätzlich zu einer Verhaltensverbesserung. Des Weiteren zeigte eine andere Studie unserer Arbeitsgruppe, dass die Transplantation von somatischen Stammzellen aus dem Nabelschnurrestblut, sogenannte „unrestricted somatic stem cells“ (USSC), die Anzahl regenerierter Axone erhöht und das lokomotorische Verhalten konstant verbessert. Aufgrund dieser Studien, ist die Zielsetzung dieser Arbeit, die Kombination der zwei Einzeltherapien in einem Nagetiermodell zur Untersuchung der Wirkung auf die Axonregeneration, die Beteiligung von propriospinalen Interneuronen, die synaptische Rekonnektivität sowie die daraus folgende funktionelle Erholung.

Um die Hypothese, dass die Kombinationstherapie der individuellen Behandlungen überlegen ist, zu verifizieren und die damit einhergehende Regeneration und synaptischen Rekonnektivität vertieft zu analysieren, wurde eine komplette Durchtrennung (Totaltransektion, Tx) auf Höhe des thorakalen Segments 8/9 (Th8/9) in immunsupprimierten Ratten ausgeführt. Sowohl eine Kurzzeit- (5 Wochen) als auch eine Langzeitstudie (21 Wochen) wurden mit einer Tieranzahl von n = 16 und n = 40 entsprechend durchgeführt. Unmittelbar nach der Totaltransektion des Rückenmarks wurden die 4 verschiedenen Behandlungen angewandt: (1) Kombinationstherapie (mMS + USSC), (2) mMS, (3) USSC und (4) Kontrolle (TX only). Zur Analyse des Gewebeerhalts, der Gefäßneubildung und der

Axonregeneration nach Rückenmarksverletzung wurden immunhistologische Färbungen in den Kurz- und Langzeittieren durchgeführt. Darüber hinaus wurde die Regeneration von propriospinalen Interneuronen (PN), durch eine retrograde Markierung, das Axonwachstum des kortikospinalen Trakts (CST), durch eine anterograde Markierung, und die Synapsenbildung nach 21 Wochen durch immunhistologische Färbungen untersucht. Zusätzlich wurde die funktionale Erholung der Hinterbeine mit Hilfe eines Offenfeldtests unter der Einbeziehung einer modifizierten Basso, Beattie, und Bresnahan lokomotorischen Skala (mBBB) wöchentlich ausgewertet.

Sowohl in der Kurzzeit- als auch der Langzeitstudie konnte durch immunhistologische Färbungen die in einer vorangegangenen Studie gesehene Migration der USSC in das Läsionsareal, sowie das mMS Lumen bestätigt werden. Zum ersten Mal konnte die Rekonnektivität regenerierter Axone mit Zielneuronen kaudal zur Läsion gezeigt werden. Eine Reduktion der Zysten und eine Zunahme der Axonregeneration konnte ebenfalls in kombinationsbehandelten Tieren beobachtet werden. Die Bildung zahlreicher Blutgefäße im Läsionsareal, sowie eine signifikante Verbesserung der lokomotorischen Funktion wurden in Tieren mit Implantation des mechanischen Mikrokonnektorsystems nach 21 Wochen beobachtet.

Die Kombination der individuellen Behandlungen (mMS, USSC) resultierte in einem erhöhten Axonwachstum, welches den jeweiligen Einzeltherapien überlegen war. Die langanhaltende Erholung der Lokomotion nach der Kombinationstherapie einer schwerwiegenden Rückenmarksverletzung zeigte sich nur im Vergleich zur USSC Behandlung, sowie zur Kontrolle, überlegen. Die Ergebnisse dieser Kombinationsbehandlung nach Rückenmarksverletzung bieten einen neuen, therapeutischen Ansatz, welcher den Fortschritt zur Lösung einer Behandlungsstrategie weiter voranbringen kann.

Summary

Spinal cord injuries (SCI) mostly lead to permanent paralysis. This is due to the limitations of spontaneous axon regeneration in the CNS caused by the formation of a glial scar and the increased secretion of inhibitory molecules at the lesion site. This multifactorial and multiphasic pathophysiology of SCI and the fact that there is no therapeutic approach that shows a long-lasting improvement leads to the assumption that a combination of various therapies are necessary to show effective outcomes. A previous study in our lab has shown that an implantation of a mechanical microconnector system (mMS), developed in collaboration with the University of Technology Hamburg-Harburg and the BG Trauma Hospital Hamburg, into the lesion site following a complete transection restored the tissue continuity and improved the behavioural outcome. Furthermore, another study from our lab demonstrated that transplantation of somatic stem cells from umbilical cord blood, so called unrestricted somatic stem cells (USSC), enhanced the number of regenerated axons and led to a constant behavioural improvement. Based on these studies, the aim of the present investigation is the combinatorial treatment of the before mentioned individual strategies in a rodent model to analyse the effect on axon regeneration, involvement of propriospinal interneurons, synaptic reconnection as well as functional improvement after SCI.

To verify the hypothesis that the combinatorial therapy is superior to the individual treatments and to further analyse the accompanied regeneration and synaptic reconnection a complete transection (TX) at the thoracic level 8/9 (Th8/9) in immunosuppressed rats was performed. A short-term study, comprised of 5 weeks, and a long-term study, comprised of 21 weeks, was performed with animal numbers of n = 16 and n = 40, respectively. Immediately after SCI, the four different treatments were applied: (1) combination therapy (mMS + USSC), (2) mMS, (3) USSC, and (4) control (TX only). Immunohistochemical stainings were performed to investigate tissue preservation, angiogenesis, and axonal regeneration in the short- and long-term study. Furthermore, regeneration of propriospinal neurons (PN) via retrograde labelling, corticospinal tract (CST) axon regrowth via anterograde (AAV) tracing, and synapse formation were examined in long-term animals with the help of immunohistochemical stainings. Additionally, hind limb function was evaluated

weekly in an open field test using a modified Brasso, Beattie, and Bresnahan Locomotor Score (mBBB).

The immunohistochemical stainings revealed migrated USSC in the lesion area and the mMS lumen. Furthermore, synaptic reconnections of regenerated axons to neurons caudal to the lesion were observed for the first time. A decrease of cyst cavities and an increase in axonal regeneration was found in combinatorial treated animals. Both of these results were detected in the short- and long-term study. The formation of numerous blood vessels in the lesion area as well as a significant improvement of the locomotor performance in mMS treated animals was observed after 21 weeks.

The combination of the individual therapies (mMS, USSC) resulted in an increase in axonal regrowth, which was superior to the single treatments. The long-lasting functional improvement in the combinatorial therapy following a severe spinal cord injury only showed a superior outcome compared to the USSC and control treatment. In conclusion, the results of this combinatorial treatment in spinal cord injuries offer a new therapeutic approach, which can further advance the solution for a treatment strategy.

Contents

List of Figures

List of Tables

1. Introduction

Traumatic injuries of the spinal cord result in lifelong, severe disabilities because of the loss of mobility with simultaneous dysfunction of the autonomic nervous system. The leading causes of spinal cord injuries (SCI) are traffic accidents, falls, and sporting accidents. With about 250 000 new incidents each year the number of people suffering from SCI constitutes at 2.7 million worldwide [6, 7]. In contrast to the peripheral nervous system (PNS), the central nervous system (CNS) is not able to regenerate spontaneously when injured [8]. In research, special attention is therefore paid to find therapeutic strategies and their matching mechanisms.

1.1. Pathophysiology of spinal cord injury

A spinal cord injury leads to a series of pathophysiological processes at the lesion site and its surrounding tissue. These processes can be summarised in three phases: the acute, subacute, and chronic phase. Furthermore, it is characterised by a biphasic pattern: the primary mechanical injury, with haemorrhage and generation of necrotic epicentre, and the secondary injury, caused by one or more additional damaging processes, initiated by the primary injury. Therefore, SCI does not only lead to an interruption of the electrophysiological signal transduction of the damaged axons but subsequently triggers secondary degenerative cascades [9]. Inflammation and immune responses [10], proliferation of progenitor cells [11-13], migration of astrocytes to the injury [14], and gliosis and cyst formation [15, 16] are concomitants of these secondary processes and cell loss. The transection of nerve fibres (axons) and their break-up caused by a trauma leads to the so-called Wallerian degeneration which results in the disintegration of the axon and its myelin sheath distal to the lesion. The debris originating from this process is phagocytised by macrophages and, to a lesser degree, resident microglia. The inhibitory environment for axon regrowth is partially created by a variety of myelin-associated inhibitors including Nogo-A, myelin-associated glycoprotein (MAG), and myelin-oligodendrocyte glycoprotein (MOG) which are present in the myelin debris [17]. Neutrophils that infiltrate the injury centre undergo apoptosis. However, if macrophages do not efficiently phagocytose apoptotic neutrophils they undergo secondary necrosis and uncontrollably release toxic intracellular contents, which causes further damage [18].

Hence, adjacent healthy tissue is affected and destruction of neuronal and glial cells lead to an increase of the initial injury area up to more than twice the size.

In conclusion, secondary injury occurs over a period of time from minutes to weeks and leads to further neurological damage, including oxidative damage [19], imbalance of ionic influx [20], apoptosis [21], vascular changes [22-24] (i.e. ischemia, edema, and disruption of the blood-spinal cord barrier), and inflammation [25] (Fig. 1). Necrosis and apoptosis of neurons and glia cells are the consequences. Moreover, this secondary degenerative cascade provokes a physical and chemical barrier to axonal extension.

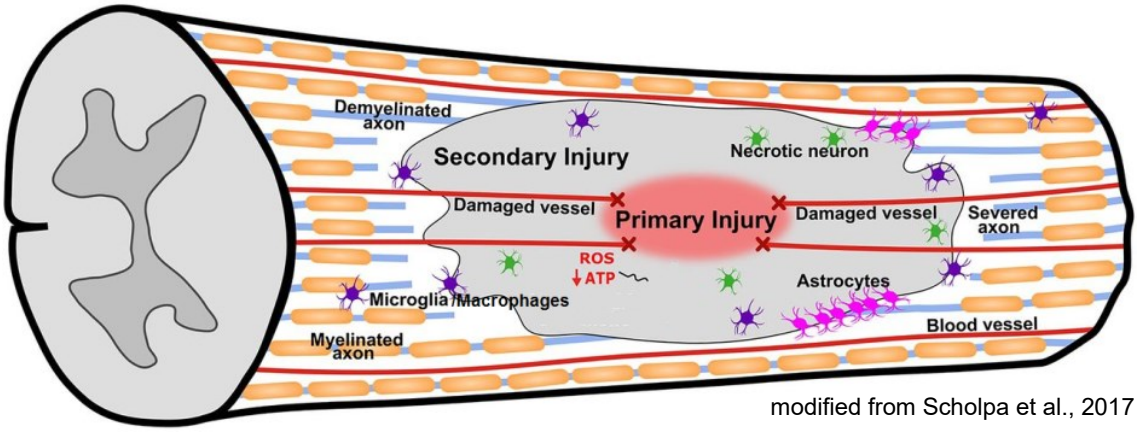

modified from Scholpa et al., 2017 [2]

Figure 1: Spinal cord injury pathology: primary and secondary injury.
A combination of primary and secondary injury leads to the entire damage after SCI. The primary mechanical injury induces vasculature disruption in the spinal cord and reduction of local oxygen delivery, which increases oxidative damage by reactive oxygen species (ROS). Following the primary insult is the secondary injury, which includes neuronal cell death, axon severing and demyelination, microglia/macrophage activation, and glial scar formation.

1.2. Scar formation

One of the major factors of regeneration failure in the mammalian spinal cord is thought to be the connective tissue at the injury site. As first described by Ramon y Cajal [26] a lesion scar occurs following a CNS injury, such as SCI. The process of scar formation starts with the breakdown of the blood-brain/blood-spinal cord barrier where haematogenous cells invade the neural tissue resulting in the activation of the inflammatory reaction by cytokine production (Fig. 2). Most important in this regard is the restriction of the initial damage by local intracellular and extracellular modifications. Therefore, the blood-brain-barrier is re-sealed to re-establish the CNS integrity. The invasion of haematogenous cells is accompanied by neural degeneration, formation of a cystic cavity, and activation of glial cells around the

lesion. There are two types of scarring tissue that eventually form the lesion scar: the glial and the fibrotic scar. The glial scar consists mainly of reactive astrocytes, which overexpress GFAP (glial fibrillary acidic protein). Their proliferation due to the injury separates the uninjured from the injured tissue by branching. It is known that the astrocytes express molecules that are assumed to be inhibitory such as tenascin, brevican, and neurocan [27-29] as well as possessing growth-promoting properties like NCAM [30]. Furthermore, oligodendrocytes and meningeal cells, which are associated with reactivated astrocytes, also express inhibitory molecules such as Nogo [31, 32]. However, the fibrotic scar, consisting of a dense extracellular matrix (ECM) network including collagen type IV (coll IV), fibronectin, and laminin, is suggested to be more impediment for axonal regeneration [33]. Reactive astrocytes and invading fibroblasts together form a continuous basal lamina at the periphery of the lesion area and a glial barrier, called glia limitants, evolves [5, 34]. Experiments in the late 1990s showed that regenerating axons came to an abrupt halt at the area of collagen type IV [35-37]. This supports the inhibitory properties of the fibrotic scar.

1.3. Axon regeneration failure after SCI

In the early 1900s, Ramon y Cajal assumed that the CNS was incapable of regeneration in contrast to PNS injuries [8, 26]. However, in 1981 this hypothesis was refuted by replacing the CNS glial environment with a transplant of peripheral nerves [38]. With that, axons from nerve cells of the spinal cord and the brainstem were able to grow for long distances. Although the rate of degeneration of damaged axons is about the same in CNS and PNS, the number of phagocytosing cells is lower in the CNS than PNS resulting in a much slower removal of cell debris in the CNS [39]. Hence, the environment of the CNS is the main cause for the limited regeneration in mammals. It has been shown that the lack of a stimulating environment, including missing growth promoting factors and massive cell death, the presence of regenerative barriers, physically aroused by the glial scar as well as physiologically up-regulated inhibitory molecules, and the deficient growth potential of adult CNS neurons causes the limited regeneration after injury of adult mammalian CNS axons [40-42]. Therefore, to overcome these barriers and to gain functional recovery following a spinal cord injury is one of the major goals for therapeutic treatments.

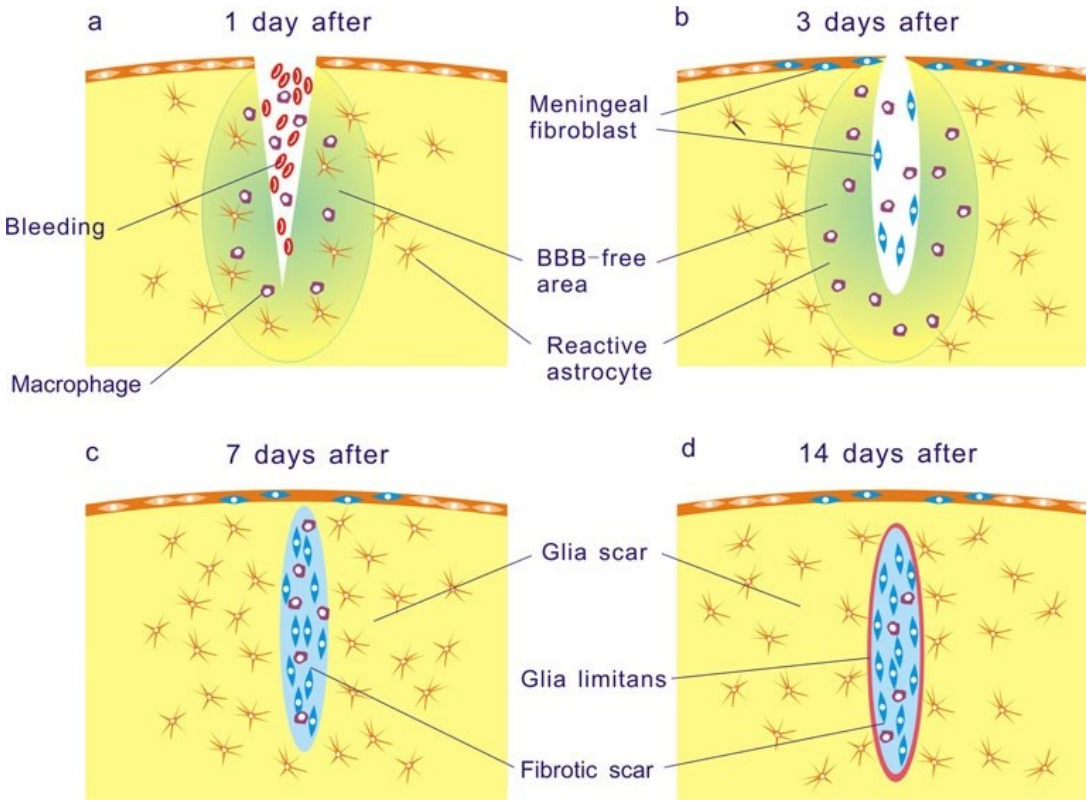

Kawano et al. 2012 [5]

Figure 2: Schematic drawing representing the process of the lesion scar formation.
Following a CNS injury, in the first day the blood-brain barrier (BBB) is disrupted and macrophages infiltrate the BBB-free area. (a) Upregulation of GFAP by reactive astrocytes. (b) Three days after injury reactive astrocytes are significantly increased and are absent from the lesion centre where the BBB is destroyed. Intrusion of fibroblasts from the damaged meninges to the lesion site. (c) One week after lesion the fibrotic scar is formed by proliferating fibroblast which secrete extracellular matrices. The BBB-free area is re-sealed and reactive astrocytes re-occupy the surrounding area of the lesion. (d) By two weeks after injury, the reactive astrocytes seal the lesion site by forming a glia limitants.

1.4. Locomotor function following SCI

Recovery of locomotor function after spinal cord injury is the ultimate goal of a therapeutic treatment. Therefore, understanding the mechanisms involved in motor control is essential for behavioural testing methods for SCI animal models. Many studies focus on the functional recovery evoked by various therapy approaches. The administration of different cell implants or substances, like mesenchymal stromal cells conditioned medium [43] or a combination of deferoxamine mesylate and stromal cell-derived factor 1α (SDF-1α) [44], via intrathecal catheter led to a significant improvement of locomotor function following SCI. Furthermore, the transplantation of stem cells into the lesion site also led to a functional recovery [45,

46]. In recent years, central pattern generators (CPG), a specialised network of interneurons within the spinal cord, have been accepted to be involved in locomotion by generating rhythmic movements [47, 48]. In accordance to this, neuromodulators, e.g. serotonin (5-HT), are able to considerably influence the locomotor CPG activity and consequently improve locomotor function following SCI [49, 50]. Currently there are no approved therapies to restore mobility and sensation following SCI. Therefore, the cellular and molecular mechanisms caused by spinal cord injury that compromise regeneration and neuroplasticity have to be further investigated to develop new strategies to promote axonal regrowth and functional recovery.

1.5. Treatment therapies

There are various ways to treat SCI. With the continuous growth of understanding the molecular processes and the pathophysiology, the number of therapeutic approaches is increasing. Regrowth of only a small number of axons can already lead to an improvement of motor and sensory function [51]. Nonetheless, axonal regeneration is not necessarily occurring to show recovery. For long-distance regeneration in the severed original pathways after SCI several criteria have to be complied. Axonal regrowth or sprouting has to be followed by elongation of respective axon fibres which in turn may grow through and beyond the lesion area and, if they find the appropriate target cells, synapse connections have to be established and remyelination has to occur to achieve functional recovery [33]. Even though CNS neurons have the intrinsic capacity to regenerate [52], it is still unclear why neurons fail to regenerate in general. Therefore, many research groups focus on identifying the components and mechanisms, which are responsible for regrowth failure, with the intent of enhancing axonal regeneration [51]. However, there is still no successful clinical therapy to protect or promote recovery after SCI. In general, therapeutic approaches can be classified into four categories [4] (Fig. 3): (1) Pharmacological approaches (e.g. growth factors), (2) reparative approaches (e.g. gene therapy, tissue engineering like biomatrices and mechanical guiding tracks), (3) cell therapies (e.g. neurotransplantation), and (4) rehabilitation.

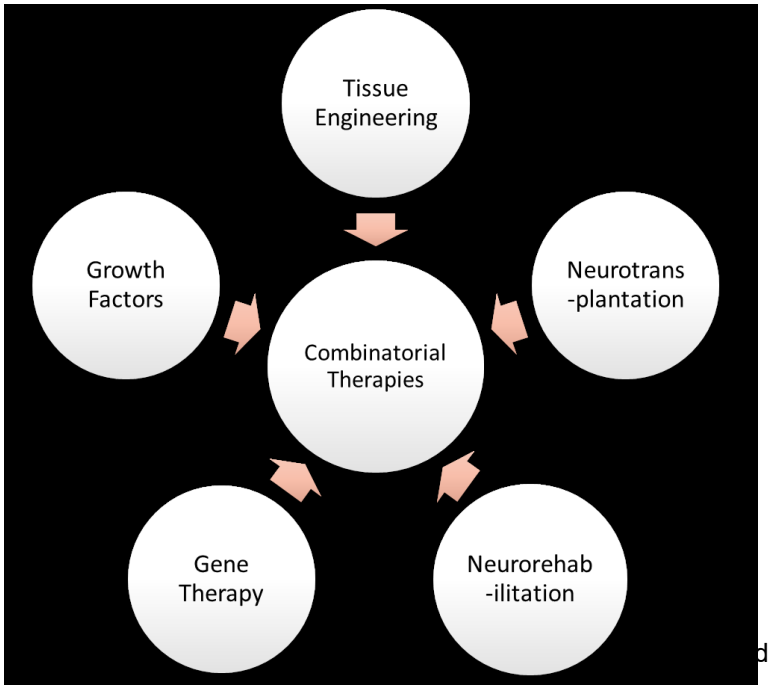

d from Dietrich et al., 2015 [4]

Figure 3: Strategies to promote spinal cord repair and regeneration.
The single therapy approaches (tissue engineering, neurotransplantation, growth factors, neurorehabilitation, gene therapy) have regenerative success only to some extent. Therefore, to combine different therapies may enhance regeneration and rehabilitation.

1.6. Pharmacological approaches

Researchers have identified various factors and mechanisms, which result in insufficient regeneration of axons and might even act synergistically. Pharmacological approaches like blocking inhibitory molecules have been attempted to disarm the inhibitory environment and hence to support axonal regrowth. Blocking the inhibitory effects of myelin [53-56], modifying the composition of the lesion scar environment, like applying an iron chelator [57, 58] or enzymatically digesting inhibitory proteoglycan molecules with a chondroitinase ABC treatment [59-62], and administering trophic factors [63-70] led to axonal regeneration after CNS injury. However, the time frame in which a treatment is applied varies in its efficacy and further the response of different neuronal subpopulations differs depending on the treatment [71].

1.1.1. Biomatrices and mechanical guiding tracks/tools

The scar formation caused by the death of neuronal cells following an SCI presents a prominent obstacle for axon growth and regeneration. One possibility to

bypass this barrier has been tested by implantation of several biomatrices in chronic SCIs. A mechanical support for axonal regrowth can be achieved by artificial tissue scaffolds. Several criteria should be met by tissue scaffolds to promote spinal cord repair, such as biocompability with host tissue to avoid adverse immune reactions and biodegradable materials with nontoxic products. Common natural substances for these scaffolds are hyaluronic acid, alginate hydrogel, collagen, agarose, chitosan, matrigel, and methylcellulose hydrogels. All of them have advantageous and disadvantageous features, like adhesion potential, cell invasion, macrophage motility, or scar reduction [72-74]. In contrast, synthetic materials for scaffold are favourable as they can be modified in a controlled fashion to achieve desired material properties [75]. For instance, a resection of the spinal cord, that means the surgical removal of the scar tissue, and the subsequent implantation of regeneration-supporting, immune inert non-toxic biopolymers, especially Polyethylenglycol 600 (PEG), has improved axon regeneration and long-lasting locomotor recovery [76]. A reduction of fluid-filled cysts was achieved by implanting a cross-linked collagen-based scaffold into the resection gap [77]. Furthermore, an alginate-based hydrogel induced a directed axonal regeneration across this artificial scaffold [78]. In the past few years, several approaches to enhance axon regeneration following SCI with mechanical guiding tracks/tools have been investigated. An example is the mechanical microconnector system (mMS) developed by Brazda and colleagues [1]. The mMS is implanted into the tissue gap following a complete transection of the spinal cord. With this device, the tissue continuity was restored and glial and vascular cell invasion, motor axon regeneration and myelination was achieved resulting in a significant functional improvement [79].

1.1.2. Stem cell transplantation

Another therapeutic concept to improve paraplegia is the transplantation of stem cells. Not just axon regeneration but also locomotor function was improved by numerous experimental studies with different types of stem cells [80-82]. Among the various stem cell types, which have been used in experimental studies are hematopoietic (HSC), mesenchymal (MSC), neural (NSC), and embryonic stem cells (ESC). HSC are multipotent stem cells of the blood system with self-renewal properties. HSC have the potential to differentiate not only into haematopoietic but also into nonhaematopoietic cells like neural lineage cells [83-85]. Furthermore,

HSC have been shown to be beneficial when transplanted after SCI [86]. MSC, also known as mesenchymal stroma cells, were originally found in the bone marrow but have been identified in other tissues as well [87]. Studies indicated the potential of MSC to support axonal regrowth and to augment tissue sparing by neuroprotection [88-90]. Another promising cell type for stem cell treatment in SCI are the NSC and their progenitors due to their potential to give rise to mature neurons, astrocytes, and oligodendrocytes [91, 92]. Several studies demonstrated that the transplantation of NSC into the injured spinal cord resulted in improved functional outcome and axonal regeneration. However, in one clinical case the development of several neuroblastomas deriving from the graft were observed suggesting tumorigenicity of NSC which has to be kept in mind for future studies [81, 93]. Embryonic stem cells have the ability to differentiate into nearly all cell types due to their pluripotency. Furthermore, under defined conditioned ESC can be cultured and expanded into sufficient numbers to be clinically relevant for transplantation. Unfortunately, ESC tend to form teratomas or other tumours and therefore require pre-differentiation and purification prior to grafting [94]. The retrieval of embryonic stem cells is ethically highly controversial. Therefore, somatic stem cells with suitable regeneration-promoting characteristics are sought-after. For example, somatic adult human MSC from the bone marrow were transplanted and resulted in improved functional outcome following SCI. However, as the transplanted cell population is often heterogeneous a certain stem cell type for therapeutic effectiveness is impossible to allocate [81]. Nonetheless, somatic stem cells can also be extracted from umbilical cord blood. Besides the uncomplicated extraction of these stem cells, their proliferation ability in cell culture is also of advantage. Furthermore, the acute “Graft-versus-Host” reaction has been shown to be much less in umbilical cord blood derived stem cells [95]. The unrestricted somatic stem cells (USSC), which are isolated from the umbilical cord blood, even exhibit features of adult stem cells from the bone marrow [96]. However, USSC can be distinguished from MSC, extracted either from umbilical cord blood or bone marrow, by the expression of delta-like 1/preadipocyte factor 1 and a USSC-specific HOX-gene code [97, 98]. It has been shown that USSC secret axonal growth permitting signals indicating a beneficial effect on axonal regrowth following an SCI [99]. In accordance, a favorable outcome, such as functional recovery, following the transplantation of USSC derived from umbilical cord blood has been described by

Schira and colleagues [100]. Moreover, USSC do not induce tumor formation which makes them an eligible tool for transplantation [101].

1.1.3. Physical therapy and stretching

A relatively high achievement of recovery in spinal cord injury in humans has been made by physical therapy including gait training [102-104]. Physical therapists commonly use stretching as an approach to reduce tendon and muscle contractures and to maintain the extensibility of soft tissue. To support probable beneficial neuroplasticity, enhance the locomotor function, and improve the final outcome intensive, repetitive task specific training needs to be performed [105-109]. Different approaches including voluntary running wheels, robotic-based training, or treadmill training in various animal and injury models have been performed [110-112]. These physical therapies resulted in facilitation of locomotor recovery in general, improvement in step shape consistency, and improvement of use of paretic hind limbs.

In conclusion, the major targets in spinal cord recovery are to limit the progression of the secondary injury, to replace lost cells, to stimulate and especially guide axonal growth, to promote remyelination, and to establish a growth permissive environment. All of these repair strategies have been shown to improve axonal regeneration and locomotor recovery to some extent. However, their efficacy was rather modest which leads to the assumption that a combination of these treatments may show a greater effect. Finally, translating the knowledge of the single and combinatorial therapies into future studies could lead to a refinement and more efficacious treatment for human patients.

1.7. Complete transection – the optimal injury model to demonstrate axonal regeneration

Research in spinal cord injury developed a number of experimental injury models mainly in rats, but also for mice, cats, and pigs. Because of several parameters, including cost and accessibility, easy care, and well-established functional analysis techniques, mice and rats are the common SCI models today [113, 114]. An enhanced knowledge of the pathophysiology and secondary mechanism of SCI have been acquired by means of experimental studies with these animal models, which in turn contributed to a better application and establishment of

novel therapeutic strategies. In general, SCI models should be able to reflect and simulate aspects of clinical SCI, should be reliable, controlled, and reproducible [115, 116]. The aim of the study plays a great role in deciding which injury model to use. The most common ones are complete or incomplete transection, as well as contusion and compression injuries. Transection models rather than contusion or compression are used to evaluate the effectiveness of therapeutic interventions to promote axonal regeneration and locomotor improvement [117]. However, the transection model does not represent the common human spinal cord injury. In humans, SCI corresponds most closely to a compression or contusion injury model with an intact *dura mater* [118, 119]. Nonetheless, the complete transection is referred to as the "gold standard" to demonstrate axonal regeneration [120], since in a complete transection the regenerated axons can be distinguished from the spared ones, if the transection was executed properly [120, 121]. To implant scaffolds a complete transection is essential to accommodate the device and further provides a good basis for the initial analysis of tissue engineering strategies, especially in regards to axon regeneration [122]. With surgeons considering re-sectioning the scar of chronic SCI patients that would leave a huge tissue gap which in turn can be compared to a complete transection, the complete transection model is not only suitable for acute but also chronic spinal cord injuries [123].

In the present study, the complete transection model was applied to facilitate the implantation of the mechanical microconnector system to analyse axonal regeneration and synaptogenesis.

1.8. Propriospinal neurons – a tool for bypassing lesion areas?

Spinal cord injuries are usually accompanied by functional deficits including impaired fore- and/or hind limb function. This is due to damage of the white matter that affects both descending and ascending systems, and to the gray matter containing the segmental circuitry for processing sensory input and generating motor output [124]. Descending propriospinal neurons are able to bridge the lesion and form new contacts to relay motor signals [125]. Propriospinal interneurons (PN) have been first described by Sir Charles Sherrington as a population of spinal cord interneurons that connect multiple spinal cord segments and participate in complex or long motor reflexes [126]. To receive a motor input signal and to conduct this signal the PNs are connected to i.e. the corticospinal tract (CST) axons. In rodents

and primates, the CST axons project mainly to the intermediate grey matter where especially descending, propriospinal interneurons are located [125, 127]. These descending PNs form direct connections between cervical and lumbar spinal circuits. This allows voluntary motor control coming from the motor cortex [128].

In incomplete spinal cord injuries, the possibility to regain functional locomotion is much higher than in complete SCIs. That especially applies to the redirection of corticospinal signals. When corticospinal tract axons are lesioned they can sprout onto spared propriospinal interneurons which could allow interrupted corticospinal signals to bypass the lesion site and reach the distal cord without the need of axonal regeneration [125, 129]. However, this plasticity seems limited to injuries where some components of the damaged projection survived which then can be expanded.

1.9. Reconnection after SCI

The transection of axon fibres and the resulting neural cell death caused by spinal cord injury leads to the disruption of the neural network, like the loss of synaptic connections, and severe functional deficits. Spared neurons remaining at the injury site have been suggested to be involved in the reconstruction of damaged neural circuits by relaying signals and to contribute to functional recovery following SCI. Even though these spared neurons build synaptic connections to rebuild the damaged neural circuits, the locomotor function is limited and spontaneous as there are only a few neurons still existing in the injured spinal cord [130, 131]. Therefore, the transplantation of stem cells, which leads to an increase of the neuron population at the injury site, might lead to an improved functional recovery. Several research groups have investigated the transplantation of neural stem cells into an injured spinal cord. Implanted neural stem cells received an extensive range of host neural inputs to the injury site and built synaptic connections to host neurons, which potentially enables functional restoration [132, 133].

2. Aim of this thesis

Diagnosis paraplegia: The loss of voluntary movement is devastating. This loss and other deficits are caused by the interruption of the electrophysiological signal transduction due to damage to the spinal pathways. With knowledge of SCI increasing considerably through research, including detailed mechanisms and pathophysiology involved in injury- and recovery-related processes, numerous treatment strategies have been developed [134]. However, the multifactorial and multiphasic pathophysiology of SCI, like physiological and physical barriers, represents a major obstacle for SCI recovery. Since single therapies have not shown a satisfactory outcome so far, a combination of different treatments is likely to accomplish the aim of SCI research to enhance locomotor function. Therefore, this study combined two therapeutic strategies, (1) the implantation of a mechanical microconnector device and (2) grafting somatic stem cells.

The purpose of the mechanical microconnector system (mMS) is to close the physical gap of separated spinal cord stumps caused by a complete transection by means of an applied vacuum [1]. The re-adaptation of spinal cord stumps through the application of the mMS by Brazda and colleagues [1], Kehl [135], and Estrada et al. [79] showed beneficial effects on the formation of a tissue bridge, vascular cell invasion, motor axon regeneration and myelination resulting in improved locomotor function.

In numerous studies, the transplantation of various stem cells has shown beneficial effects on regeneration following SCI. With the transplantation of human unrestricted somatic stem cells (USSC) Schira and colleagues [100] demonstrated a significant improvement of axonal regeneration and locomotor recovery in a rat hemisection model.

The aim of this thesis was to investigate the synaptic reconnection of regenerated axons and the involvement of propriospinal interneurons in functional recovery following a complete spinal cord transection and the subsequent mMS implantation and USSC transplantation as a combinatorial treatment. These individual therapies as well as their superior combination have been shown to be beneficial and were to verify in this study. In particular, the following aspects were addressed:

a) Efficacy of the combinatorial treatment on regenerative axonal growth, synaptogenesis, and reduction of cystic cavities compared to the individual treatments.
b) Involvement of descending propriospinal interneurons in hind limb locomotion by bridging motor signals through the lesion site into the caudal spinal cord.
c) And finally, evaluation of the effect of the combinatorial therapy for significant improvement in locomotor function.

3. Materials and methods

3.1. Buffers, solutions and antibodies

3.1.1. Buffers and solutions

Buffers and Solutions	Composition/Manufacturer
DPX for tissue mounting	Merck
DS, 5 %	50 µl DS (Sigma) 1 ml PBS
Ethanol denatured	Fischar
Gelatine, 10 % for tissue embedding	10 g DifcoTM gelatine (BD) 100 ml 0.1 M PB 100 mg sodium azide (Roth), 0.1 % 60 °C for solving, 37 °C for embedding
Immu-Mount for tissue mounting	Thermo Scientific
Masson's Trichrome	Solution A: 1 g Acid Fuchsin (Merck) 1 g Xylidine Ponceau (Sigma) 198 ml aq. bidest 2 ml Acetic Acid (Merck) Solution B: 2 g Phosphomolybdic Acid (Merck) 200 ml aq. bidest Solution C: 4 g Light Green SF yellowish (Merck) 4 ml Acetic Acid (Merck) 200 ml aq. Bidest
NaOH	Merck

NGS, 10 %	100 µl NGS (Vector) 1 ml PBS
Paraffin	100 g Paraffin (Merck) 5 g Wax (Cera Alba, CAELO) at 56°C
PB 0.2 M, pH 7.4	45.5 g Na_2HPO_4 (Merck) 12 g NaH_2PO_4 (Merck) 2000 ml aq. bidest.
PBS 0.1 M, pH 7.4	100 ml 10xPBS (Roche/Sigma) 900 ml aq. bidest
PFA 4 %, pH, 7.4	40 g PFA powder (Merck) 1000 ml 0.1 M PB pH titration with 5 M Sodium Hydroxide (NaOH)
Proteinase, bacterial, Type XXIV (7.0 – 14.0 units / mg, solid)	9 U / mg 1,9 mg Proteinase (Merck/Sigma) 5 ml Tris Buffer
Rotihistol	Roth
Sucrose for cryoprotection, 30 %	9 g sucrose (Merck) 30 ml PBS 0.01 % sodium azide (Roth)
Sudan Black (SB) 0.3 %	0.6 g SB (Fluka) 200 ml Ethanol (70 %) stir over night and filter next day

Tissue-Tek O.C.T. Compound	VWR
Tris Buffer 20 mM, pH 7.9	500 ml aq. Bidest 1.12 g Tris (Sigma) pH titration with 3 M hydrochloric acid (HCl, 37 %, Merck)
Triton X-100, 0.03 % in PBS	1.5 µl Triton X-100 (Sigma) 5 ml PBS
Triton X-100, 0.1 % in PBS	5 µl Triton X-100 (Sigma) 5 ml PBS

3.1.2. Primary antibodies

Antibody	Class	Antigen	Dilution	Manufacturer
5-HT	rb IgG	5-hydroxytryptamine, Serotonin	1:40	Biologo
ED1	ms IgG	Macrophage-activation Antigen (CD68)		Bio-Rad (former AbD Serotec)
FG	gpig	Fluorogold, fluorescent dye	1:500	Protos Biotech Corp
GFAP	ms IgG	glial fibrillary acidic protein	1:500	Merck
hNuc	ms IgG	human nuclei	1:500	Millipore
NeuN	ch IgY	neuronal nuclei	1:250	Millipore
PAM	ms IgG	phosphorylated neurofilament	1:1000	Biolegend
RFP	rb IgG	Red Fluorescent Protein	1:1000	Rockland, Biomol

Synaptophysin	gpig IgG	synaptophysin (synaptic vesicle protein)	1:500	Synaptic Systems
Synaptophysin	rb	synaptophysin	1:500	Millipore
TH	rb IgG	tyrosine hydroxylase	1:750	Abcam
v.W.F.	rb IgG	von Willebrand Faktor (factor VIII related antigen)	1:1000	Dako

3.1.3. Secondary antibodies

Antibody	Class	Dilution	Manufacturer
Alexa Fluor® 488 anti mouse	dk IgG	1:500	Molecular Probes
Alexa Fluor® 488 anti mouse	gt IgG	1:500	Molecular Probes
Alexa Fluor® 488 anti rabbit	dk IgG	1:500	Molecular Probes
Alexa Fluor® 594 anti chicken	dk IgG	1:500	Jackson Immuno Research Laboratory
Alexa Fluor® 594 anti guinea pig	dk IgG	1:500	Molecular Probes
Alexa Fluor® 647 anti guinea pig	dk IgG	1:500	Jackson Immuno Research Laboratory
Alexa Fluor® 647 anti rabbit	dk IgG	1:500	Molecular Probes

3.1.4. Tracer substances and reagents

Substance	Dilution	Manufacturer
Baytril ®	-	Bayer Health Care
Carprofen ®	1:20	Pfizer GmbH
Temgesic ®	-	Indivior
Cyclosporin A	1:20 (2.5 mg / ml)	Novartis
DAPI (4,6'-Diamino-2-Phenylindole)	1:10.000	Roche Diagnostics
Fluorogold (FG)	2 % (in NaCl)	Invitrogen

3.2. Adeno-associated viral vector (AVV) for axonal anterograde tracing

A recombinant adeno-associated viral vector (AAV9-mCherry) construct was used for anterograde axonal tracing. Axons thereby were tracked from their cell body (soma) to their synapses. The AAV constructs were manufactured in cooperation with Prof. Michel and Prof. Lingor from the Georg-August-University Goettingen (Fig. 5). The AAV plasmid is comprised of a mCherry fluorophore in a plasmid of the serotype 9, which possesses a great transfection rate. The fluorophore mCherry is a monomeric form of dsRed, which is isolated from the sea anemone *Discosoma* and has an emission maximum of 610 nm and an excitation maximum of 587 nm. The induction of the AAV construct occurs without integration into the nucleus genome.

Anterograde tracing was performed stereotactically 3 weeks prior to perfusion. For that, the animals were anesthetised via inhalation of isoflurane (Forene; 2-3 % in O_2 and N_2O at a ratio of 1:2). The injection of the AAV for CST axon tracing was performed by drilling a hole into the skull in each hemisphere to inject into the region of the sensorimotor cortex (Fig. 4, Table 1). Injection coordinates were measured from the bregma -0.2 cm to the rostrocaudal and +/- 0.24 cm to the

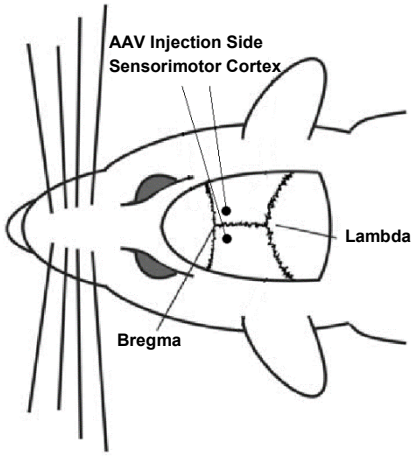

Figure 4: Schematic illustration of experimental rat for AAV injection.

lateral axis. A volume of 2 µl AAV was slowly injected over four minutes via a Hamilton syringe (24G needle) topped with a glass capillary at a depth of 0.13 cm measured from the contact of the glass capillary to the dura. The syringe was left in place for additional four minutes to avoid leakage before taken out. Prior to injecting into the other hemisphere, it had to be ensured that the glass capillary was not clogged. Subsequently, the scalp was closed with metal clips.

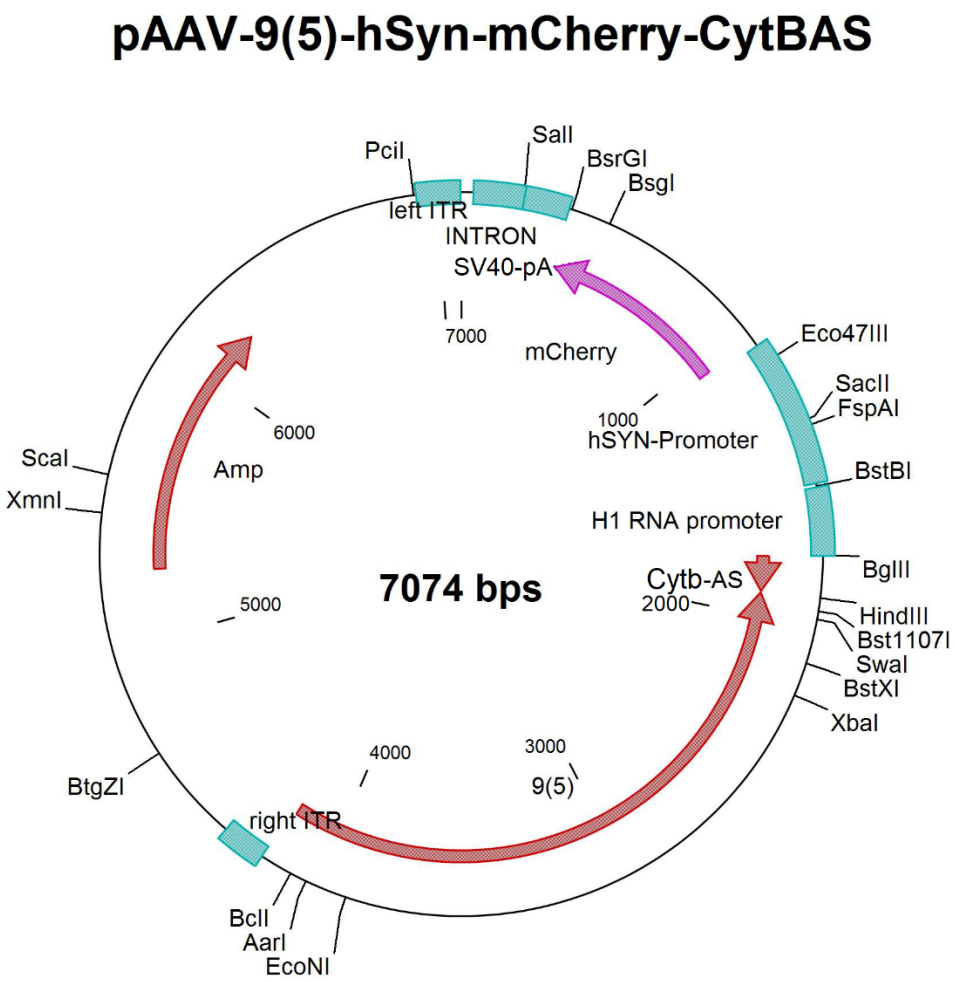

Figure 5: Detailed map of the AAV plasmid with a mCherry tag.

Table 1: Coordinates for anterograde CST tracing with an AAV.

Bregma reference point	**Rostrocaudal**	**Lateral**		**Depth**	
		left	right	left	right
	-0.2 cm	0.24 cm	-0.24 cm	0.13 cm	

3.3. Retrograde tracing with Fluorogold (FG)

To retrogradely trace cells/axons the marker Fluorogold (2 % in NaCl) was injected into the thoracic spinal cord segments 10/11 (Th10/11) in a volume of 2 µl four days prior to perfusion. Fluorogold was injected into the posterior median sulcus. The injection was performed stereotactically with a Hamilton syringe (24G needle) topped with a glass capillary over four minutes. The syringe was left in place for four more minutes to avoid leakage before taken out. As FG is known to be necrotic and to avoid necrosis at the lesion side the distance to the lesion area was estimated to be about 1 cm [136]. Therefore, FG was injected at the lower thoracic level 10/11.

3.4. Therapeutic components

3.4.1. The mechanical microconnector system (mMS) – design, structure, and mechanics

The mechanical microconnector system, consisting of polymethylmethacrylate with honeycomb-structured walls, is a device to reconnect severed tissues, in this case the spinal cord stumps after a complete transection (Tx). Two elliptical discs form the device with a thickness of 350 µm and outer diameters of 1.7 mm and 2.7 mm, which corresponds to the oval cross section of the thoracic rat spinal cord, resulting in a surface of 3.6 mm^2 for the microchamber (Fig. 6). The distance between the two discs, which constitutes the system chamber, is 3 µm adding up to a total thickness of the assembled mMS of 1000 µm [1]. Furthermore, the honeycomb structure permits migration of cells and exchange of trophic factors as it has been described in earlier publications [137, 138] (Fig. 7). To connect the two spinal cord stumps a negative pressure was applied for 10 min with about 250 mbar to suck the stumps into the mMS where they remain in place after removal of the vacuum. The rough surface of the walls of the honeycomb structure allows the spinal cord stumps to adhere to the walls without detaching when the vacuum pump is switched off. The vacuum pump was removed when the pressure was back to 0 mbar. The mMS has been designed and constructed in collaboration with the Institute of Microsystems Technology (Head: Prof. Dr. Hoc Khiem Trieu at University of Technology Hamburg-Harburg).

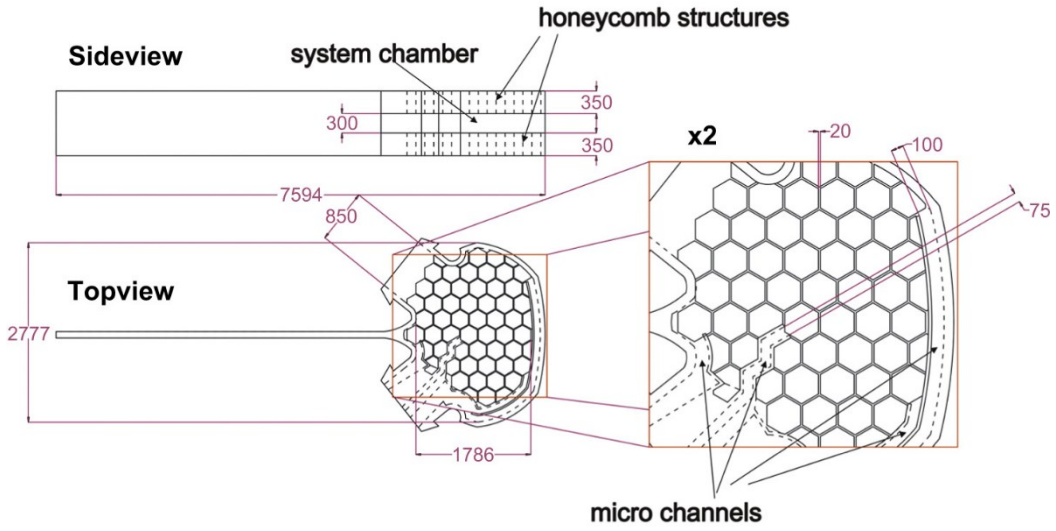

Figure 6: Technical drawing of mMS for dimensional purposes.
All dimensions are given in µm (Brazda et al. 2013 [1]).

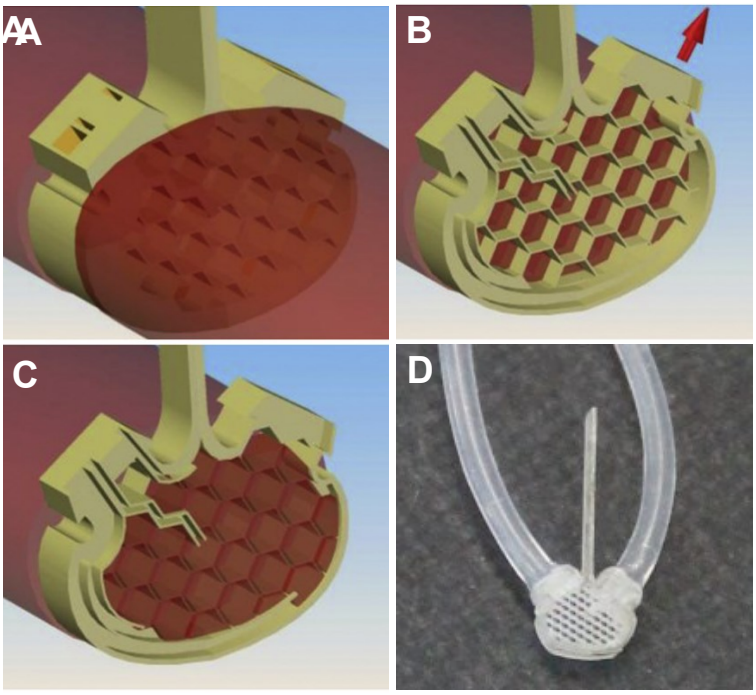

Figure 7: Design and principal use of mMS.
(A-C) Schematic drawing: (A) mMS implantation into the spinal cord lesion following a complete transection. (B) The two spinal cord stumps are drawn into the honeycomb structure by vacuum application (red arrow: negative pressure). (C) Spinal cord stumps are kept several micrometres apart by adhesive force. (D) Photographic image of the mMS and the tubes for vacuum application and drug infusions.

modified from Brazda et al. 2013 [1]

3.4.2. Unrestricted somatic stem cells (USSC)

USSC were isolated from human umbilical cord blood. Besides their beneficial proliferation ability, USSC possess characteristics of mesenchymal stem cells from human umbilical cord blood [95, 96]. USSC were obtained in consent of donors at the Institute of Transplantation Diagnostic and Cell Therapeutics (ITZ, Prof. G. Kögler) of the University Hospital Duesseldorf (UKD) and were provided anonymously. The following procedures were performed by working group

members of the ITZ (3.4.2.1.) and the Laboratory for Molecular Neurobiology. They are listed for the sake of completeness.

3.4.2.1. Isolation, expansion, and characterisation of USSC

The isolation of USSC was performed by the research group of Prof. Kögler. First, the USSC were generated from a cord blood samples and then isolated as previously described [96]. In summary, the mononuclear cell fraction was obtained using a standard Ficoll-gradient separation followed by ammonium chloride lysis of red blood cells. Subsequently, cells were plated out in culture flaks in the presence of dexamethasone. The growth and expansion of adherent USSC colonies were initiated by a DMEM (*Lonza*) medium containing 30 % heat-inactivated fetal bovine serum (FBS, *Lonza*), 2 mM glutamine (*Gibco*), and penicillin/streptomycin (100 U / ml, *Gibco*). Finally, cells were incubated at 37 °C in 5 % CO_2 in a humidified atmosphere.

3.4.2.2. Freezing and storage of USSC

With a confluency of 80 % the USSC were detached from the culture flasks with trypsin / EDTA (1x, 0.05 %; *Gibco*) for 3 min at 37 °C. The trypsin reaction was stopped using DMEM / 10 % FBS and the cells were centrifuged for 5 min at 1200 rpm. With a mixture (1:1) of culture medium and freezing medium, containing DMEM / 40 % FBS and 20 % DMSO (*Sigma*), the USSC were resuspended. Subsequently, the USSC were frozen at -20 °C for 30 min before they were stored at -80 °C overnight. Finally, tubes were transferred to liquid nitrogen and stored until usage.

3.4.2.3. Preparation of USSC for transplantation

USSC were thawed, seeded into T12.5 cell culture flasks and incubated at 37°C. Confluent cells were washed with PBS, and trypsin was applied for detachment and incubated for 4-5 min at 37 °C. The trypsin was applied reaction was stopped using DMEM / 10% FBS. USSC were separated by using a cell separation filter and subsequently centrifuged for 7 min at 900 rpm. The pellet was resuspended in 1 ml Glutamaxx medium without FBS. USSC were counted and transferred into an Eppendorf tube and centrifuged for 2 min at 1200 rpm. To obtain the desired amount of 55 000 cells / µl the pellet was diluted with culture medium (12-22 µl). USSC of passages 7-9 were used for transplantation.

3.5. Experimental animals and surgical procedure

3.5.1. Animals

Adult female Wistar rats (*Janvier Labs*) weighing between 210 – 250 g were used. For the duration of the experiments, the animals were housed in groups of 3 - 4 in a 12-hour light / 12-hour dark cycle. Purified water (pH 2) and pelletized dry-food was available ad libitum.

Institutional guidelines for animal safety and comfort were adhered to. All surgical interventions as well as pre- and post-surgical animal care were provided in compliance with the German Animal Protection law (State Office, Environmental and Consumer Protection of North Rhine - Westphalia, LANUV NRW: AZ 84-02.04.2014.A195, AZ 84-02.04.2014.A136).

The following table (Table 2) provides an overview of the experimental animal groups.

Table 2: Experimental animal groups.
Tx = complete transection, mMS = mechanical Microconnector System, USSC = Unrestricted Somatic Stem Cells, ST = short-term study, LT = long-term study, SM = survival and migration

Treatment/Therapy	Treatment Group Name	Survival Time	Animal # / Group	Study
Tx + mMS + USSC	Combination	5 wpo	4	ST
Tx + mMS	mMS	5 wpo	4	ST
Tx + USSC	USSC	5 wpo	4	ST
Tx only	Control	5 wpo	4	ST
Tx + mMS + USSC	Combination	21 wpo	15	LT
Tx + mMS	mMS	21 wpo	15	LT
Tx + USSC	USSC	21 wpo	15	LT
Tx only	Control	21 wpo	15	LT
Tx + mMS + USSC	Combination	5 wpo	5	SM

3.5.2. Complete transection of the spinal cord between the thoracic segments Th8/9

Adult female Wistar rats were anesthetised with isoflurane (Forene; 2-3 % in O_2 and N_2O at a ratio of 1:2) and buprenorphine (0.1 ml s.c. pre- & postoperation, Temgesic ®, 0.02 mg / kg, *Indivior*) and a subcutaneous injection of Carprofen (0.5 ml, 5 mg / kg, Rimadyl ®, *Pfizer GmbH*) to perform the surgery. The fur was removed at the dorsal site for about 2/3 of the back with an electric shaver and the skin was disinfected. Subsequently the animals were placed on a heating pad to regulate their body temperature. To prevent dehydration of the eyes they were covered with an eye ointment (Bepanthen, *Roche*). All surgical instruments were disinfected with 70 % ethanol before usage. A dorsal skin incision along Th6 to Th11 was made, the muscle tissue was exposed, and a blunt cut was made at the level of the *transverse process*. This was followed by the removal of the *Ligamenti supraspinale*, *interspinale*, and *transversarium* between the thoracic vertebras. With fine pliers the *spinous processes* of the thoracic segments 8 and 9 were removed as well. Next, a small incision in the *Dura mater spinalis* was made so that the spinal cord could be lifted with the help of a spinal cord hook and completely transected with fine spring scissors. The *Dura mater spinalis* was subsequently sewed with a 9.0 thread (2 - 3 sutures) (9.0 Ethilon, *Ethicon*). The muscles and skin were resutured with resorbable threads (4.0 Vicryl, *Ethicon*). The complete transection was performed in all four groups.

3.5.3. mMS implantation

The implantation of the mechanical microconnector system was followed by the complete transection of thoracic segments 8 and 9 (Th8/9). The mMS was implanted with the help of a stereotactic device into the tissue gap and fixated via 2 knots (Fig. 8, A, white arrows) at the muscle tissue to prevent movement of the connector. To be able to create a vacuum the dura was sutured across the device (Fig. 8, B, white arrows). The micro vacuum pump was attached to one of the tubes (Fig. 8, A, red arrow) of the connector while the other one is pinched off. The two spinal cord stumps were brought together via the applied vacuum (~10 min at 250 mbar). The vacuum was applied with the lowest possible pressure in order to avoid further damage to the spinal cord tissue. Subsequently, the tubes were cut close to the mMS once the vacuum was applied and left in place until the pressure decreased back to 0 mbar. Finally, the muscle tissue as well as the skin was resutured.

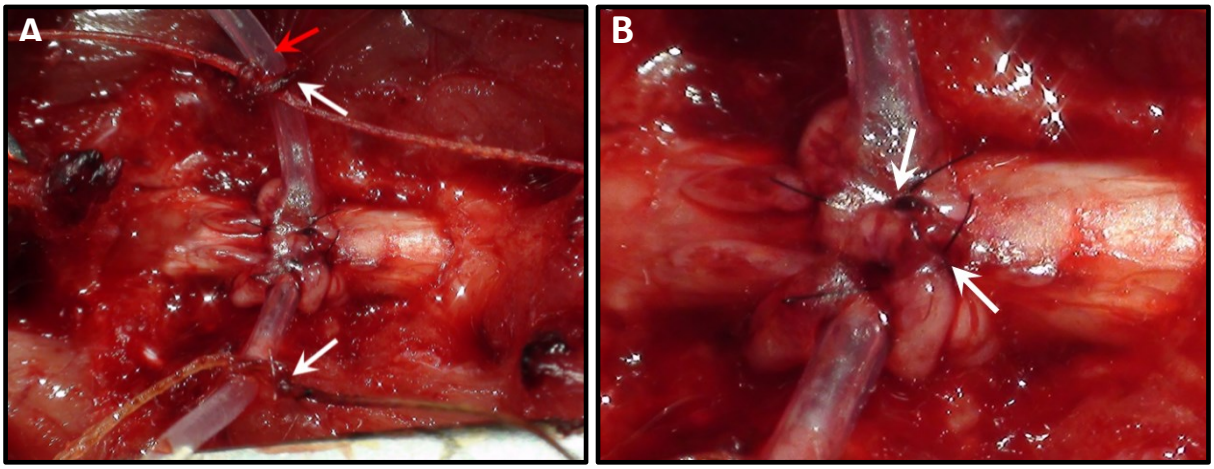

Figure 8: Surgery images of the mMS implantation.
(A) The microconnector was fixed by its tubes (red arrow) at the muscle tissue (white arrows) to prevent movement at the time of vacuum application. (B) The *dura mater* was sutured across the mMS (white arrow).

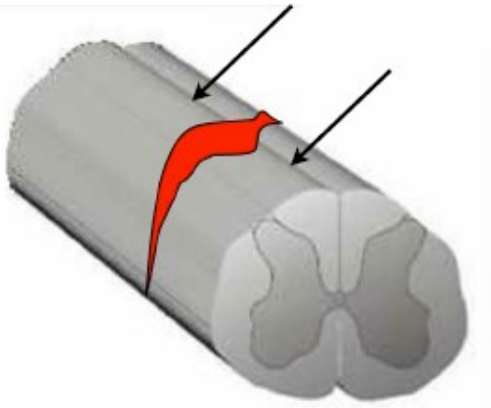

Figure 9: Schematic drawing of a spinal cord with the USSC injection sites above and below the lesion.
The injection of USSC into the spinal cord is performed 2 mm rostral and 2 mm caudal to the lesion (marked by arrows). The complete transection, here marked in red, is performed at Th8/9.
Kehl et al., 2012 [3]

3.5.4. USSC transplantation

Following the complete transection USSC were stereotactically injected with a Hamilton syringe (24G needle) supplemented by a glass capillary attached (Micropipette Puller, Table 3). The injections were carried out 2 mm rostral and 2 mm caudal to the lesion (Fig. 9, arrows) in four different depths (1.3, 1.0, 0.7, and 0.4 mm when in contact with dura) with a volume of 0.5 µl each. To avoid any leakage or reflow the injections were performed very slowly and the syringe was left in place for two more minutes before taken out thereby the stem cells were able to settle. The number of cells per µl was 55 000, thus the total amount of cells transplanted into the spinal cord was about 220 000. All animals received the immunosuppressive

cyclosporine A (15 mg / kg, *Novartis*) one day before the surgery and subsequently three weeks post injury to reduce cell rejection reaction.

Table 3: Setting of micropipette puller, Model P-37, *Sutter Instruments Co*, for glass capillaries.

Program 9	Heat	Pull	Velocity	Time
01	**700**	**40**	**20**	**50**
02	**665**	**-**	**15**	**100**

3.5.5. Physical therapy

In addition to the before mentioned treatments, all animals received a daily four minute hind limb stretch for the first four weeks followed by two days a week for the remaining survival time. The four minutes were divided in two minutes for each limb. The hind limb was grasp by the ankle and carefully stretched to the point of the highest resistance and slowly releasing the tension to its normal position. This stretch was performed in three different directions, backwards, sidewards, and downwards. As animals differed in their flexibility due to the tendons, the furthest point of stretching varied as well. Once the two-minute period was over, the stretching was performed on the other hind limb. This physical therapy was applied to prevent shortening of the tendons.

3.5.6. Survival and migration analysis of transplanted stem cells (USSC)

To confirm survival and migration of the transplanted USSC a short-term study of 5 days post injury (dpi) was performed. Adult female Wistar rats received a complete transection at the thoracic level Th8/9 followed by mMS implantation and USSC transplantation as described above. All rats were immunosuppressed for the entire survival time. For the confirmation of survival and migration of the stem cells the spinal cord tissue was embedded, sectioned, and immunostained with the human nuclei antibody (see 3.7 Immunohistochemistry).

3.5.7. Combinatorial treatment

The combinatorial treatment of mMS implantation and USSC transplantation was applied to achieve a possible synergistic effect. As described above, the mMS was implanted into the lesion gap following a complete transection of the spinal cord at the thoracic level 8/9. Subsequently, the USSC were transplanted rostral and

caudal to the transection via injections. Animals were prepared for transplantation via an immunosuppressive injection one day prior to the stem cell injection.

3.5.8. Postoperative care

Immediately after surgery, the animals received a subcutaneous injection of 2 x 2.5 ml NaCl (0.9 %) at room temperature for rehydration. To ensure the well-being of the animals they were observed until full consciousness was regained. A prophylactical daily oral antibiotic (0.1 ml, Baytril ®, *Bayer Health Care*) was administered for one week (7 days). Further, an analgesic (5 mg / kg, Carprofen ®, *Pfizer GmbH*) was administered at the day of surgery and the following two days. As the bladder function is lost due to the inflicted injury daily manual bladder emptying up to two times a day was performed. Routinely inspections of animals were performed to prevent infections, dehydrations, or injuries. If signs of these abnormalities were present, appropriate veterinary assistance was sought.

3.6. Behavioural analysis

The locomotor behavioural testing and subsequently the analysis were performed in a blinded manner regarding the treatment groups. The locomotor recovery following the complete transection was evaluated with a well-established open-field test. The open-field test was carried out in a 1 m x 1 m plexiglass pool with up to four animals at a time (Fig. 10). The reason for multiple animals inside the pool is a motivational one. Animals could be more motivated to move around when they were in a group. To evaluate the locomotor function of the hind limbs of completely transected animals a modified Basso-Beattie-Bresnahan (mBBB) Locomotor Score [139] was applied (Fig. 11). The analysis with the mBBB score allows the recording of a videotape since toe clearance, which is important in the BBB, is absent in animals with a complete transection. Furthermore, the number of up to four animals in the pool per behavioural test is manageable and was proven to be most effective. Four-minute videos of the animals were recorded weekly for 21 weeks and used for behavioural analysis with the help of a score sheet (Fig. 11). The first thing that was looked at was the movement of the hip, knee, and ankle joints with either “no”, “slight”, or “extensive” movement. Furthermore, the trunk position (left, right, or mid) and the general movement of the left and right hind limb was evaluated. Additionally, alteration and amplitude of the hind limbs had to be observed. Moreover, weight support as well as the plantar foot placement were analysed for occasional, frequent,

and consistent appearance. Although not belonging to the locomotor score, the spasticity in general, its amplitude, and the affected body parts were monitored.

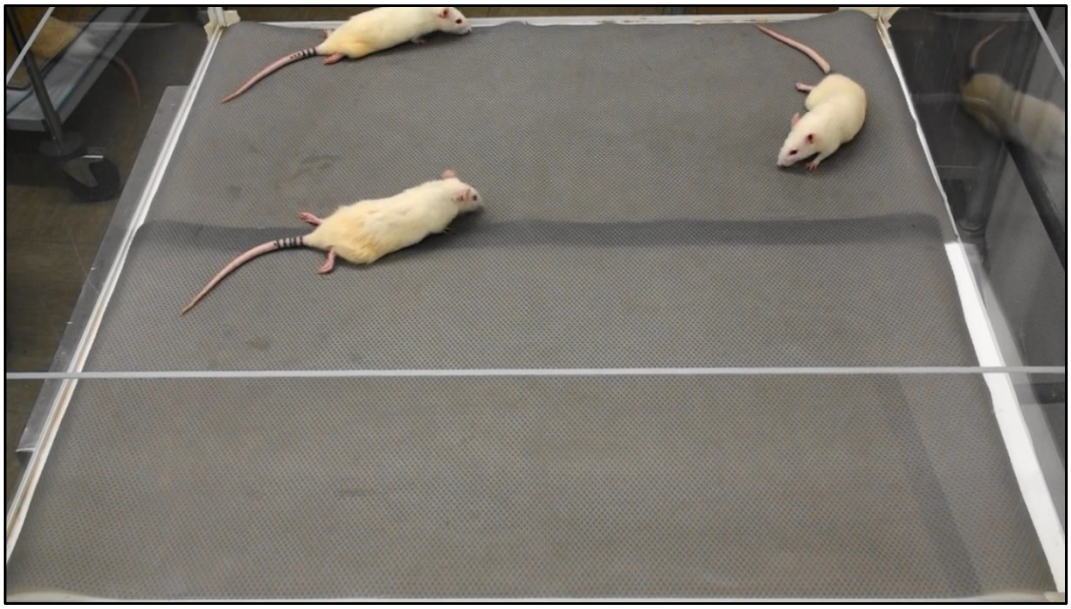

Figure 10: Open field test to evaluate the functional improvement in experimental animals following a spinal cord injury and potential treatments using the mBBB locomotor score.

Tier_____ Datum_____ wpo_____ Scorer _____

Movement						Trunk position		Movement general		rate	R-L Alterations	Amplitude	
Hip		Knee		Ankle				L	R				
L	R	L	R	L	R	L	R	no	no	O	no	L	R
no	no	no	no	no	no	mid		weak limb jerks	weak limb jerks	F	O	weak	weak
S	S	S	S	S	S			yes	yes	C	F	large	large
E	E	E	E	E	E						C		

Videos: ja / nein

weight supp. L	weight supp. R	Plantar paw placement L	Plantar paw placement R	Spasm		
				general	Amplitude	affected body parts
no	no	no	no	no	weak	hind limbs
O	O	O	O	O		tail
F	F	F	F	F	large	toes
C	C	C	C			

Figure 11: mBBB score sheet to assess the locomotor improvement.
wpo = weeks post operation, R = right, L = left, S = slight, E = extensive, O = occasional, F = frequent, C = consistent.

3.7. Tissue collection

The rats were anesthetized with a lethal dose of pentobarbital (2 ml / kg, i.p.) and transcardially perfused for 2 - 3 minutes via the ascending aorta with ~300 ml 0.1 M phosphate buffered saline (PBS), pH 7.4, and, subsequently 14 minutes with 400 – 500 ml of ice-cold fixative (4 % paraformaldehyde (PFA), *Merck*, in 0.2 M PB). Spinal cords were removed from the vertebral columns and postfixed in PFA overnight at 4 °C. The tissue was then cryoprotected in 30 % sucrose (in PBS with 0.01 % sodium azide) for at least one day. For further processing, the tissue must have sunk to the bottom in the 30 % sucrose solution. Free floating parasagittal or horizontal sections (20 – 50µm) were collected of the lower thoracic segments via the freezing microtome (*Microm GmbH*, HM 430, Type K400) in PBS + 0.01 % sodium azide (Th8/9, Th10/11) or the cryostat (*Leica*, CM 3050S) (Th6/7) on microscope slides (Menzel Gläser, Superfrost® Plus, *Thermo Scientific*).

3.8. Immunohistochemistry (IHC)

For the immunohistochemical stainings the free-floating tissue sections were washed in PBS (3 x 10 min) and then incubated in a blocking solution (5 % Donkey Serum, Sigma, in PBS or PBS / 0.03 % Triton) for 1 ½ hours at room temperature. Subsequently, the first antibodies were diluted in their respective concentrations in either PBS or PBS / 0.1 % Triton and then incubated overnight at 4 °C. The antibodies used were rabbit polyclonal anti-5-hydroxytryptamine (5-HT, 1:40, SE100, *Biologo*), rabbit polyclonal anti-Tyrosine Hydroxylase (TH, 1:750, ab112, *Abcam*), rabbit polyclonal anti-von Willebrand Faktor (v.W.F., 1:1000, A008202, *DAKO*), mouse monoclonal anti-Glial Fibrillary Acidic Protein (GFAP, 1:1000, MAB3402, *Merck Millipore*), mouse monoclonal anti-Neurofilament Marker (PAM, 1:1000, 837904, *Biolegend*), guinea pig polyclonal anti-Synaptophysin 1 (1:500, 101004, *Synaptic Systems*), rabbit polyclonal anti-Synaptophysin (1:500, ab9272, *Merck Millipore*), guinea pig anti-Fluorogold (FG, 1:500, NM-101 FluGgp, *Protos Biotech Corp*), and chicken polyclonal anti- Neuronal Nuclear (NeuN, 1:500, ABN91, *Merck Millipore*). After washing the tissue (3 x 10 min) the secondary antibodies were applied in their respective concentrations for 1 - 4 hours at room temperature (see 3.1.3. Secondary antibodies). Another washing step (3 x 10 min) was needed before the tissue was first treated with 70 % alcohol (5 min) followed by Sudan Black (7 min) at room temperature to reduce the background fluorescence. Dried tissue sections

were mounted on glass slides with Immu-Mount, then microscoped and imaged at either the fluorescence microscope (BZ-8000K, *Keyence*) or the confocal Laser Scanning Microscope (cLSM 510, *Zeiss*).

The survival and migration of the stem cells (USSC) were confirmed with the mouse monoclonal anti-human Nuclei (hNuc, 1:500, MAB1281, *Merck Millipore*). For this staining the tissue was first embedded in gelatine (10 % gelatine, *Difco*, in 0.1 M PB and 0.1 % sodium azide) (Table 4) and then parasagittally sectioned with the freezing microtome (50µm). An antigen-retrieval with proteinase type XXIV (see table 5), which was pre-heated at 37°C for about 10 min, was applied to the sections and incubated for five minutes at room temperature. To stop the proteinase reaction the tissue was washed with PBS for 3 x 5 min at RT. The blocking procedure was performed with normal goat serum (NGS) and antibody procedures were the same as above.

The orientation of the tissue sections is seen in Fig. 12.

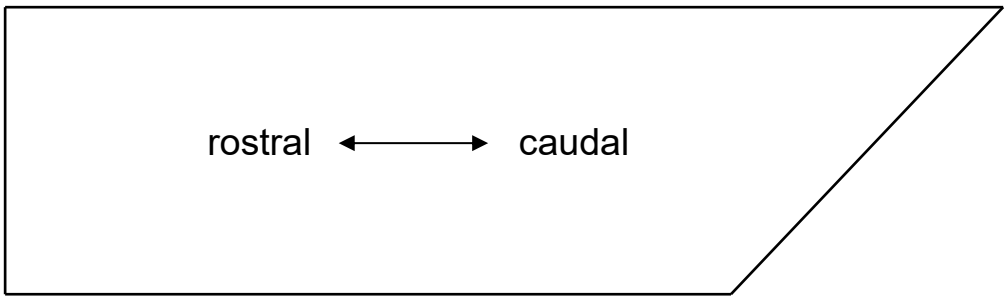

Figure 12: Tissue section orientation.
All sections were mounted with an orientation of the rostral side to the left and the caudal part to the right. The caudal part is marked by the pointed end.

Table 4: Gelatine embedding protocol.

Gelatine embedding
• 30 % sucrose (in 0.1 M PB with 0.01 % sodium azide) overnight at 4 °C
• Transferred to 10 % gelatine (*Difco*) and kept at 37 °C overnight   ○ Gelatine dissolved in 0.1 M PB with 0.1 % sodium azide under heat (not over 60 °C) and stored at 37 °C up to two days
• A base of gelatine was poured into the mold and tissue was placed on cooled gelatine block
• tissue was carefully covered with gelatine and cooled at room temperature for ~30 min (align spinal cord in correct position)
• Mold was placed at -20 °C for 2 - 5 min

• Block was carefully removed from the mold, cut in desired size, and put into 4 % PFA overnight at 4 °C
• Transferred in 30 % sucrose (in 0.1 M PB with 0.01 % sodium azide) overnight at 4 °C before sectioning

Table 5: Antigen-retrieval with proteinase type XXIV

Antigen-retrieval – proteinase type XXIV
Concentration: 9 U / mg = 1.9 mg / 5 ml 20 mM Tris
warm up proteinase up to 37 °C
add 1 ml proteinase to each well
incubate for 5 min at RT
stop reaction by washing 3 x 5’ PBS

3.9. Histochemistry (HC)

After retrieval (see 3.7) the Th8/9 spinal cord tissue was embedded in paraffin (see Table 6) and cut into parasagittal sectioned with the microtome (20 µm). Before staining, the tissue sections needed to be dried at 55 °C for 10 h. For the Masson’s trichrome staining the slides were deparaffinised before incubated in the three different solutions (see Table 7).

Table 6: Paraffin embedding protocol.

Paraffin embedding		
• Dehydration	**70 % EtOH**	**30 min**
	90 % EtOH	**60 min**
	100 % EtOH	**60 min**
	100 % EtOH	**60 min**
	100 % EtOH	**60 min**
	Methyl benzoate	**O/N**
• Glass vial was filled with 1 ml benzene and towel dry spinal cord was transferred into benzene. Spinal cord was incubated for 15 min at RT. (Exact time needed to be complied as benzene acts highly dehydrating.)		
• Glass vial was filled up to 10 ml with paraffin (56 °C) and incubated at 60 °C for 30 min. (Exact time needed to be complied as benzene acts highly dehydrating.)		

• Benzene-paraffin mixture was discharged, vial was filled with pure paraffin (10 ml), and incubated at 60 °C for 60 min.
• Paraffin was exchanged two more times with the same incubation time.
• One more paraffin exchange to let it incubate overnight.
• Bottom of rubber box was filled with paraffin, spinal cord was placed into mold, filled up with paraffin, and aligned into parasagittal position.
• Bock was cooled at RT for 30 min without moving. Stored in the fridge overnight before further processing.

Table 7: Masson's trichrome staining protocol for paraffin embedded tissue.

Masson's trichrome staining		
• Deparaffinisation	**Rotihistol I**	**10 min**
	Rotihistol II	**10 min**
	Rotihistol III	**10 min**
	100 % EtOH I	**5 min**
	100 % EtOH II	**5 min**
	100 % EtOH III	**5 min**
	90 % EtOH	**5 min**
	70 % EtOH	**5 min**
	50 % EtOH	**5 min**
	aq. dest.	**5 min**
• Solution A		**10 min**
• Wash in aq. dest.		**5 min**
• Solution B		**10 min**
• Wash in aq. dest.		**5 min**
• Solution C		**10 min**
• Wash in aq. dest.		**5 min**
• Dehydration	**50 % EtOH**	**1 min**
	70 % EtOH	**1 min**
	90 % EtOH	**1 min**
	100 % EtOH I	**1 min**
	100 % EtOH II	**1 min**
	Rotihistol I	**3 min**

	Rotihistol II	**3 min**
• Mounting with DPX		

3.10. Analysis and documentation

3.10.1. Final animal numbers

As an increased number of anaesthesia application leads to an increased risk of a fatal surgery outcome, the sum of animals applicable for behavioural and histological analysis in the long-term study decreased from the initial 15 per group. Furthermore, premature death due to infection or autotomy also reduced animal numbers (Table 8).

Table 8: Actual number of animals per group in the long-term study for histological analysis

Treatment/ Therapy	**Treatment Group Name**	**Animal # / Group**	**Final Animal # / Group** (cyst analysis)	**Final Animal # / Group** (axonal stainings)
Tx + mMS + USSC	Combination	15	9	5
Tx + mMS	mMS	15	11	6
Tx + USSC	USSC	15	12	8
Tx only	Control	15	8	6

3.10.2. Blinding procedure

Animals have been assigned to a treatment group dependent on the surgery procedure including combination, mMS, USSC, and control. Following the postoperative care, a third person allocated new random tail numbers to the animals to blind the analysis. This key has been kept secret until the behavioural and histochemical-/immunohistochemical stainings were finished. This study is therefore considered a double-blinded study.

3.11. Histological evaluation

3.11.1. Cyst analysis

The size of the cyst was calculated to compare the cavity formation between the groups. For an optimal comparison a region of interest (ROI) was defined with a total length of 8 mm. It was measured 4 mm rostral and caudal from the lesion centre (Fig. 13, white lined box). To calculate the cyst area the scale was set by measuring the

scale bar of the corresponding image with imageJ (*Fiji*, freeware, image editing software). The area of the cysts was quantified by marking the borders of all cysts inside the ROI (Fig. 13, green lined area). The sum of the cysts was then put into relation to the tissue enclosed in the ROI (Fig. 13, yellow lined area; Table 9). Five tissue slides per animal were analysed. For the localisation of the cyst, either rostral or caudal to the lesion, it should be kept in mind that in some animals cavities were present rostral as well as caudal. Therefore, the side (rostral or caudal to the lesion) with the largest cyst areas was determined to detect a possible prevalence of the cavity for their location.

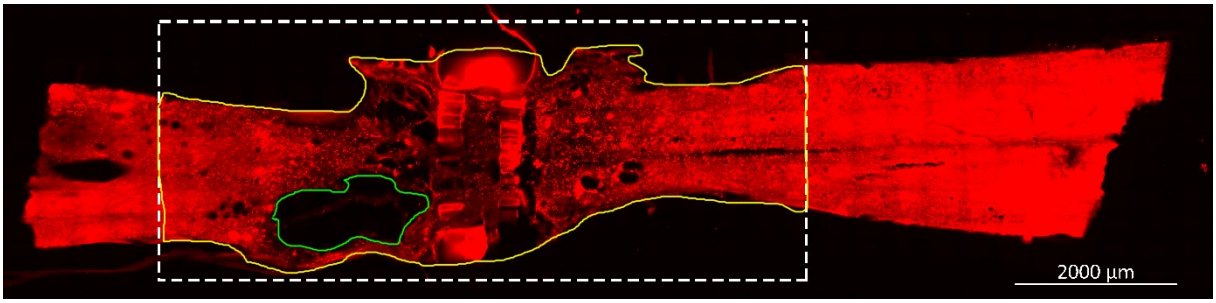

Figure 13: Analysis of cystic cavities following SCI.
Five horizontal 50 µm thick spinal cord tissue sections were analysed for cysts next to the lesion site. The region of interest (ROI, white lined box) was defined with a total length of 8 mm. It was measured 4 mm rostral and caudal from the lesion centre. The cyst area (green) was then calculated and put in to relation to the total tissue area (yellow) enclosed in the ROI.

Table 9: Calculation of cyst area in relation to the total tissue size inside the ROI.
The size of the scale bar was measured in pixel/µm and was then used to determine the cyst area in μm^2 as well as the total tissue size in μm^2. The percentage of the cyst area was then computed by using these numbers.

Animal	Cyst Area Pixel/μm^2	Scale bar (Pixel/µm)	Cyst Area μm^2	Total Tissue Size Pixel/μm^2	Total Tissue Size μm^2	Cyst Area in %	Mean Value (out of 5) %
H68-1	764713,595	2,096	364844,27	20818077,24	9932288,76	3,67	
H68-2	886593,329	2,096	422993,00	20301759,58	9685954,00	4,37	
H68-3	826380,632	2,088	395776,16	20323482,53	9733468,64	4,07	3,82
H68-4	602587,055	1,494	403338,06	20487376,1	13713103,15	2,94	
H68-5	815337,168	2,097	388811,24	20024537,4	9549135,62	4,07	

3.11.2. Quantification of 5-HT- and TH-positive axon profiles

To analyse the number of 5-HT- and TH-positive axon profiles in the lesion area as well as caudal to the lesion (up to 8 mm) three 50 µm thick horizontal sections of the spinal cord of analogous regions were stained for each of these two neurotransmitters in each animal. The quantification was performed by counting the

5-HT- and TH-positive axon profiles under the Nikon Diaphot 300 with the 20x-objective. As the background noise is relatively high, the counting was done manually. If the identification was ambiguous, the 40x-ojective was used for validation. The staining of 5-HT and TH axons appear in a shape of “beads on a string” (Fig. 14). To distinctively identify 5-HT and TH axons at least three “beads on a string” (= axonal profiles with neurotransmitter-filled vesicles) had to be present to be counted.

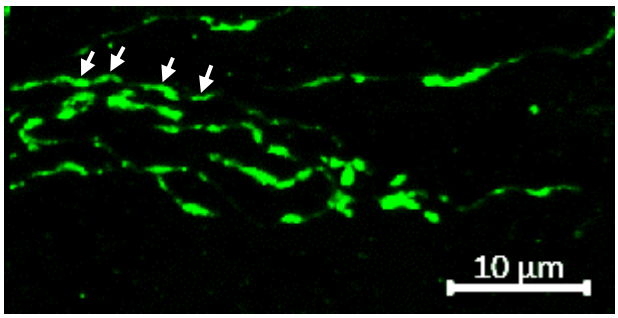

Figure 14: Appearance of 5-HT staining in the spinal cord tissue.
In a horizontal 50 µm thick tissue section of the spinal cord 5-HT appears as beads on a string (arrows).

3.11.3. Analysis of angiogenesis

The formation of new blood vessels (angiogenesis) inside the lesion area was evaluated qualitatively (Fig. 15).

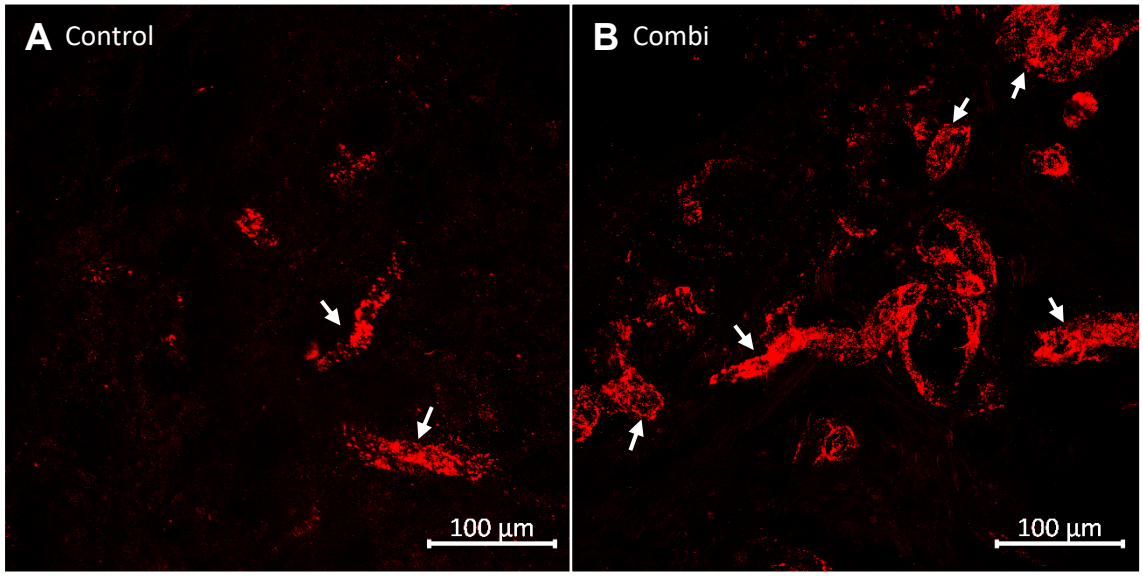

Figure 15: Angiogenesis in the lesion area following SCI.
(A) Lesion area of a control animal with a low amount of new formed blood vessels (white arrows). (B) Lesion area of a combinatorial animal with a high amount of new formed blood vessels (white arrows).

3.11.4. Statistics

All statistics were performed with SPSS Statistics 17.0. Depending on the normality of the evaluated data, calculated with the Shapiro-Wilk test, either the Kruskal-Wallis or the One-Way ANOVA test was used for all axon profile numbers, cavity formation, and functional recovery, i.e., over all different experimental groups in total. The one-sided Mann-Whitney U-test was applied for paired comparison including a Holm-Bonferroni correction for multiple testing with the type I error rate $\alpha = 0.05$ as a post hoc test. The paired comparisons were performed to test for significant elevation in axon profiles, cystic cavity, and locomotor recovery of treated with control animals. The experimental groups were considered significantly different at $p \leq 0.05$. All data are presented as mean ± SEM. Correlation analysis were performed with the Spearman's rank correlation coefficient to identify any statistical dependence between the rankings of two variables.

4. Results

4.1. Migration of stem cells into the injured spinal cord and the mMS lumen

The migration of USSC in a model of complete transection of the spinal cord, including the mMS implantation, was investigated. Therefore, a 5-day study was performed and the tissue was stained with hNuc, labelling human nuclei, to explicitly identify these human stem cells. Five days after the transplantation (5 dpo), the cells were detected rostral and caudal to the lesion (Fig. 16, A + B) Furthermore, adjacent to the lesion site the cells were orientated alongside the central canal and thereafter migrated into the lesion zone and the mMS lumen (Fig. 16, C - G). USSC were detectable under the treatment of immunosuppressive drugs but were untraceable after withdrawal of the immunosuppressant [100]. In conclusion, within five days USSC survived the transplantation and migrated from the injection site towards the injury site under the treatment of immunosuppressive drugs.

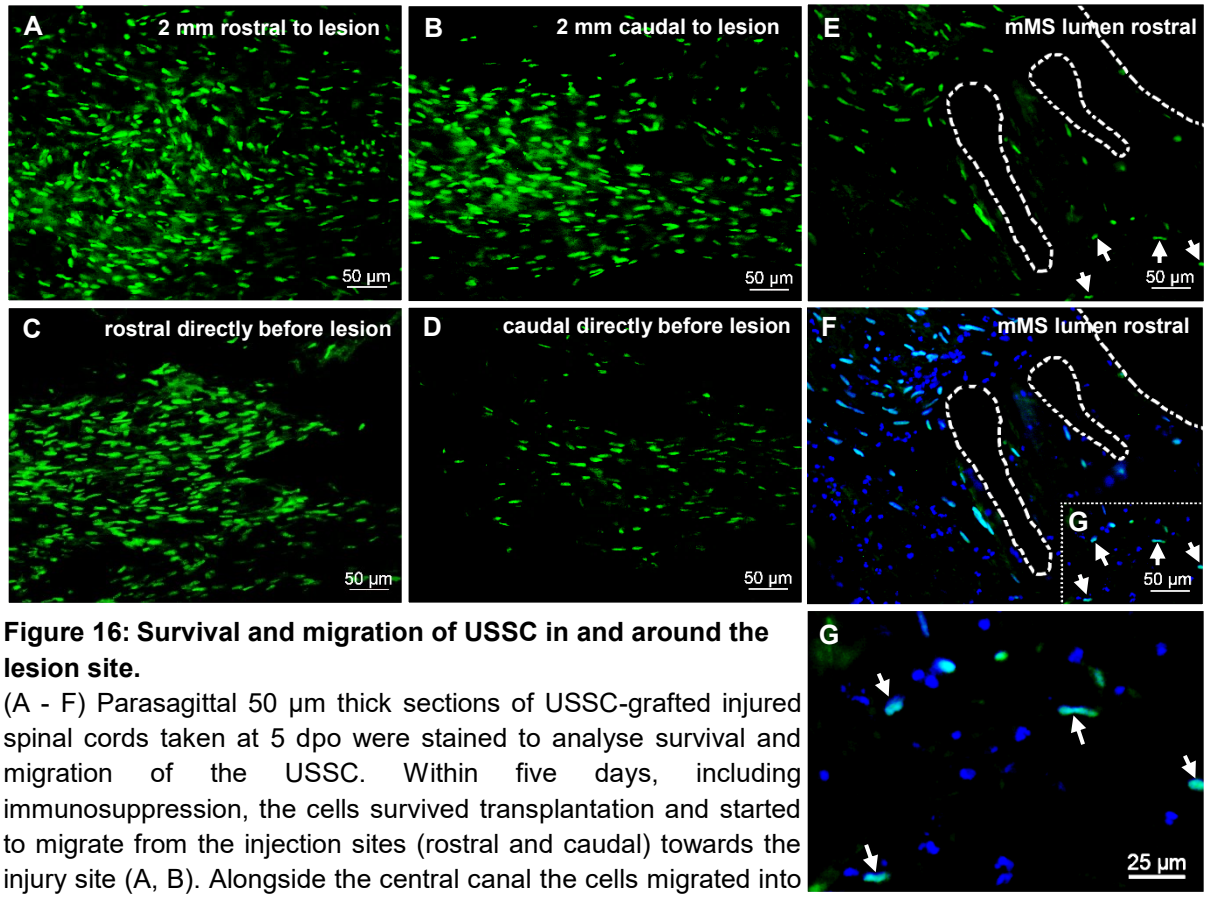

Figure 16: Survival and migration of USSC in and around the lesion site.
(A - F) Parasagittal 50 µm thick sections of USSC-grafted injured spinal cords taken at 5 dpo were stained to analyse survival and migration of the USSC. Within five days, including immunosuppression, the cells survived transplantation and started to migrate from the injection sites (rostral and caudal) towards the injury site (A, B). Alongside the central canal the cells migrated into the lesion zone (C + D). (E - G) In mMS-grafted animals, the USSC migrated into the microconnector lumen. The white dotted lines mark the honeycomb walls of the mMS and the white arrows label USSC inside the lumen. Magnification of the mMS lumen (white dotted box in F) shows USSC (green) in an overlay with DAPI (blue).

4.2. Cyst formation following spinal cord injury with or without treatment

4.2.1. General tissue formation

To evaluate the tissue formation in the mMS, a trichrome staining on 20 µm parasagittal, paraffin sections (see 3.9, Table 7) was performed on combinatorial animals that died two weeks post operation. It was observed that some mMS implants were tilted, however, the majority was aligned perpendicularly (Fig. 17). The tissue preparation revealed some difficulties: when sectioning the tissue with the freezing microtome small pieces of the mMS broke out of the tissue. Moreover, in some cases parts of the mMS were washed out of the free-floating sections during the staining process. However, in general the mMS lumen became completely filled with tissue (Fig. 17). The red in the trichrome staining in the mMS lumen represents the newly developed tissue, which offers an environment for axon regeneration.

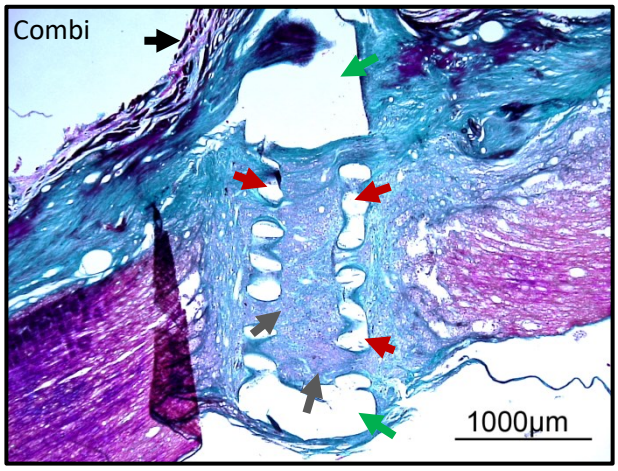

Figure 17: Tissue formation in the mMS. Trichrome staining of a 20 µm parasagittal paraffin tissue section showed tissue formation inside the mMS lumen two weeks post injury (red/purple, grey arrows). Fibrin, erythrocytes, and cytoplasm are stained in red/purple. Collagen, which is a major component of the scar, is seen in green. Furthermore, the mMS implant was aligned perpendicularly in the majority of animals. At the dorsal part of the tissue section, a callus (area of thickened and hardened tissue at the injury due to friction) was formed (black arrow). The smaller rectangular shaped holes (red arrows) represent the honeycomb walls of the mMS whereas the bigger ones (green arrows) are caused by the tubing system. The fold on the left side of the section is an artefact from the mounting procedure.

Big cavities were observed when sectioning the tissue (Fig. 18). Further quantification was performed regarding the total cyst area and the localisation of the majority of cysts (rostral or caudal).

4.2.2. Occurrence of cavities rostral and caudal to the lesion

To identify the distribution of the cystic cavities found in the tissue, a region of interest was determined (see 3.11.1., Fig. 18, white dotted rectangle). The total size of all cavities found either rostral or caudal from the lesion was estimated by visual judgement and the larger number determined the distribution of the cavities in either the rostral or caudal part (Fig. 18). For this quantification, five sections per animal

were analysed and the cyst location was defined to either the rostral or the caudal site to the lesion. An animal that showed a cyst majority in the caudal part in 4 out of 5 sections was assigned to the caudal part and vice versa. The short-term study only comprised four animals per group and therefore the number of animals to analyse the cyst distribution does not exceed 16, whereas the number of animals in the long-term study is 40. In the short-term study (5 wpo), the majority of cysts independent of the treatment group was found caudal to the lesion (Fig. 19, A). When looking at the treatment groups individually the quantification of the cyst distribution shows the majority in the caudal part in each group (Fig. 19, B). In contrast, the majority of cavities found in the spinal cord in the long-term study (21 wpo) were mostly located rostral to the lesion, which was also seen in the individual groups (Fig. 19, C + D).

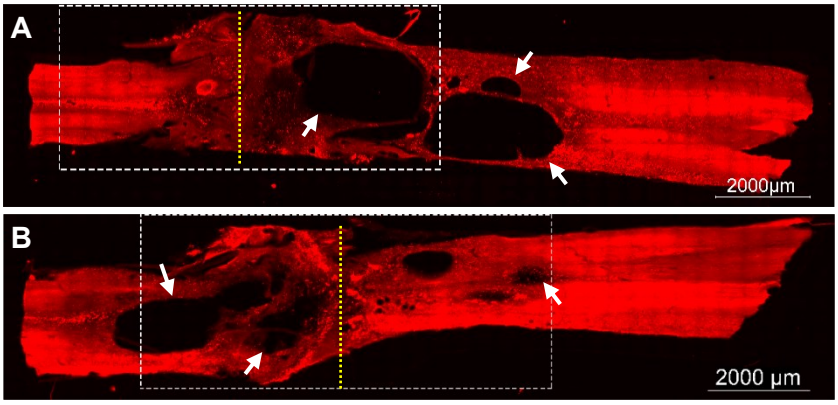

Figure 18: Cyst occurrence – rostral or caudal to lesion.
(A-B) Example images to demonstrate the size of cysts to detect their distribution. (A) In this horizontal, 50 µm thick section the cavities (white arrows) were found caudal to the lesion centre (yellow dotted, vertical line). (B) Although some smaller cysts were detected caudal to the lesion (yellow dotted, vertical line) here, the total size of cysts (white arrows) in the rostral part is greater and therefore predominantly located rostral to the lesion. The red signal of the images is the autofluorescence of the tissue itself.

4.2.3. Size of the cyst area differs between treatments

To assess the efficacy of the combinatorial treatment to spare tissue and therefore reduce cavity formations after a complete transection the total area of cysts in relation to the total tissue size inside the ROI was measured (Fig. 20). As described in chapter 3.11.1. the cyst area is calculated in percentage (%) for the short- (5 wpo) as well as for the long-term (21 wpo) study. In both experiments, the smallest cyst area could be found in the combinatorial treatment (5 wpo: 2.11 %, 21 wpo: 1.48 %), followed by the mMS (5 wpo: 2.7 %, 21 wpo: 3.83 %) and USSC (5 wpo: 3.37 %, 21 wpo: 7.6 %) treatment, respectively. Furthermore, the control group exhibits the largest area of cavities (5 wpo: 6.77 %, 21 wpo: 16.78 %) (Fig. 21).

Whereas the short-term study only showed a trend of the control group having the largest cystic cavities, the long-term study displays a significant difference between the combinatorial and control group ($p = 0.000004$) as well as the mMS and control group ($p = 0.000198$), confirming that the Tx-control group exhibits the largest cavity area. Moreover, the combinatorial treatment leads to further reduction of cavities compared to the individual treatments indicating a synergistic effect of the mMS implant and the transplanted USSC on cyst formation.

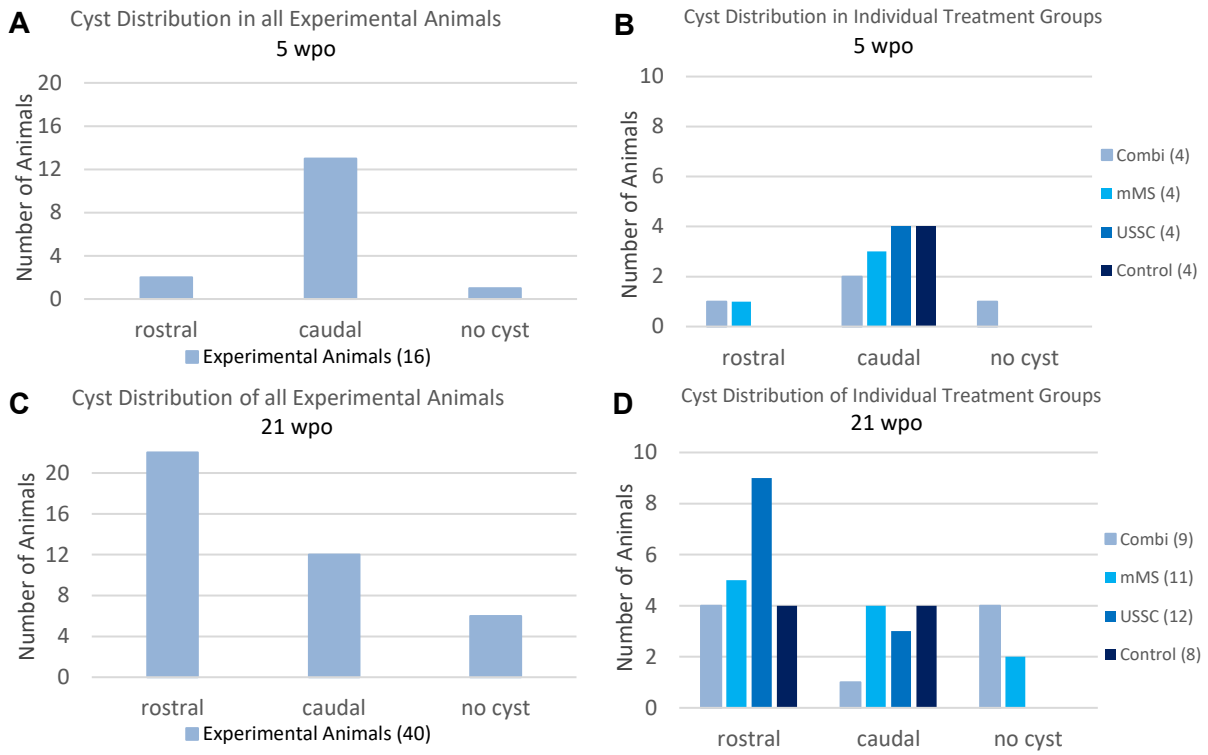

Figure 19: Cyst distribution in experimental animals – rostral or caudal to the lesion.
Five horizontal 50 µm thick sections per animal were analysed to determine the cyst distribution. (A) In the short-term study (5 wpo), the majority of cysts were found caudal to the lesion. Only a small amount was observed rostral to the lesion and some animal did not have any cysts at all. (B) The majority of cavities in the individual treatment groups were also detected in the caudal part and do not show any inconsistency with the overall distribution. (C) In the long-term study (21 wpo), cysts were seen mostly in the rostral part of the spinal cord. (D) The individual treatment groups show a larger variability of distribution of the cavities. However, the majority is still observed in the rostral part in all treatment groups.

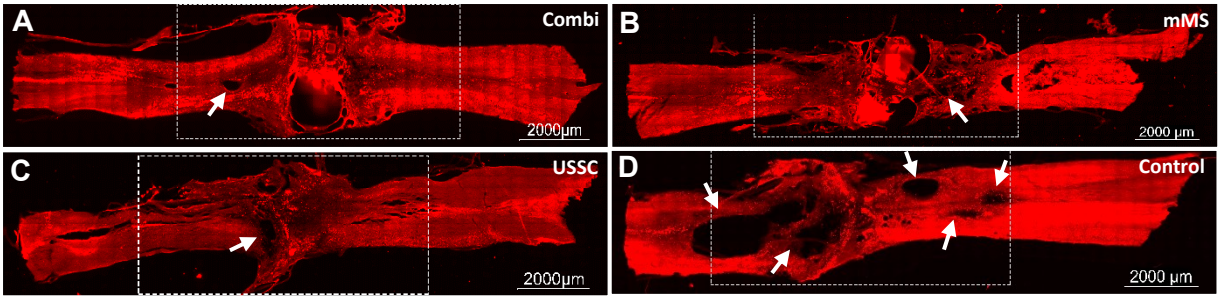

Figure 20: Cavity formation after SCI.
Example images of horizontal 50 µm thick spinal cord tissue sections for representation of cysts found next to the lesion area. The combinatorial group (A) only showed small cavities, whereas the individual treatment groups, mMS (B) and USSC (C), already displayed greater cyst sizes. However, the largest cavities were detected in the control group (D). Cysts are marked by white arrows.

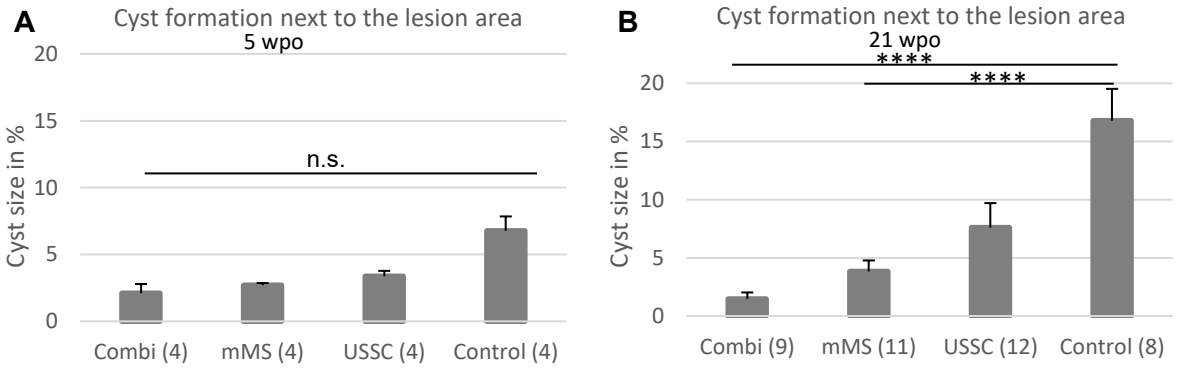

Figure 21: Cavity formation differs between groups following complete SCI.
Five horizontal 50 µm thick sections per animal were investigated to analyse the cavity formation. (A) In the short-term experiment, the largest cavities were observed in the control group, whereas the combinatorial, mMS, and USSC treatment groups displayed a smaller cyst size, respectively. However, no significant (n.s.) differences were detected between the groups. (B) The same observation was made for the long-term study. Moreover, a significant difference of the cyst size was detected between the control and the combinatorial ($p = 0.000004$) and mMS ($p = 0.000198$) treatment.

Statistics: One-Way ANOVA, with Bonferroni Correction. *$p \leq 0.05$, **$p \leq 0.01$, ***$p \leq 0.001$, ****$p \leq 0.0001$. Results are shown as mean ± SEM.

4.3. Angiogenesis in the lesion site following treatment

Angiogenesis in the damaged spinal cord tissue and thus the facilitated transport of molecules and nutrients supporting regeneration constitutes an important aspect in this event [140]. To analyse the formation of new blood vessels in the lesion site, horizontal 50 µm thick spinal cord tissue sections were stained with the marker “von Willebrand Faktor”. Blood vessels were identified in the lesion area in all four groups independent of the treatment or time point (5 wpo, 21 wpo) (Fig. 22, A - H).

However, in the long-term study, more blood vessels were detected in animals with an mMS implant than in the USSC and control group (Fig. 22, I).

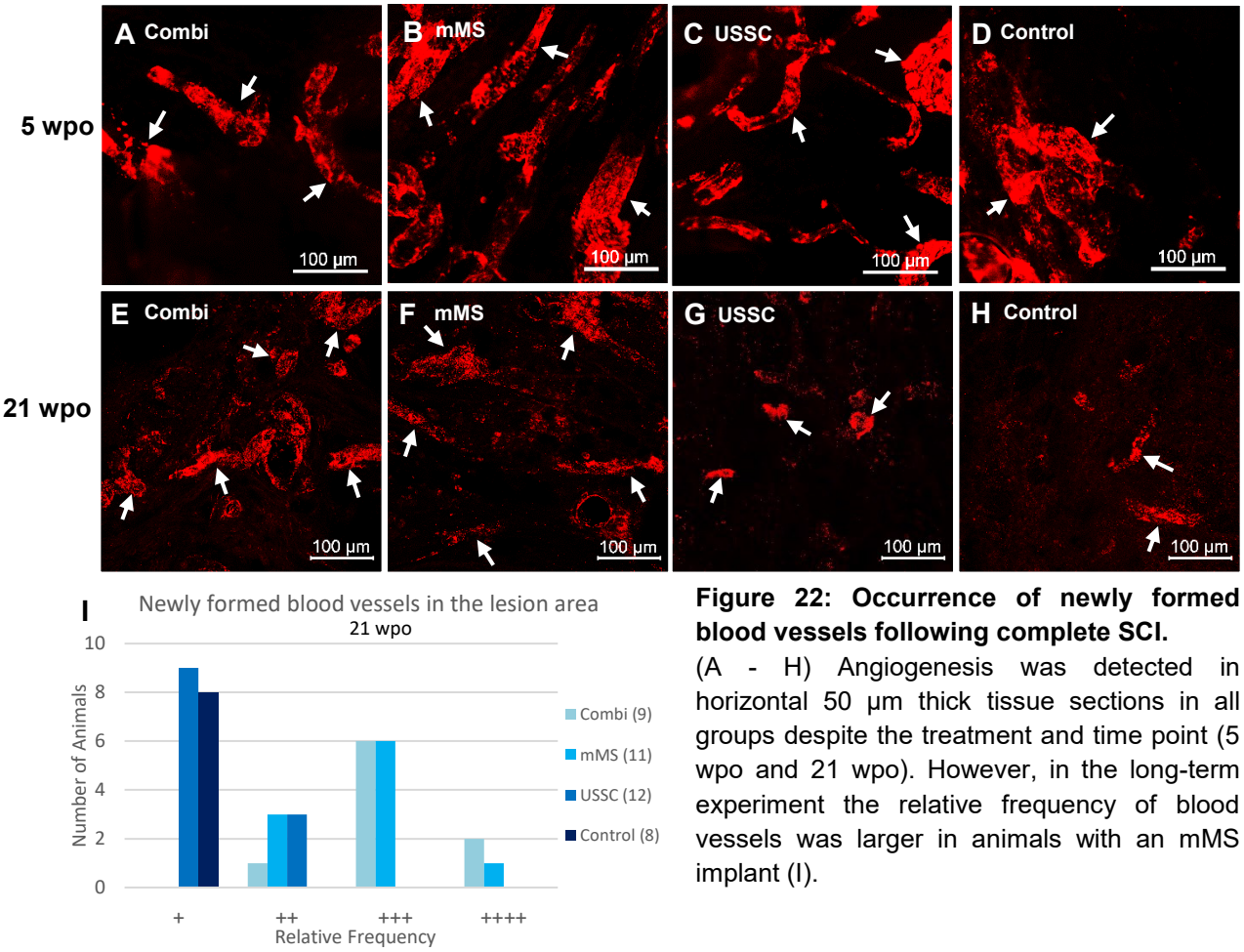

Figure 22: Occurrence of newly formed blood vessels following complete SCI.
(A - H) Angiogenesis was detected in horizontal 50 µm thick tissue sections in all groups despite the treatment and time point (5 wpo and 21 wpo). However, in the long-term experiment the relative frequency of blood vessels was larger in animals with an mMS implant (I).

4.4. Axon regeneration and growth into and beyond the lesion

One of the vital elements in spinal cord repair is the regeneration of axons since it has been shown that only a small number of regenerated axons may be sufficient to partially improve locomotor recovery and sensory function [141-143]. A general axonal staining after 5 wpo was performed with the neurofilament marker PAM to obtain an overview of the axonal population in the lesion area (Fig. 23). Furthermore, staining of the serotonergic (5-HT) and catecholaminergic (TH) axons, which are involved in motor function, showed regeneration to some extent into the mMS lumen as well as caudal to the lesion of combinatorial and mMS treated animals. For the quantification, axon profiles (5-HT, TH) were counted manually because of the relative high background noise. The quantitative analysis of the axon profiles of the neurotransmitter 5-HT and TH was performed on three 50 µm thick, free floating,

horizontal tissue sections per animal under the 20x objective of the Nikon Diaphot 300 fluorescent microscope. Any discrepancies were validated under the 40x objective to identify the single axon profiles. Axon fibres were observed and counted in the lesion area as well as the adjacent caudal part of the lesion. Moreover, only distinctively identified 5-HT- and TH-positive axon profiles were counted.

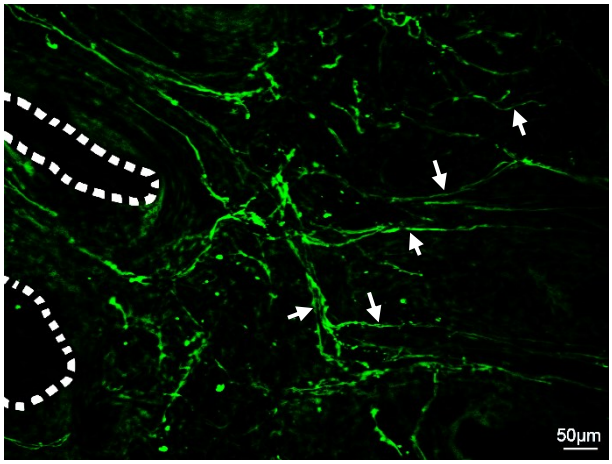

Figure 23: Exemplary general axonal staining (PAM) in the lesion area of an mMS animal
Axonal staining (PAM) of a parasagittal, 50 µm thick tissue section of an mMS animal showing a vast axonal population (white arrows) in the mMS lumen after 5 wpo. White dotted lines represent honeycomb structures.

4.4.1. 5-HT regeneration following therapy

Regeneration of serotonergic (5-HT) axons were analysed at 5 wpo and 21 wpo. Quantification of 5-HT axon profiles in the lesion site after 5 wpo showed a great number of 5-HT fibres in the control group (Fig. 24, D + E). Furthermore, a lower amount of 5-HT was observed in the USSC (C), mMS (B), and combinatorial (A) group, respectively (7 versus 5.75, 4.25, 3.5 average axon profiles). Given that there was no significant difference found between the groups, the enhanced 5-HT axon profiles in the control compared to the other three treatment groups can only be referred to as a trend. The number of 5-HT fibres in the lesion area were only counted in the short-term experiment as the lesion tissue was not greatly preserved in the 21 wpo specimen due to the cutting procedure.

After 21 wpo, 5-HT axon profiles were detected caudal to the lesion up to a distance of 5 mm (Fig. 25, A - D). Comparing the number of 5-HT fibres found between the groups, the greatest amount was seen in the combinatorial treatment with a significant difference to the control group (14.2 versus 2.66 average axon profiles, $p = 0.006$), which displays the lowest number of 5-HT (Fig. 25, E). The mMS and USSC group showed only 2/3 and 1/3 of the amount of 5-HT fibres observed in the combinatorial group, respectively (9.72, 5.08 vs. 14.2 average axon profiles). In

contrast, no 5-HT fibres were detected caudal to the lesion after 5 wpo independent of the treatment.

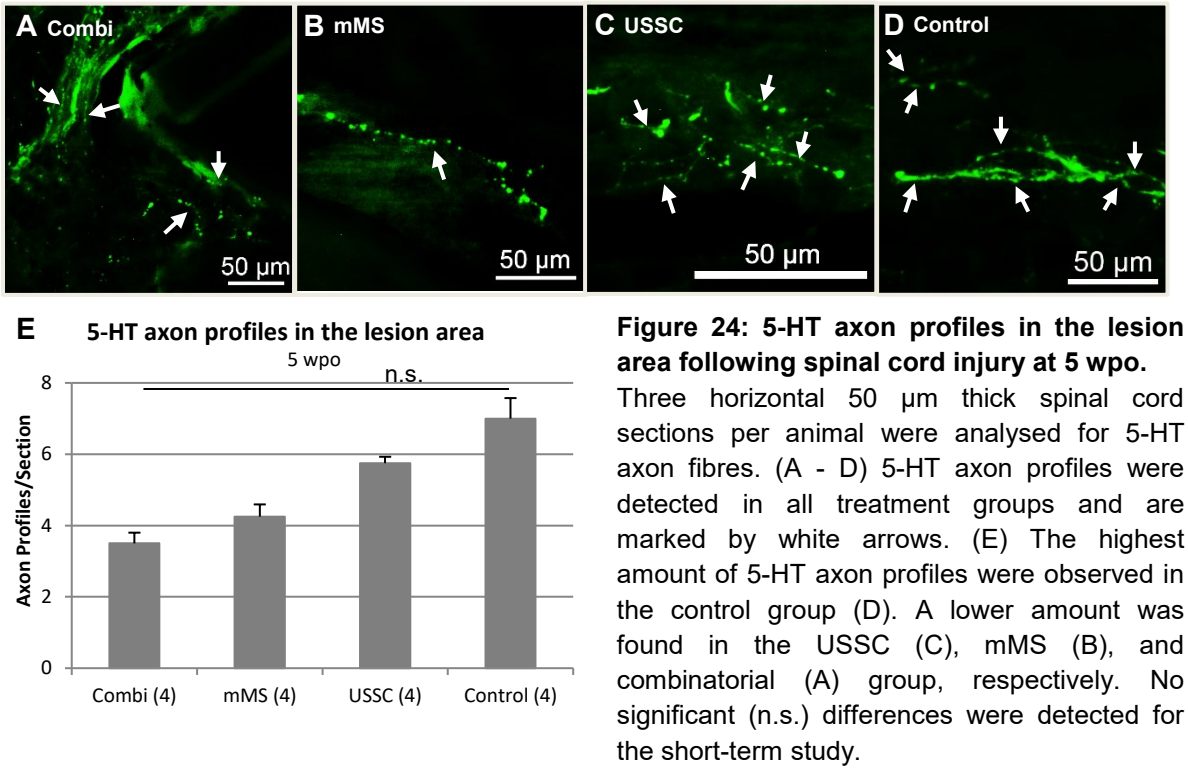

Figure 24: 5-HT axon profiles in the lesion area following spinal cord injury at 5 wpo. Three horizontal 50 µm thick spinal cord sections per animal were analysed for 5-HT axon fibres. (A - D) 5-HT axon profiles were detected in all treatment groups and are marked by white arrows. (E) The highest amount of 5-HT axon profiles were observed in the control group (D). A lower amount was found in the USSC (C), mMS (B), and combinatorial (A) group, respectively. No significant (n.s.) differences were detected for the short-term study.

Statistics: Kruskal-Wallis with Bonferroni Correction. Results are shown as mean ± SEM.

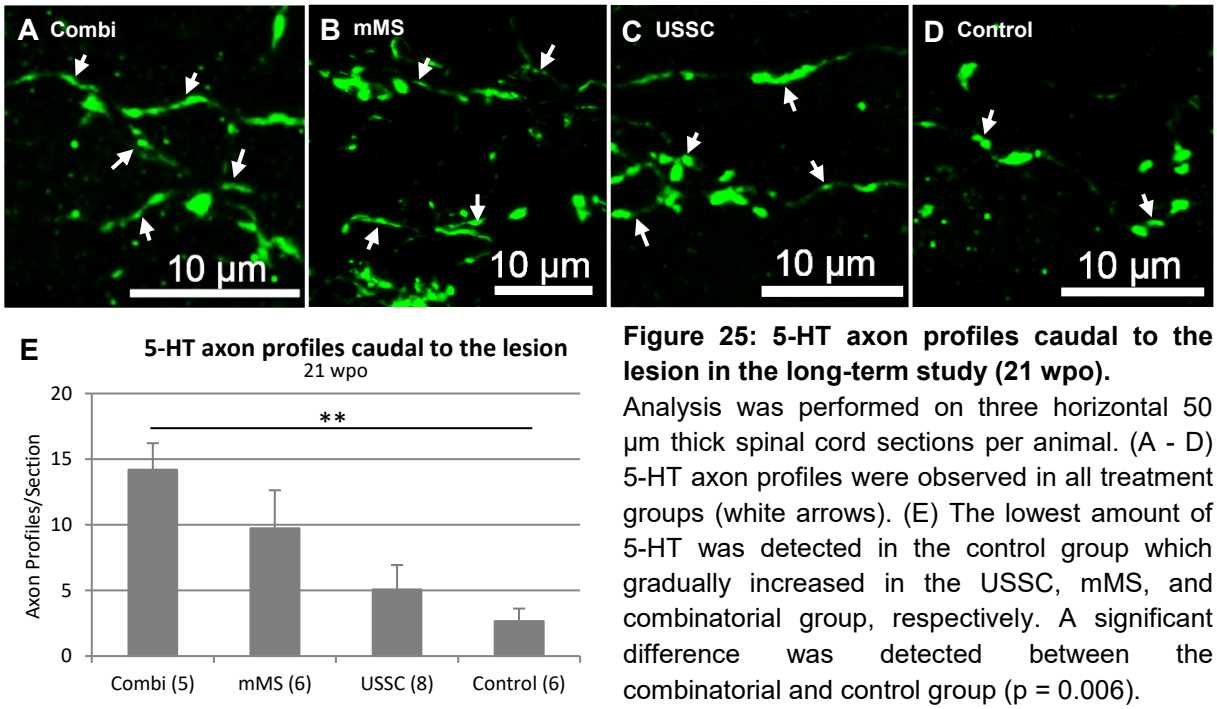

Figure 25: 5-HT axon profiles caudal to the lesion in the long-term study (21 wpo). Analysis was performed on three horizontal 50 µm thick spinal cord sections per animal. (A - D) 5-HT axon profiles were observed in all treatment groups (white arrows). (E) The lowest amount of 5-HT was detected in the control group which gradually increased in the USSC, mMS, and combinatorial group, respectively. A significant difference was detected between the combinatorial and control group ($p = 0.006$).

Statistics: Kruskal-Wallis with Bonferroni Correction. *$p \leq 0.05$, **$p \leq 0.01$. Results are shown as mean ± SEM.

In Figure 26 A - D the number of 5-HT axon profiles after 21 wpo were counted in various distances to the lesion, starting from 0-1 mm up to 7-8 mm from the lesion centre. This was analysed to get an overview of regenerated 5-HT axons as the probability to include endogenous 5-HT axons increases with greater distance to the lesion. In all three treatment groups, combinatorial (A), mMS (B), and USSC (C), 5-HT axon profiles were seen at all distances (up to 8 mm) from the lesion centre. The control group, however, only showed a small number at few distances (D). As there was almost no 5-HT present in the lesion site in the control, the number of 5-HT caudal to the lesion counted in the control was subtracted from the three treatment groups to obtain the number of regenerated 5-HT axons.

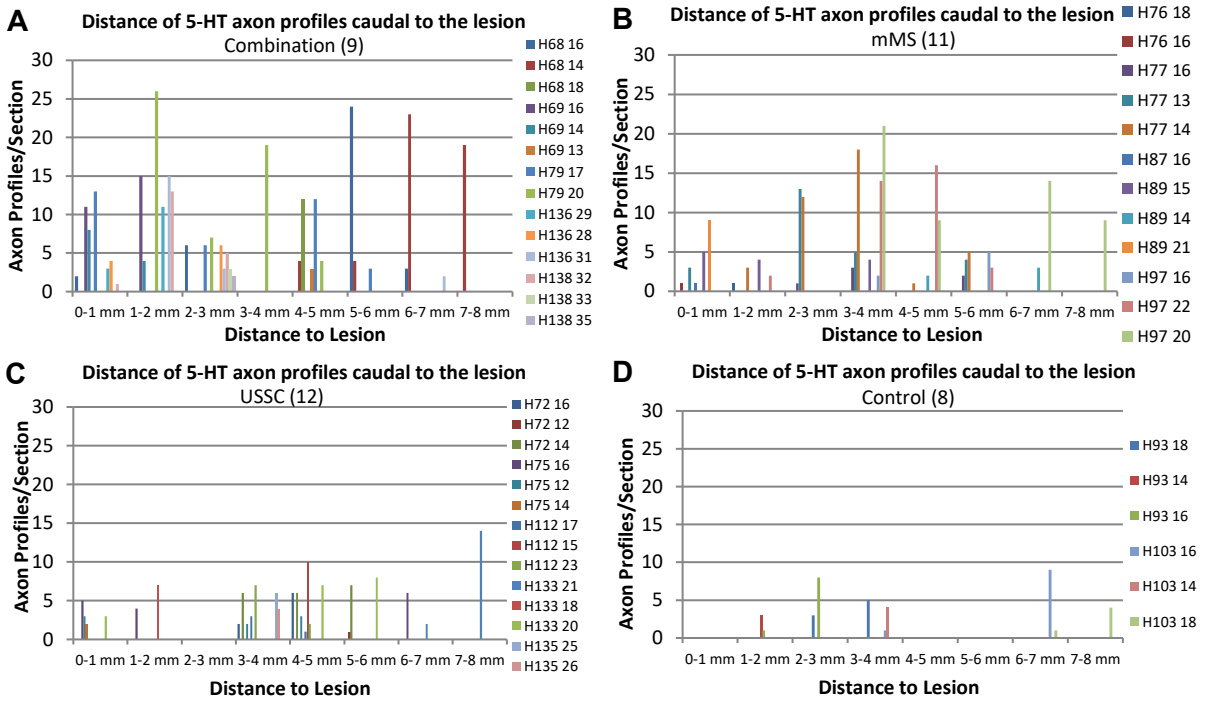

Figure 26: Distance of 5-HT axon profiles caudal to the lesion centre.
Three horizontal 50 µm thick tissue sections of all animals of each group (each colour represents one tissue section) were analysed to calculate the number of 5-HT axon profiles in various distances caudal to the lesion. Only sections where axon profiles were observed are listed. 5-HT fibres were detected at all distances in the combinatorial (A) and mMS (B) group. A lower amount of 5-HT axons was found in the USSC (C) and control (D) groups.

4.4.2. TH axon regeneration after treatment

To quantify the regeneration of TH axons, the TH axon profiles were counted in the lesion site (21 wpo) and caudal to the lesion (5 + 21 wpo). The number of TH fibres in the lesion area were only counted in the long-term experiment, as the lesion tissue was not greatly preserved in the 5 wpo specimen due to the cutting procedure. In the lesion area the highest number of TH axon profiles were observed in the combinatorial group (Fig. 27, A), whereas the number was lower in the mMS (B), USSC (C), and control (D) group (18.87, 11.27, 2.33, 1.73 average axon profiles) (Fig. 27, E). No significant differences were detected between the groups. However, a trend of augmented TH fibres following the combinatorial treatment is observed.

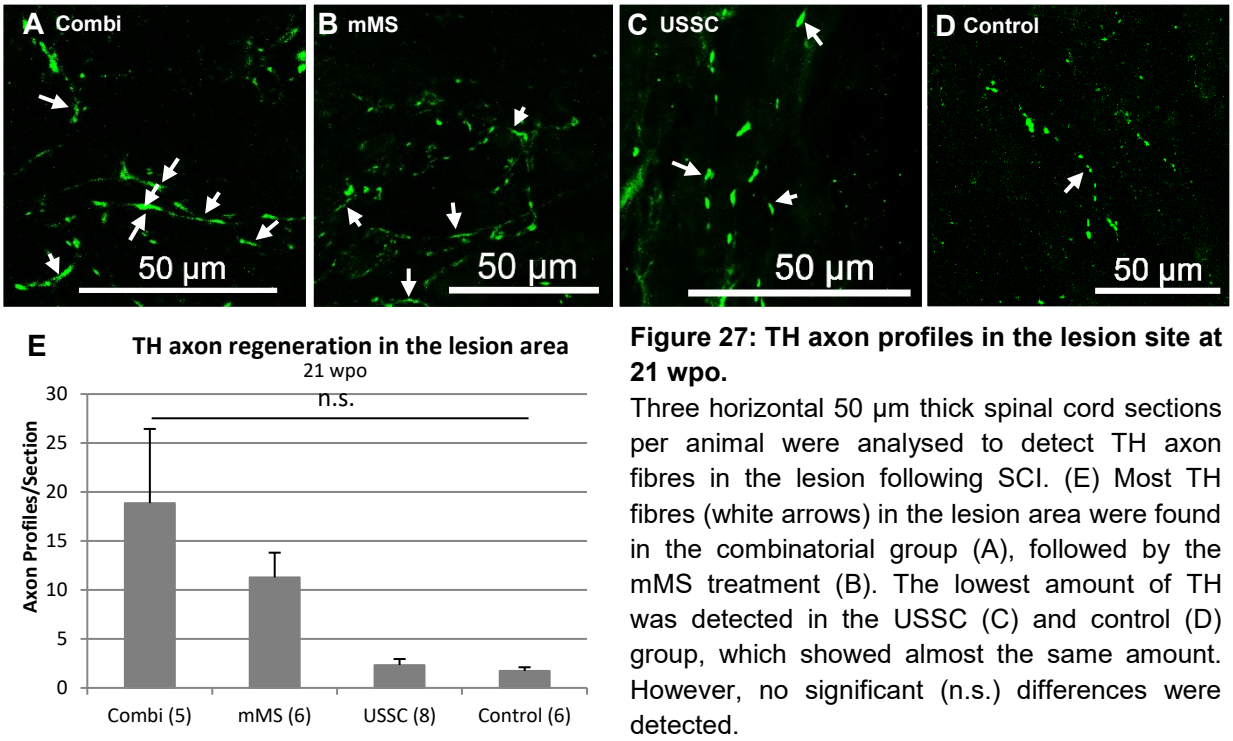

Figure 27: TH axon profiles in the lesion site at 21 wpo.
Three horizontal 50 µm thick spinal cord sections per animal were analysed to detect TH axon fibres in the lesion following SCI. (E) Most TH fibres (white arrows) in the lesion area were found in the combinatorial group (A), followed by the mMS treatment (B). The lowest amount of TH was detected in the USSC (C) and control (D) group, which showed almost the same amount. However, no significant (n.s.) differences were detected.

Statistics: Kruskal-Wallis with Bonferroni Correction. Results are shown as mean ± SEM.

Both time points, 5 and 21 wpo, showed an enhanced growth of TH axons caudal (up to 5mm) to the lesion in the combinatorial group. In the short-term study (Fig. 28, A - D) the amount of TH fibres was similar in the mMS, USSC, and control group (11.6, 10.05, 10.9 average axon profiles). Furthermore, a significant difference between the combinatorial and USSC (18.25 versus 10.05 average axon profiles, $p = 0.006$) as well as the combinatorial and control (18.25 versus 10.9 average axon profiles, $p = 0.015$) group was observed (Fig. 28, I). For the long-term study, the

number of TH axon profiles was highest in the combinatorial group compared to the other three groups while the lowest amount was detected in the control group (17.07 versus 10.61, 5.05, 2.28 average axon profiles) (Fig. 28, E - H, J). The effect of the combinatorial treatment to increase TH axon regrowth, which was significant in the short-term experiment, could also be detected as a trend after 21 wpo.

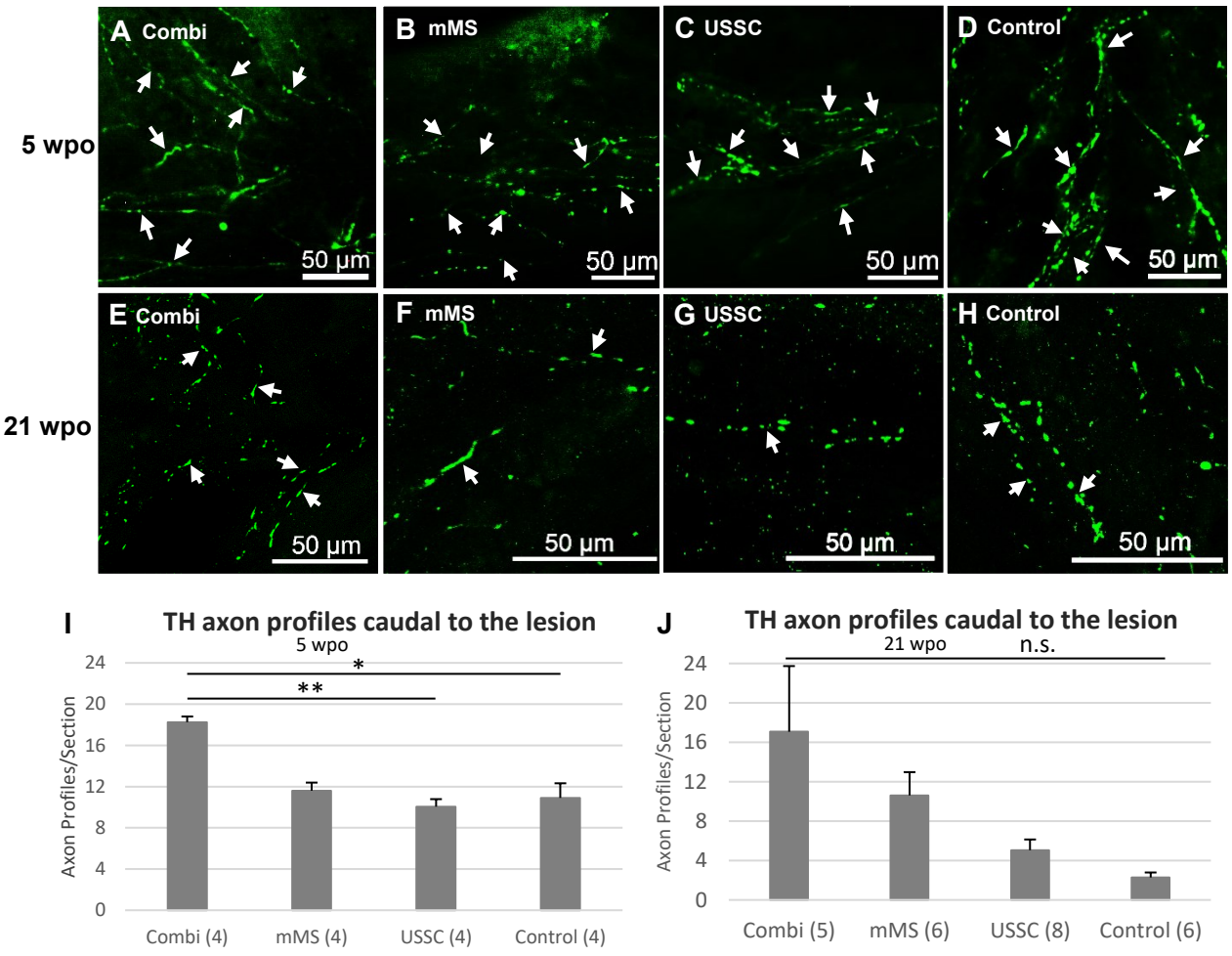

Figure 28: TH axon profiles caudal to the lesion following SCI.
Three horizontal 50 µm thick spinal cord sections per animal were analysed to detect TH axon profiles caudal to the lesion. (A - D) TH fibres were found caudal to the lesion in the short-term study (5 wpo) (white arrows). (E - H) TH axon profiles were also observed caudal to the lesion in the long-term experiment (21 wpo) (white arrows). (I) After 5 wpo the number of TH axon profiles were enhanced in the combinatorial group compared to the other three groups (mMS, USSC, control), which show about the same level of TH fibres. A significant difference was detected between the combinatorial and control ($p = 0.015$) as well as the combinatorial and USSC ($p = 0.006$) group. (J) In the long-term experiment, the largest amount of TH was found in the combinatorial group whereas TH axon profiles were less in the three other groups with the lowest amount in the control group. No significant (n.s.) differences were detected.

Statistics: One-Way ANOVA with Bonferroni Correction. *$p \leq 0.05$, **$p \leq 0.01$. Results are shown as mean ± SEM.

As some animals showed a remarkably enhanced growth of TH axon fibres into and out of the mMS lumen, the question arose if the axon growth of 5-HT was as good in these animals (Fig. 29, A-D). However, compared to TH serotonergic axons were not as abundant in the mMS lumen and adjacent to it in these animals.

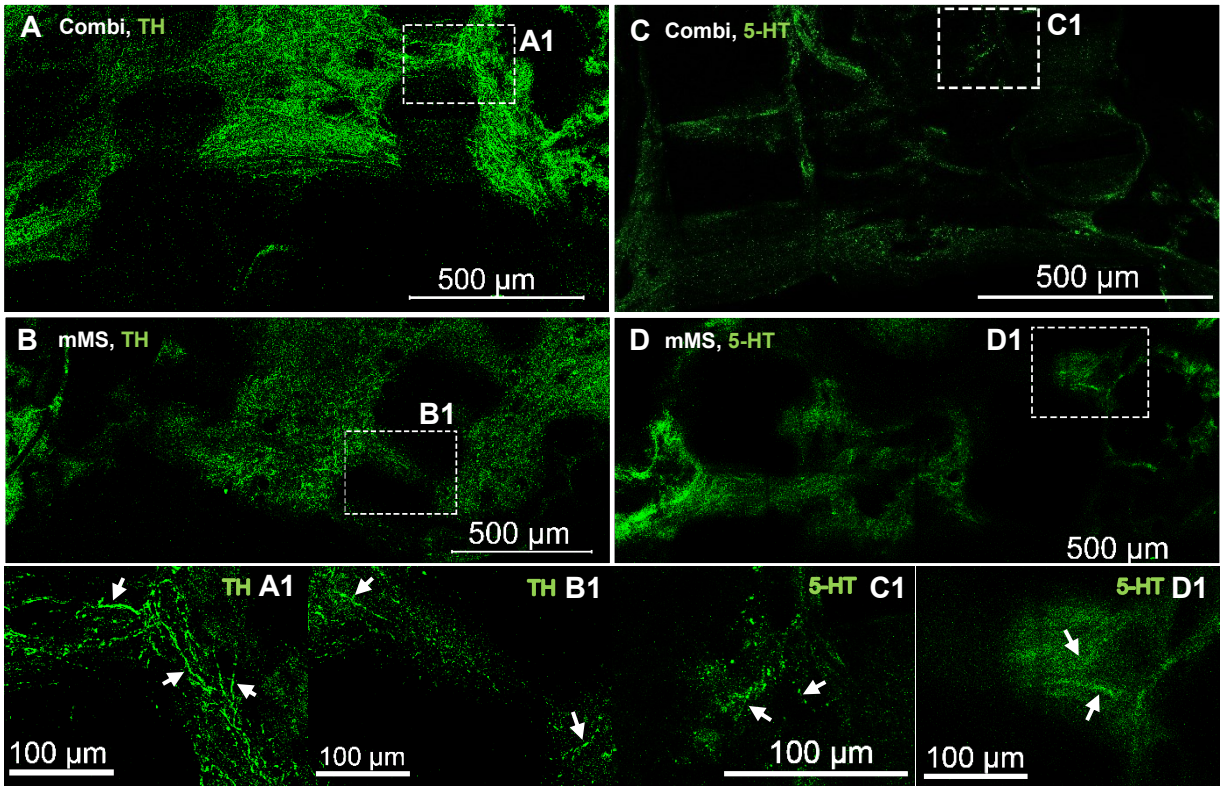

Figure 29: Axon regeneration through mMS implant of individual animals.
Two neighbour horizontal 50 µm thick spinal cord sections of two animals with an mMS implant were analysed for 5-HT and TH axon profiles. Images A and C are from the same animal as well as B and D. A high amount of TH fibres grew through the mMS (A + B). However, almost none 5-HT axon profiles were observed in exactly the same animals in the mMS lumen as well as adjacent to it in these sections (C + D). (A1 - D1) The rectangles in A - D are magnifications of the sections adjacent to the caudal part of the mMS with TH and 5-HT axon profiles (arrows).

4.4.3. Comparable number of macrophages in the lesion area in all treatment groups

Following a spinal cord trauma, macrophages infiltrate the lesion site immediately and remain at the injured spinal cord [144]. A high amount of unspecific staining, especially prominent in 5-HT immunofluorescent images, is due to the uptake of antibodies by macrophages [145]. Therefore, a staining for CD68 was performed to verify the unspecific-labelled cells as macrophages. Stained macrophages detected in the lesion area differed in size, which was also observed in previous studies of other labs [146, 147]. Furthermore, they appeared in comparable

density in all four groups and are thus likely responsible for the high unspecific staining (Fig. 30).

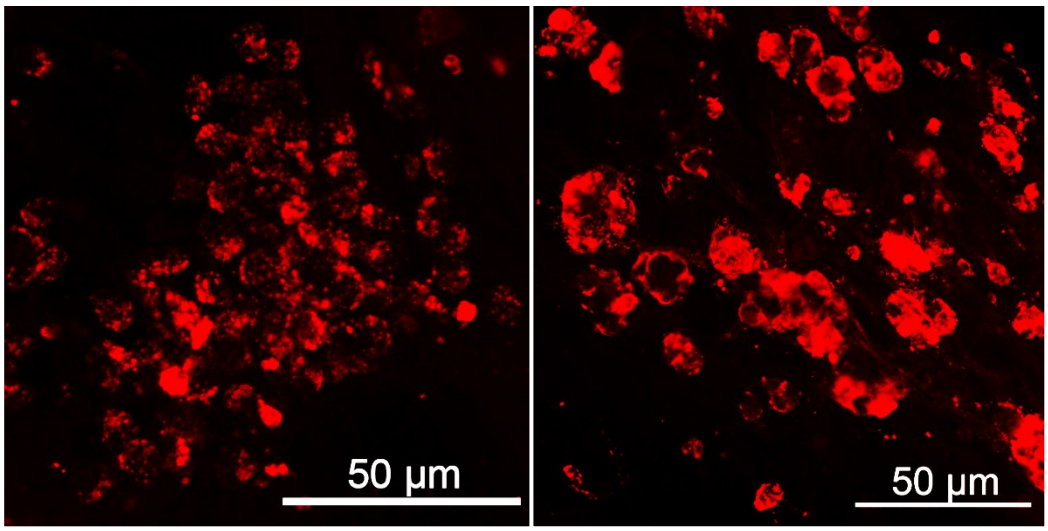

Figure 30: Example images of macrophages in the lesion area following SCI. Staining of horizontal 50 µm thick spinal cord sections for macrophages with the marker ED1, a CD68 clone, displayed a vastly amount of macrophages in the lesion site in all four treatment groups.

4.5. Formation of new synapses on regenerated axons

The possible synaptic reconnection of regenerating axons with neurons caudal to the lesion was analysed. Horizontal 50 µm thick spinal cord sections were stained for synaptophysin, a presynaptic marker, NeuN, a neuronal marker, and the neurotransmitter 5-HT. With this staining, synaptic connections of regenerating 5-HT fibres on host neurons were detected caudally in close proximity to the lesion site (Fig. 31, A - H). These newly formed synaptic contacts of regenerating 5-HT axons were identified by the overlay of the green 5-HT axons and the red synaptophysin resulting in yellow point-shaped structures (Fig. 31, A - D). Apparently, more synaptic contacts of regenerating 5-HT fibres appeared to be present in the treatment groups, especially in the combinatorial group, compared to the control group. However, due to the low number of labelled synaptic contacts no reliable quantification could be performed.

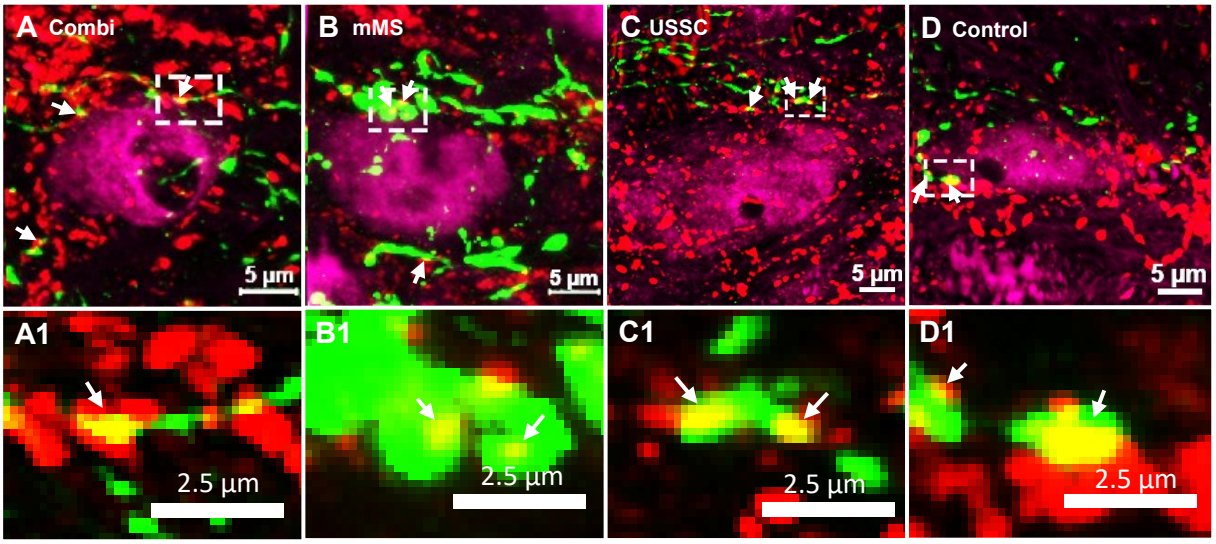

Figure 31: Regenerating 5-HT axons formed synaptic contacts on neurons caudal to the lesion. To analyse the synaptic reconnection of regenerating 5-HT axon fibres caudal to the lesion horizontal 50 µm thick spinal cord sections were investigated. (A - D) The triple staining of 5-HT (green), synaptophysin (red), and NeuN (magenta) showed potential new synaptic contacts (white arrow) on neurons in the caudal spinal cord stump. The amount of those synaptic contacts was smallest in the control group (D) and more frequent in the treatment groups (combi, mMS, USSC). However, no quantification was performed. (A1 - D1) The rectangles in A - D are magnifications of synaptic contacts (white arrow) of regenerating 5-HT fibres. Synaptic contacts could be identified by yellow point-shaped structures (white arrows), which emerged from an overlay of green 5-HT and red synaptophysin.

4.6. Observation of regenerated CST traced axons

Regeneration of CST axons was visualised via an anterograde tracing with an AAV. The tagged fluorophore mCherry of the AAV was stained with a respective antibody, as its endogenous fluorescence was insufficient after IHC procedures. As expected in an intact spinal cord the anterograde tracing of the CST showed mCherry labelled axons fibres in the entire spinal dorsal corticospinal tract, including the thoracic segments 8/9 (Fig. 32, A). For a verification of the antibody, 50 µm thick horizontal spinal cord sections rostral to the lesion, where the mCherry signal was visible, were stained with the red fluorescent protein (RFP) antibody. An overlay of the mCherry signal and the stained RFP demonstrated a specific (dotted) staining, as seen in the Fig. 32, B. It has been shown that injury of the spinal cord leads to dieback of the CST axons resulting in spherical swellings (retraction bulbs) at the proximal endings of the severed axons [148]. These spherical swellings were also observed in anterograde traced CST axons in spinal cord injured animals showing axonal dieback of the CST up to Th6/7 (Fig. 32, C + D, white arrow). In one animal of the mMS group regenerating axons of the CST distal to the lesion were detected in the thoracic segments 10/11, which is about 1 - 2 segments caudal to the lesion (Fig. 32, E). CST axons apparently formed synaptic contacts (Fig. 33, F, white arrow).

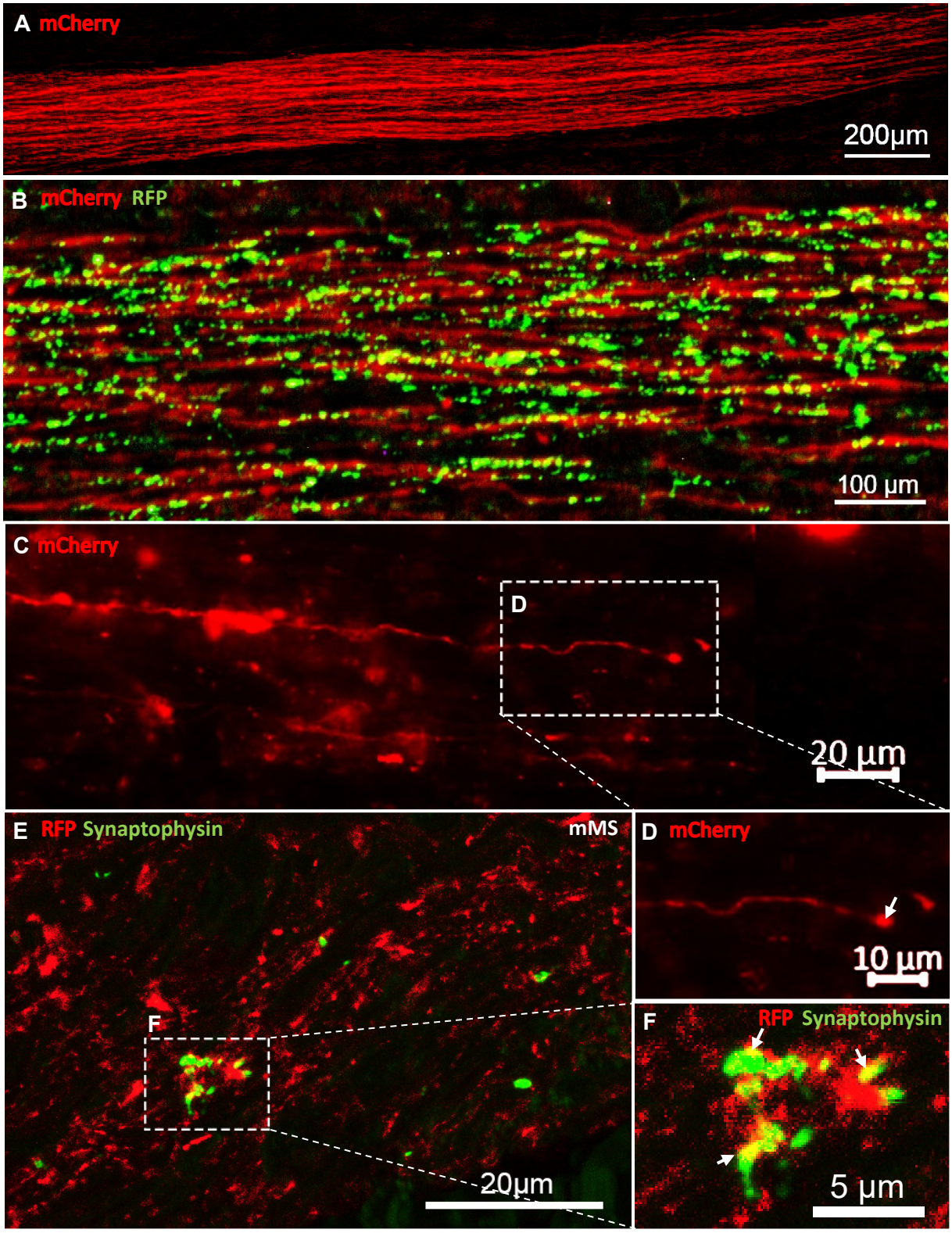

Figure 32: Traced CST axons in the thoracic spinal cord.

(A) A horizontal 50 µm thick tissue section of an uninjured spinal cord. CST axons were labelled by the fluorophore mCherry after AAV injection. (B) The overlay of the RFP stained CST axons (green) with the mCherry signal (red) of CST traced axons in the spinal cord thoracic segment 6/7 confirmed the specificity of the RFP antibody. (C) CST mCherry-traced axons at the thoracic levels 6/7 show spherical swellings (retraction bulbs), which are characteristic of axonal dieback following an injury. (D) Magnification of a CST axon with a spherical swelling (white arrow). (E) In one animal regenerating mCherry traced CST axons (red) were detected in the thoracic segments 10/11 following SCI. (F) The magnification of CST axons shows costaining with the presynaptic marker synaptophysin (green, white arrows).

4.7. No detection of FG traced interneurons proximal to the lesion

To trace descending propriospinal interneurons that potentially regenerate through the lesion zone the retrograde marker Fluorogold was injected caudally to the lesion (Th10/11). At first, the FG tracer was injected into an uninjured spinal cord at the thoracic level Th10/11 for validation of the tracing method. When analysing the uninjured traced tissue, FG was detected in cells rostral to the injection site at the thoracic segments 8/9 (Fig. 33, A + B). Additionally, it could be traced up to the cortex in layer V, where FG fluorescent pyramidal cells were observed (Fig. 33, C + D). In experimental animals, FG had to be stained with an antibody for a triple staining with NeuN and synaptophysin. The staining was performed not just to look for FG traced interneurons rostral to the lesion, but also to find any possible connections with neurons and synapses. The staining did not reveal any Fluorogold traced cells rostral to the lesion or in the cortex. However, FG was detected up to the lesion site where it overlapped with NeuN and connected to synapses (Fig. 34, B + C, white arrows).

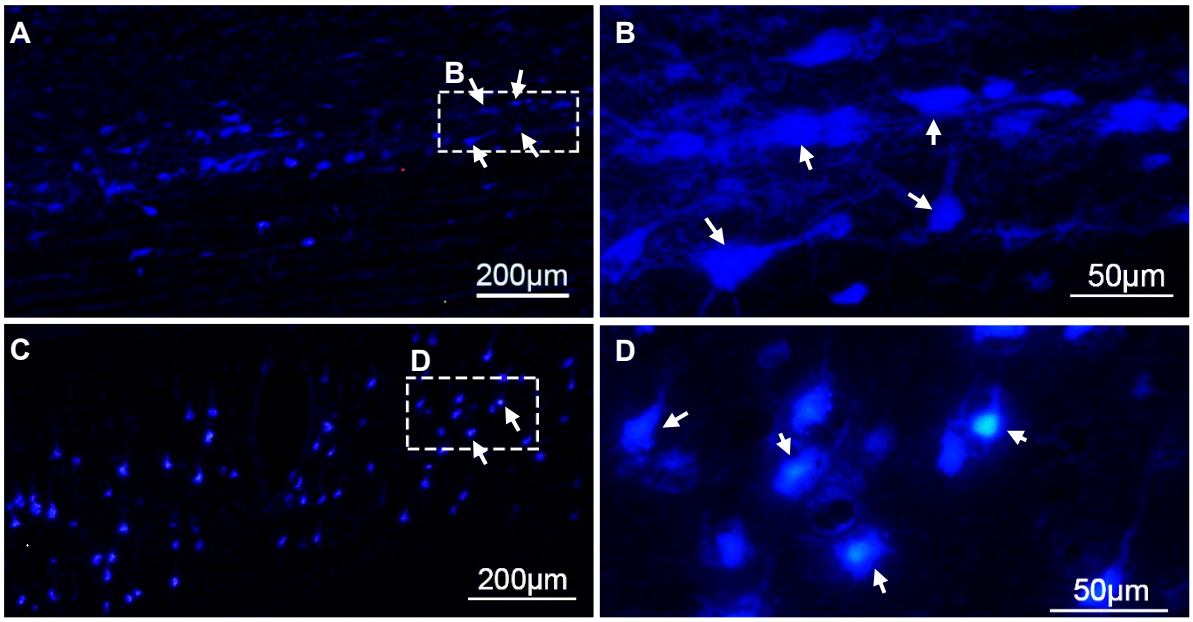

Figure 33: FG traced neurons of an uninjured animal in the spinal cord and brain.
Parasagittal 50 µm thick tissue sections were analysed for FG traced cells. (A-B) Fluorescence of FG-labelled cells in the spinal cord (Th8/9) after FG injection at the thoracic level Th10/11. (B) The magnification shows distinct cells traced by FG in the spinal cord (white arrows). (C-D) Primary motoneurons were retrogradely traced with FG in cortical layer V. (D) With the magnification, traced pyramidal cells, which can be recognised by their explicit form, could be observed (white arrows).

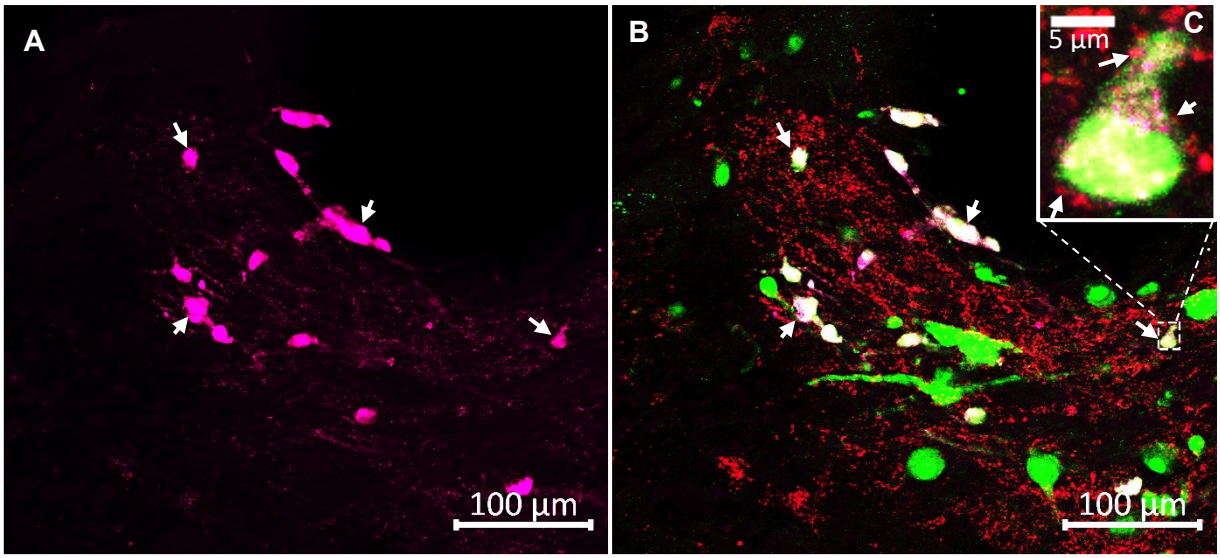

Figure 34: FG staining caudal to the lesion of experimental animals following SCI.
Three horizontal 50 µm thick spinal cord tissue sections of each FG traced animal were investigated for FG traced cells. (A) Retrogradely FG traced neurons were detected close but caudal to the lesion (white arrows). (B) Triple staining of FG (magenta) with NeuN (green) and synaptophysin (red). A small number of NeuN-positive cells overlapped with the FG tracer (white arrows). (C) At higher magnification, connections of synaptophysin (red) to FG-traced neurons could be detected (white arrows). However, FG traced cells could not be found rostral to the lesion.

4.8. Functional improvement after spinal cord injury following mMS implantation

4.8.1. Influence of the combinatorial and individual therapies on locomotor recovery

As anticipated the mBBB score dropped initially to 0 – 1, as seen in Fig. 35, following a complete spinal cord transection and the subsequent treatment, reflecting the transection of the spinal cord pathways due to the injury. An average mBBB score of 2 was reached within three weeks post injury in all groups. A notable spreading of the mBBB score of the different groups was detected after 8 – 9 weeks. The maximum average mBBB score of the control group was 7 after which it decreased until the end of week 21 (final week). With level 7 the animals were able to frequently alternate (L-R) their hind limbs whilst moving. The USSC treatment led to a maximum average mBBB score of 8 at which the animals showed a consistent alternation of the hind limbs. In contrast, the combinatorial and mMS groups attained a maximum average mBBB score of 11 and therefore revealed an improved locomotor function to the level of rhythmic movements and plantar foot placement after which they remained at a plateau up to week 16 – 17. Animals of the

combinatorial and mMS group displayed a significant increase in locomotion compared to the control group at week 13 (combi: 11 vs. control: 6.1, p = 0.00053; mMS: 9.9 vs. control: 6.1 p = 0.0062), 16 (mMS: 10.8 vs. control: 6.75, p = 0.0044), 17 (combi: 9.8 vs. control: 6.1, p = 0.007), 19 (mMS: 8.7 vs. control: 4.6, p = 0.0019), and 20 (combi: 7.25 vs. control: 3.45, p = 0.0025; mMS: 8.1 vs. control: 3.45, p = 0.0015). Hence, a significant locomotor improvement was observed in animals with an mMS implant. The monotherapy of USSC remained between the mMS implant animals and the control group.

A large degree of variation was seen in each group as the average mBBB score in Fig. 35 A could not show the heterogeneity within a group and the inter-individual differences in animals, which could profoundly be observed in the scatter plots. With the highest mBBB scores in the combinatorial and mMS group, the variability increases as well (Fig. 35, B + C). In contrast, the USSC and control animals, which already show a lower mBBB score in general, the variability is smaller as well (Fig. 35, D + E). A high mBBB score was reached with the combinatorial and mMS treatments indicating a promising effect following spinal cord injury.

4.8.2. Maximum mBBB scores differ between groups

The proportion (%) of animals of each group to reach a respective mBBB threshold was portrayed in histograms (Fig. 36, A - D). As the number of animals per group showed some variation (see 3.10.1.), the proportion (%) was calculated to identify the mBBB threshold for better comparison. Animals of all groups obtained an mBBB score of 4 (Fig. 36, A). Furthermore, 93 % of the mMS group were able to reach the threshold of mBBB 10, which includes occasional weight support (Fig. 36, B). A minimal lower amount of 76 % of combinatorial animals attained this level. The control and USSC group, however, showed an even lower percentage for the mBBB 10 level, 36 % and 35 %, respectively. A cut was observed at the mBBB of 15, where animals show occasional to frequent weight support with possible plantar foot placement. Control animals uniformly failed to exceed this threshold (Fig. 36, C). Yet, treatment groups of mMS (40 %), USSC (14 %), and their combination (30 %) were able to pass this stage with the USSC group showing the lowest number. Consequently, the USSC group did not reach an mBBB level of 17 (Fig. 36, D). Animals of the combinatorial and mMS group, however, accomplished to acquire this score with the combination having a slightly higher number of animals reaching this level, 23 % versus 20 %, respectively.

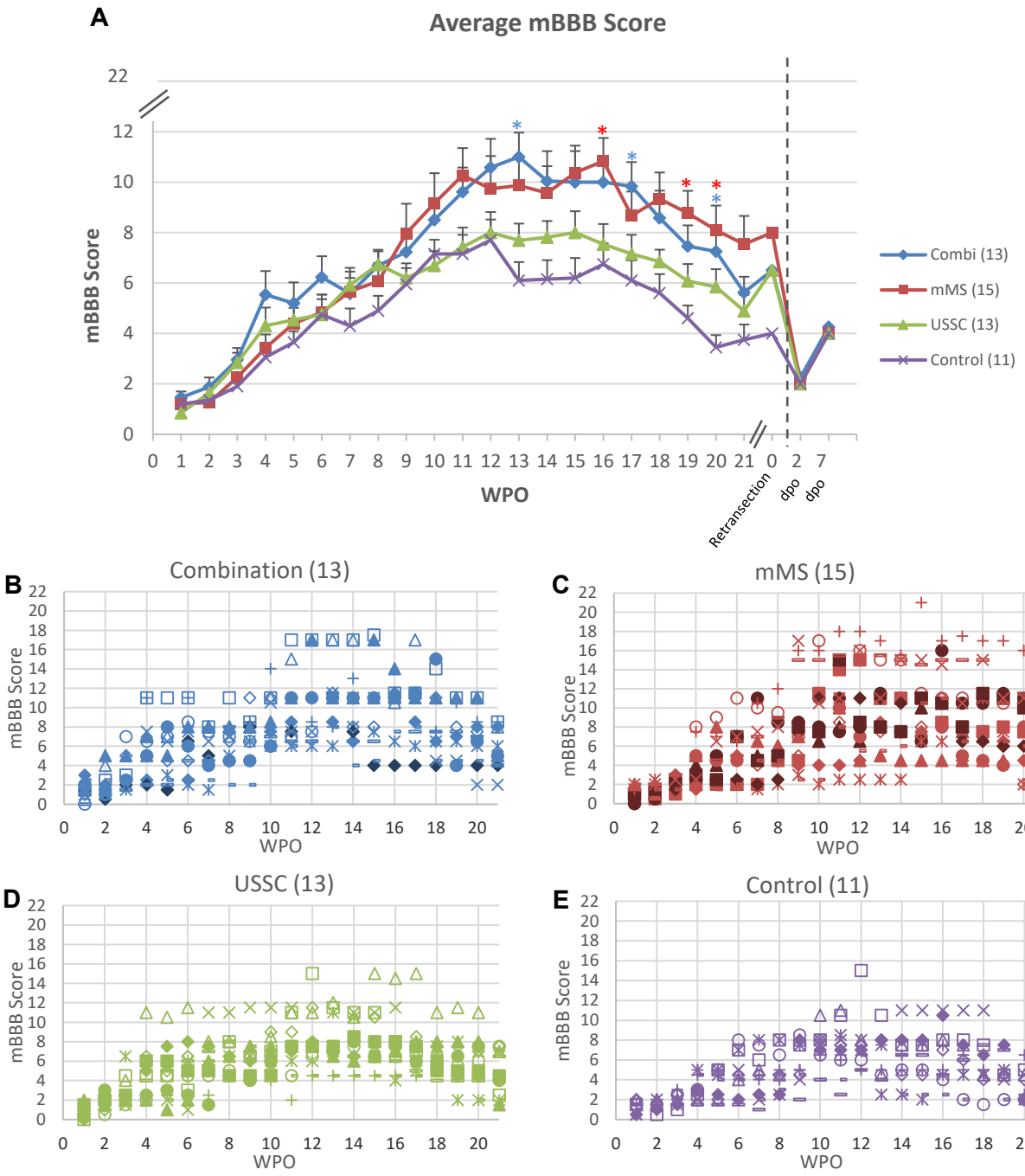

Figure 35: Comparison of mBBB scores between treatment groups.
(A) Average mBBB scores over a time course of 21 weeks resulted in a significant increase in locomotor function in mMS implanted animals (combinatorial and mMS group) compared to the USSC therapy and control group. Data was assessed with a modified Basso-Beattie-Bresnahan locomotor score (mBBB), which has a maximum of 22. Locomotor function following retransection was analysed after two and seven days. Open field test was performed at the day of retransection (0 dpo), which showed a similar mBBB as in week 21. Two days post retransection (dpo) the mBBB level dropped to 2 for all animals. After seven days, the mBBB score increased to 4 with no differences between the groups. (B-E) Scatter plot diagrams of the mBBB scores of the treatment groups, combinatorial (B), mMS (C), USSC (D), and control (E), showing the individual scores for each animal per day. Except one outlier, the control group did not exceed an mBBB level of 11. In contrast, animals of the other treatment groups reached higher mBBB scores. One mMS treated animal even obtained scores up to 21.

Statistics: Kruskal-Wallis with Bonferroni Correction. *p ≤ 0.05, **p ≤ 0.01, blue * = Combi vs. Control, red *

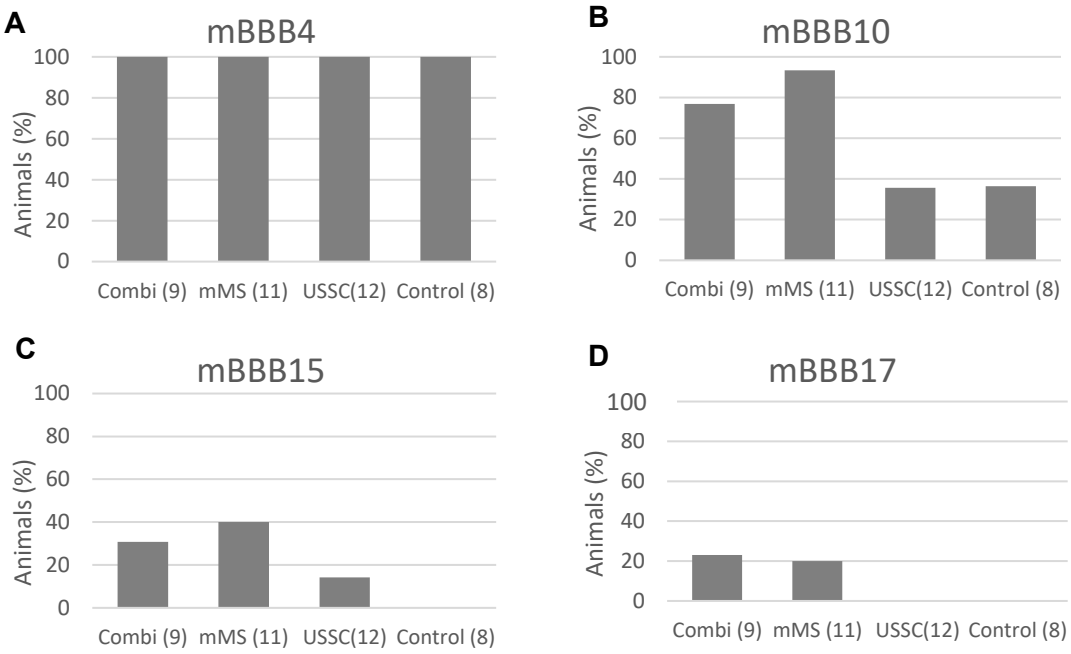

Figure 36: mBBB threshold in experimental animals differ between groups.
Animals receiving mMS and combinatorial treatment obtained the highest mBBB scores, compared to the USSC and control group. Thresholds are given in percentage of animals per group. Proportion of animals reaching mBBB 4 (A), mBBB 10 (B), mBBB 15 (C), and mBBB 17 (D) are shown. Control animals did not reach the threshold of mBBB 15 and 17. An mBBB of 17 was not observed in animals treated with USSC. Only combinatorial and mMS animals attained an mBBB score of 17.

4.8.3. Decrease of mBBB score following retransection

To find out if regenerated axons were involved in locomotor recovery a complete transection at the thoracic level Th6/7 was performed on a small number of animals. Following week 21 the spinal cord of two animals per group were retransected. Unfortunately, three animals died during the surgery. Therefore, the mMS, USSC, and control group only comprised one animal per group. Previous to the retransection, the open field test was performed to gain a current locomotor score. Here, the animals showed a similar mBBB as the week before. However, two days post retransection the mBBB score dropped to about level 2 (Fig. 35, A). Five days later a small increase up to mBBB score 4 was observed for all animals independent of the group.

5. Discussion

Findings of this study could reveal for the first time that the combinatorial treatment of the mechanical microconnector system (mMS) implantation together with unrestricted somatic stem cell (USSC) transplantation results in axon regeneration and formation of new synaptic connections caudal to the lesion at 21 weeks post operation. The fibres regrew through and beyond the lesion area in the white and grey matter. However, with respect to functional improvement the combinatorial treatment does not differ from the individual mMS treatment in locomotor recovery. Behavioural testing revealed significant functional recovery of hind limb usage, which may be partially mediated by axonal regeneration. In contrast, control animals only showed low degrees of spontaneous axon regrowth but no long distance regeneration of axons.

5.1. Decrease of cyst formation following SCI and subsequent combinatorial treatment

Following spinal cord injury, cavities are formed in the chronic lesion site. These consist of fluid-filled cavities separated into chambers by cellular tissue bridges, which are enclosed by partially demyelinated axons and spared fibres [149-154]. In the progressive phase of cavity formation within the first two weeks, the size of the cavity can expand up to multiple times of the initial wound. Moreover, this physical barrier interrupts neuronal pathways in the central part of the spinal cord. To support axonal regeneration and functional improvement after SCI, tissue preservation and therefore prevention of cyst formation is generally considered as an essential requirement [155, 156].

In the present study, a considerable number of cysts was observed, especially when compared to previous studies from our lab. Therefore, it has been of great interest to further investigate the influence of the different treatment strategies on cavity formation. To examine any cyst size differences between the groups and whether the individual treatment or their combination reduces the cavity formation the complete cyst area in a region of interest (ROI) has been measured and put in relation to the total tissue area of the ROI. Histological evaluation has revealed an increased cyst formation compared to previous animal experiments in our lab. Possible causes may be the pressure force and duration of the vacuum application as well as the rat breed and thus the supplier. All data of the pressure forces and

their possible variation have been documented in the surgery protocols. No significant differences between the applied pressures and no correlation between the pressure forces and the cyst formation could be determined. Furthermore, the application of the mMS device cannot explain the increase in cavity formation in the USSC and control group as there was no device implanted. Previous experiments have been performed with Wistar rats provided by the animal facility of the Heinrich-Heine-University Duesseldorf whereas in the present study animals were supplied by Janvier Laboratory. Moreover, the former study of the combinatorial treatment has used Janvier animals and has shown enhanced cyst formation as well [135]. Others have demonstrated an increased cavity formation in substrains of Sprague-Dawley rats following an SCI [157]. Regardless of the survival time, either 5 or 21 weeks, the control group displayed the largest cavity area compared to the treatment groups, which coincides with previous studies from our lab.

Taking into account that both the short- and long-term study showed a trend and sometimes even a significant decrease in cavity formation when treated with stem cells (USSC), microconnector (mMS), or the combination thereof, a positive influence of these treatments regarding the cyst formation is assumed. In accordance with other research groups, who accentuated the success of therapeutic treatments concerning cavity reduction, observations made in the present study accommodate this. One approach is the transplantation of (stem) cells. In support, several studies have observed that the transplantation of various cells (T-cells [158], MSC [159], OPCs [160], USSC [100]) resulted in a reduction of cyst formation. Hence, transplantation of (stem) cells seems to have a beneficial effect in reducing cystic cavitation and on tissue preservation, which has also been observed following USSC treatment in this study.

Concerning growth factors, the application of the vascular endothelial growth factor (VEGF) following a contusion injury in the spinal cord revealed only small cavities [161]. But not just VEGF but also SDF-1 (stromal-derived factor-1) and HGF (hepatocyte growth factor) are known to have neuroprotective effects and are released by USSC [96]. Similar mechanisms and functions of the USSC associated with neuroprotection have been reported previously [96, 100]. Thus, the secretion of compounds involved in nerve regeneration may mediate the observed tissue preservation following USSC transplantation in the present investigation.

Results of this study show occurrence of macrophages in the lesion site, which can influence the formation of cavities. The infiltration and activation of peripheral macrophages and residential microglia following an SCI has been described to initiate post-traumatic cystic cavitation [156]. The size of macrophages in the rat is in average 14 µm [162]. In this study, macrophages have been found in the lesion site with a size ranging between 7 and 20 µm (Fig. 31). Those differences in dimensions found in the spinal cord of experimental animals in the present study could be in conjunction with a study where different sizes of macrophages were observed in the rat liver showing a functional heterogeneity in secretory properties [146]. Furthermore, the ED1 antibody stains not only macrophages but also activated microglia, which could be another possible explanation for the various sizes of ED1-positive cells. Therefore, macrophage occurrence could be involved in the increase in cyst size observed in the treatment groups of this investigation.

However, not just molecular effects of various cell types can decrease cystic cavitation but also mechanical strategies appear to be supportive. In order to support tissue restoration, reduce glial scar, and establish a permissive environment for cellular ingrowth it is necessary to fill the gap left by the lost cell population, including neurons. To fill this gap there are numerous cellular and acellular materials/scaffolds that can be implanted. For example, the Implantation of a cross-linked collagen-based scaffold into the resected spinal cord resulted in a reduced formation of fluid-filled cysts, especially in combination with an GDNF plasmid [77]. However, not just collagen-based scaffold but also alginate-based ones inhibited cyst formation when implanted into cervical hemisections [78]. Instead of preventing cavity formations Paino and Bunge [163] induced a cystic cavity by a phototrombic lesion in the spinal cord. Subsequently, they implanted polymerised collagen channels enclosing Schwann cells (SC). With these implants, axons were able to grow into the graft. The mMS also seems to serve as a mechanical guiding tool to support axon growth into and beyond the lesion site. To fill the cystic cavity with growth supporting material can invert the inhibitory effect of cysts. With this method it may be possible to apply a treatment to promote a growth permissive environment in human patients that suffer chronic SCI. The emphasis is here on chronic SCI because in acute SCI patients there is still a chance of functional recovery through spontaneous regeneration and/or relay of signal transduction. However, in chronic SCI patients, where the functional recovery is absent, the possibility to implant a mechanical guiding tool

through resection of inhibitory scar tissue increases the chance of locomotor recovery. In this study, the mechanical microconnector system seems to support the reduction of cavity formation too, as the cysts were lowest in animals receiving a mMS implant. The stabilisation of the spinal cord through the mMS as well as the close approximation of the two spinal cord stumps appears to enhance tissue preservation and regeneration, which in turn decreases the cavity formation. Furthermore, the inhibitory environment at the lesion site may also be reduced by the close proximity of the spinal cord stumps as the release of compounds beneficial for tissue preservation can act more rapidly at the required location. In addition to the mMS, the USSC transplantation further reduced the cavity formation possibly through the release of cytokines and growth factors known to be neuroprotective [164].

5.2. USSC migrate to the injury site and promote axon regrowth following spinal cord injury

In accordance with previous studies, targeted migration of USSC towards the lesion site in immunosuppressed animals was observed. In the combinatorial treatment USSC were detected in the mMS lumen. The migration of transplanted USSC, adjacent to the injury, was previously also shown by Schira and colleagues [100]. Even though the two studies used different injury models, Schira et al. performed dorsal hemisections, whereas in the present study a complete transection model was used, the behaviour of the human USSC following their transplantation into rat spinal cord did not differ. To avoid host-vs-graft immune reaction, which occurs when allografts are implanted, animals receiving an USSC transplant were immunosuppressed. USSC survived for about three weeks as the immunosuppression was discontinued at this point in time.

As stem cells are considered to counteract some detrimental characteristics following a spinal cord injury, like secondary injury, and cavity formation and further facilitate secretion, differentiation, axonal regeneration and myelination, they are of great benefit. In accordance, a secretome analysis of USSC revealed the secretion of a number of proteins involved in cell adhesion, cell motion, blood vessel formation, cytoskeleton organisation, and extracellular matrix organisation [99]. USSC treated animals in this study showed successful axon regrowth after injury even when inhibitory molecules were present indicating the release of growth permitting signals by USSC. Thus, a shift of the balance towards an axon growth permissive microenvironment through USSC released factors thereby promoting axonal regrowth

is likely. In conclusion, the innate targeted migratory potential of USSC and their secretion of proteins involved in nerve regeneration are of great advantage and represent innovative possibilities for the release of therapeutic molecules into the injury site.

5.3. mMS – an approach to overcome CNS regeneration failure

Stabilisation of the spinal cord after a complete transection injury in rats was achieved by general tissue preservation following the implantation of the mMS and further in combination with the USSC transplantation. A highly desirable property of biocompatible conduits is the structural stability of the injured cord [165]. Additionally, the lumen of the mMS exhibited a large number of newly formed blood vessels, which supports regeneration through molecule and nutrient supply. The higher frequency of the blood vessels inside the lumen of mMS implanted animals compared to the other two groups (USSC, control) is explainable by the tissue preservation induced by the spatial proximity of the spinal cord stumps through the microconnector. Preventing the reduction of the spinal cord diameter is another benefit of the mMS. These findings are in accordance to previous results of our research group [1, 79].

Mechanical support for axonal regrowth can be provided by artificial (tissue) scaffolds. However, there are a couple of characteristics that bridging devices, like the mMS, should contain. First of all, the device should have mechanical properties which include a certain elasticity to mimic the soft tissue environment of the spinal cord [137]. This is important in order not to cause any further damage to the spinal cord. Hence, many researchers prefer the use of a gel-like scaffold. These hydrogels have the ability to adapt the chemical, physical, and mechanical properties of the spinal cord tissue creating an environment where neurons and endogenous repairing cells can adhere to [166]. Although the mMS is made of an inflexible material, a great integration of the mMS into the spinal cord and, as mentioned before, a stabilisation of the cord devoid of additional trauma was observed. Therefore, the flexibility of the scaffold does not seem to be implicitly essential or rather is not exclusively responsible for the beneficial effect, when the device provides other positive features. Another important aspect is the biocompatibility of the scaffold to permit axon growth. In order to assure biocompatibility the devices/scaffolds need to first be tested in vitro [166]. Subsequently, the criteria to not trigger any immune response from the host

need to be met. In this study, the inflammatory response towards the mMS seems to be at a minimum. The staining of ED1 showed that macrophage infiltration was about the same amount in all groups independent of the implant. Therefore, the biocompatibility has generally been met. However, a biodegradable adaptation of the mMS would be of great advantage and is also applicable for the mMS. A crucial feature for biodegradable devices is the initial stability given to the spinal cord with the subsequent degradation to restore its flexibility. As the implanted material needs to be replaced by regenerating cells and their extracellular matrix (ECM) to maintain a growth-promoting environment the challenge is to determine the optimal time frame of degradation. Once the optimal time frame has been detected a suitable material, which will degrade in this specified time, needs to be found. Another beneficial property for a scaffold would also include a multi-channel structure for axonal guidance [167]. So far, most scaffolds are designed for rodents, as this is the main model organism to experiment with. Therefore, the conduit needs to be adjustable for different spinal cord diameters to allow the same regeneration effect to occur. To be able to adjust the scaffold is highly important for the transfer to clinical applications. In accordance to the multi-structure system, like the honeycombs in the mMS, stands the capability for cell adhesion. In contrast to a single lumen tube, the surface area of a multi-structured design is much greater, allowing more cells to attach as well as local release of integrated growth factors. Taking into account the design of the mMS, described in 1.4.1., the honeycomb walls supply such a multi-structured organisation and support cell adhesion, which supports regeneration.

The development of such a mechanical device is merely possible with the cooperation of different medical and scientific staffs. Here, we were able to collaborate with the Institute of Microsystems Technology (University of Technology Hamburg-Harburg) and the BG Trauma Hospital Hamburg (Department of Trauma Surgery, Orthopedics and Sports Traumatology) with whom it was possible to generate the mMS. The various characteristics of a suitable scaffold listed above fortify the application of the mMS to support spinal cord recovery.

In conclusion, the mMS is a promising device to adapt and stabilise the injured spinal cord. The application could range from massive tissue damage in severe traumatic injuries to a considerable loss of tissue following surgical scar resection in chronic patients. Of great advantage is the possible adaptation of the mMS in respect to the lesion size for individual customisation. The characteristics of a perfect scaffold

include many aspects. However, not all of these are mandatory to show success in spinal cord treatment. The mMS already combines many of these aspects and the reconnection of the spinal cord stumps alone are already be very effective [1]. Placing the spinal cord stump in close proximity with the mMS and applying a vacuum already led to an increase in locomotor recovery and promoted axon regeneration into and partially beyond the lesion area in this study. Furthermore, the combinatorial treatment showed an even greater regrowth of severed axons indicating an additional beneficial effect of USSC transplantation. Thus, combinatorial treatments, which have been shown to enhance spinal cord recovery [77, 142, 163, 168, 169], are a promising strategy. Moreover, these combinatorial therapies are applicable with this device through the internal microchannel system (e.g. drug application via a connected mini-pump).

5.4. Axonal regeneration is increased following combinatorial treatment

The enhancement of axonal regrowth is a leading goal for SCI recovery. Previous studies showed that already a small number of regenerated axons were accompanied by motor and sensory function improvement [51]. Tissue preservation/formation, reduced cavity formation, and angiogenesis alone cannot explain the functional recovery of the mMS and combinatorial treatment groups. The preserved/newly formed tissue as well as the number of new blood vessels in the lesion area were not significantly different. The reduced cystic cavity in the mMS and combination groups, which did show a significant difference to the control group, is suggested to partially contribute to the improved locomotor function. As the decreased cavitation cannot explain the complete functional recovery, the involvement of axonal regrowth to improve locomotor outcome stand to reason.

Several factors have been associated with the failure of axonal regeneration following a CNS injury. These factors include a lack of neurotrophic support [170, 171], the presence of myelin- [172-174] and ECM-associated inhibitors [175-177] in the lesion area, and a possible deficiency of intrinsic gene expression to facilitate an active axonal growth state [178]. The capability of stem cells to regenerate CNS tissue and the feasible transplantation has made them a popular tool for CNS trauma. Transplants of bone marrow stromal cells (MSC) into the SCI lesion cavity induced an augmented growth of axons with a longitudinal direction [179, 180]. Furthermore, Lu and colleagues [181, 182] grafted olfactory ensheathing cells into the injury site

resulting in the improvement of axonal regrowth and locomotor function. In accordance to these findings, USSC treatment following an SCI induced an increase in axon regrowth in the short- and long-term study underlining the beneficial effect of USSC cytokine secretion.

Since the extent of the axonal growth is rather modest and limited, it demands further insight into axonal regenerative mechanisms. The loss of tissue and the formation of cystic cavities are consequences of spinal cord injury. The physical gap as well as the inhibitory environment impedes axon regeneration. Thus, replacement of lost tissue and reattachment of the spinal cord stumps after a complete SCI or scar resection need to be included for an effective treatment. Furthermore, a combinatorial treatment, which targets more than one of these mechanisms, potentially enhances axonal extension beyond the lesion site. There are several studies that include a bioengineered scaffold with either stem cells or growth factors inducing directed axon regeneration across the artificial scaffold [93, 183]. The present study supports the assumption of a combinatorial treatment. The data shows that the implantation of the mMS and transplantation of the USSC in combination promote axonal regeneration after severe SCI. The individual treatments of mMS and USSC, in contrast to the control, exhibit a higher but not particularly a significant increase in axon regrowth. Comparing this study with other investigations it is important to consider the lesion model used. A complete transection of the spinal cord understandably results in a severe disturbance of axonal connections whereas in a contusion or hemisection spared axon fibres can take over the lost function of axons.

Axon regeneration in the present study was investigated by analysing the 5-HT- and TH-immune positive fibres and the anterogradely traced CST axons. Surprisingly, the 5-HT axon amount in the lesion site after 5 wpo was highest in the control group followed by the USSC, mMS, and combination, respectively. It is possible that the severed axon stumps in the lesion zone are not immediately degraded and therefore counted as axon profiles [184]. As the lesion area does not contain tissue when an mMS is implanted, there are no axon fragments that can be counted misleadingly. Abundance of terminals caudal to the lesion site of TH and 5-HT, re-established through axonal regrowth beyond the lesion site, is associated with functional recovery [185]. In the present study 5-HT and TH axon regrowth was also detected caudally and therefore suggests an involvement of these axons in the observed functional recovery. More complex, on the other hand, is the regeneration

of CST fibres. However, because of its restricted regeneration capability it serves as a great model organism for regeneration. The implantation of different scaffold in combination with stem cells or neurotrophic factors led to regrow of some CST fibres into the graft and reduced axonal dieback [186-189]. The CST tracing in this study revealed regeneration of CST axons in the caudal part of the spinal cord after SCI and the subsequent mMS treatment suggesting that the microconnector supported this outgrowth. In rats, CST axons end up in the dorso- or ventrolateral white matter [190, 191] relating to the numerous CST fibres observed in the white matter of an mMS animal caudal to the lesion. As the locomotor function not only showed a significant improvement in the mMS treatment but also in the combinatorial group, where CST fibres could not be detected, it suggests that the CST is only partially involved in the enhancement of basic hind limb movement observed in this study. It is known that the CST is subjected to axonal dieback following an SCI even up to 19 mm rostral to the site of injury [192]. Together with the limited regeneration of CST axons, it may explain the low number of animals in this study where CST fibres could be observed caudal to the lesion. Additionally, the anterograde tracing method could partially be responsible for the low number, as the injection of the tracer in chronic injured animals only led to labelled axons at the cervical levels, whereas an injection immediately following the transection resulted in labelled axons at the thoracic levels proximal to the lesion [193]. As no neuronal cell bodies were detected in close proximity to the CST axons with synaptic contacts, the possible synaptic connection may be of axo-dendritic or axo-axonic origin.

5.5. Synaptic reconnection following SCI treatment

The synaptic reconnection of axonal fibres plays an important role for signal transduction and the accompanied motor output. Many a time the formation of synapses on newly regenerated axons is marginal. It is well known that the dysfunction of locomotion pattern generators is triggered by the loss of inhibitory neurotransmission [194]. However, the formation of terminal bouton-like structures in the grey matter can occasionally be observed [132, 195]. As expected, the data of the present study showed a vast density of synapses, marked by the synaptophysin antibody, caudal to the lesion. However, a triple immunofluorescent labelling for 5-HT, synaptophysin, and NeuN revealed synapse formation of regenerated axons and host neurons caudal to the lesion for the first time in our research group. In

conclusion, the formation of synapses in the lesion area of the injured spinal cord promoted by therapeutic strategies are of immense relevance to the reorganisation of a segmental neural pathway and reconstruction of synaptic connectivity for functional restoration. Furthermore, not the axon regeneration alone but the functional reconnection is important for the locomotor recovery.

5.6. Propriospinal interneurons may not be the suspected neurons for signal transduction after spinal cord injury

Propriospinal interneurons (PNs) are neurons that are intrinsic to the spinal cord and whose axons terminate within its boundaries [196]. PNs constitute a considerable amount of the spinal cord white and grey matter. Even more so, it is believed that the number of propriospinal neurons in the grey matter is much greater than the number of motoneurons [197]. Propriospinal projections are involved in various physical and behavioural processes, such as modulation of ascending and descending input to the central pattern generators (CPG) for locomotion [198-205] along with autonomic functions like visceroreception and pain perception [206, 207]. Next to N-methyl-D, L-aspartate (NMDA) and dopamine (DA), serotonin (5-HT) is a key element in the participation of propriospinal circuits during motor and locomotor functions [208-210]. Although propriospinal neurons are attributed to be involved in the activation of locomotion, the present study could not detect any retrogradely FG-traced propriospinal neurons rostral to the lesion, which would support this involvement. There are several possible explanations, e.g., the tracing method. The FG-tracer is injected at TH10/11 as it induces necrosis. However, if propriospinal axons regenerate only as far as right behind the lesion site, these axons are not able to absorb FG at this distance from tracer injection site. An injection closer to the lesion, on the other hand, may lead to an uptake of regenerated propriospinal axons, but would eliminate further investigation of regeneration. Even though new circuits are formed after complete SCI it cannot be expected that these circuits acquire function spontaneously, but may require rehabilitation to be integrated into functional networks via use-dependent plasticity [131, 211-213]. Propriospinal interneurons can act as a relay where lesioned axons can sprout onto to transmit signals to the distal cord [125, 129]. When regenerated axons grow through the lesion, they could therefore connect to propriospinal interneurons, which would then receive the signal for further processing. In a complete transection, in contrast to a hemisection or contusion, no axon fibres in the lesion centre are left intact which reduces a

redirection of interrupted signals via propriospinal interneurons immensely. Therefore, the absence of FG-traced propriospinal neurons rostral to the lesion in the present study underlines the hypothesis that in a complete transection the relay of signal transduction is nearly vanished. Anderson and colleagues described robust propriospinal axon regrowth through astrocyte scar periphery and across lesion centres of non-neuronal tissue, however, the propriospinal regrowth did not improve locomotor function [211]. Although they found synaptic connections of propriospinal axons with local neurons, it does not seem like this connection is required for the functional recovery. This is in accordance with the present study as locomotion was improved but no propriospinal interneurons were detected rostral to the lesion underlining Anderson's hypothesis of PNs not being involved in locomotor recovery.

5.7. Locomotor function – recovery of hind limb movement following mMS treatment

Functional recovery after SCI is one of the major tasks to accomplish in research in order to improve the life of SCI patients. As of this point in time, physical training is the principal clinical therapy used to aid rehabilitation of movements of individuals after SCI. It has been shown that exercise restores neurotrophin levels and synaptic plasticity, which in turn facilitates locomotor recovery [110]. On the other hand, a few studies from the Magnuson group investigated daily stretching of the hind limb in contusion animals showing a negative effect of locomotor recovery at acute and chronic time points [214, 215]. Nonetheless, because of its importance for the rehabilitation in human patients, in the present study experimental animals were subject to daily physical stretching of the hind limbs for the entire experiment. Comparing the mBBB scores of these animals to the study performed by Kehl [135] with the same combinatorial treatment but without hind limb stretching the mBBB score is increased in all four groups. Especially when comparing the control groups, a higher functional score was observed in this investigation than by Kehl. As the stretching by the group of Magnuson only included a stretch-and-hold application, which resulted in a negative effect on functional locomotion, in the present study stretching was performed by holding as well as a continuous movement of the hind limbs. Therefore, a possible explanation for a higher mBBB score is the applied physical therapy, which intended to reduce tendon and muscle contractures as well as to maintain the extensibility of soft tissue.

A correlation of the number of 5-HT axon fibres and the cavity size has been calculated and no statistical correlation was detected. The same applies to the correlation analysis of the number of 5-HT and the mBBB score. The latter was surprising as the functional recovery represented a considerable improvement and was expected to be accompanied by an increase of 5-HT. A staining of a general axonal marker after 5 wpo does show more fibres in the lesion area than can be stained with the specific marker for 5-HT or TH. This suggests that a high number of axons from various populations are also present after 21 wpo. Furthermore, axon regrowth would lead to motor signal transduction and therefore explain the increase of locomotor function. Considering these results, the involvement of other axonal population, such as the reticulospinal or rubrospinal axons, in the locomotor recovery is likely. As mentioned before, the regeneration capability of corticospinal axons is limited but can be promoted. Compared to CST axons, brainstem-derived spinal axons, e.g. raphespinal or reticulospinal fibres, appear to have an increased sensitivity to regrow after axotomy, especially when provided with a submissive growth environment. It has been shown that brainstem-derived spinal axons, but not corticospinal axons, are able to grow into peripheral nerve grafts as well as Schwann cell (SC) grafts with exogenous factors added [38, 216]. The reticulospinal tract is involved in the initiation of limb movement, postural control, and modulation of some sensory and autonomic functions underlining a beneficial effect on functional improvement [217-219]. Furthermore, propriospinal and vestibulospinal axons are suggested to initiate robust regenerative responses following injury [220-224]. The vestibulospinal tract is responsible for coordinated postural extensor activity in the limbs and trunk [225]. Another tract contributing to locomotion is the rubrospinal tract. Together with the reticular, vestibular, and raphe formations the rubrospinal tract provides a significant regenerated descending input to the lumbar spinal cord after complete transection when a receptor, which prevents axonal regeneration, is knocked out [226]. Furthermore, regeneration and collateral sprouting from corticospinal and serotonergic fibres is promoted by antibodies directed against neurite growth inhibitors and leads to improved locomotor function after SCI [227]. Descending raphespinal and coeruleospinal tracts, to which the here studied neurotransmitter 5-HT and TH belong to respectively, have neuromodulatory influences on motor function, such as facilitation of rhythmic locomotor activity [218]. In conclusion, next to the serotonergic and catecholaminergic neurotransmitter and

CST fibres, which were investigated here and are participating in locomotor recovery, other tracts like the vestibulo-, rubro-, and reticulospinal tracts are probably involved in functional improvement. The most likely tract to additionally participate in the observed locomotion, besides 5-HT and TH, is the reticulospinal tract as it is involved in the initiation of limb movement.

The present data suggests that the combinatorial treatment has a beneficial effect, especially concerning the microconnector system, as both groups with this implant have shown improved locomotion. Combinatorial therapies, where polymer scaffolds were implanted with neurotrophins or stem cells, described an increase in functional recovery indicating to have created a microenvironment that supports reduction in tissue loss and differentiation of stem cells [168, 228]. The greater decrease in cavity formation detected in the combinatorial group supports the hypothesis of the formation of a regenerative microenvironment even though the locomotion did not differ much between the mMS and combinatorial group. Furthermore, looking at the degree of variation in the mBBB, a high mBBB score results in a high variability. With an mBBB of 17 – 21, a large amplitude of alternated hind limb movement with occasional weight support and even plantar foot placement was observed in some animals of the combinatorial treatment and especially the mMS group. The control group, not taking into account the outlier, did not reach the level of weight support. The monotherapy of USSC attained a large amplitude of alternated hind limb movement with occasional weight support or plantar foot placement and therefore only reached an mBBB score of 15. In contrast to the results of the axon (5-HT, TH) regeneration analysis, these results do not show a great add-on effect in locomotor recovery when USSC were transplanted. A possible explanation could be the secretion of neural regenerative permitting cytokines of the grafted human stem cells [100]. These indeed support axonal outgrowth through neurite growth-promoting factors. However, next to the mMS, the locomotor function is not additionally facilitated through USSC treatment. On the one hand, this would indicate that the additional regenerated axons did not reconnect to (moto-) neurons to provide signal transduction. On the other hand, however, it would support the hypothesis that propriospinal neuron regeneration is not essential for the hind limb locomotor recovery, as PNs were not detected rostral to the lesion by the applied investigation method.

Excitation of spinal motor neurons has been shown to be regulated by brainstem-derived 5-HT [229, 230]. If regulation from the brain also occurs through regenerated 5-HT fibres, it suggests an increase in functional recovery. Without regulation, debilitating muscle spasms are the consequences. Therefore, the improved locomotor function in this study implies that despite the relatively low 5-HT regeneration the required regulation from the brain is present. As mentioned before, the regenerative ability of the CST is fairly limited. In lesion models where there are still axons left intact the corticospinal signals can bypass the lesion to reach the distal cord without axon regeneration. A complete transection of the spinal cord, on the other hand does not present such a loophole for corticospinal signals to be transmitted. However, because of its rather poor regeneration the CST still serves as a good model tract for robust axonal regeneration. Further, in this study we were able to detect CST axonal regrowth caudal to the lesion. Therefore, taking into account the limited contribution of the CST to gross locomotor control in rats, it may not be the most essential part to regain the locomotor hind limb function but is additionally involved in other regenerative processes [231]. Since prominent descending tracts such as the corticospinal, coeruleospinal (TH), and raphespinal (5-HT) tracts only regenerated through the bridge to a certain proportion, it is likely that other population of regenerated fibres were also involved in locomotor function. The retransection of the spinal cord rostral to the initial injury led to a drop of locomotor function two days post injury and increased to an mBBB 4 five days later. The loss of locomotor function indicates the involvement of regenerated axons in the observed functional recovery.

5.8. Conclusion and further considerations

In this study, I could show for the first time for our combinatorial treatment the formation of synaptic connections with regenerated axons and host neurons caudal to the injury site. Synaptic connections are important for signal transduction and hence motor output. Therefore, the detection of newly formed synapses on regenerated axons caudal to the lesion seems to be involved in the observed locomotor functional recovery. Since it is known, that replication of an experimental study rarely confirms previous results, the validation of the combinatorial treatment in SCI on the therapeutic effects seen in previous findings is a great success. Axonal regeneration and locomotor function could be improved by implantation of the mMS

into a complete spinal cord transection. Furthermore, stabilisation of the spinal cord, preserving tissue in place after vacuum removal, and neovascularisation in the mMS lumen were also accomplished with this implantation. There was only a small increased trend in the functional recovery of the combinatorial treatments towards the mMS. For this result is has to be considered that the behavioural test performed here, open field test, is solely a functional test. To further investigate the functional recovery different and/or more tests, as well as electrophysiological recordings would need to be performed, which in turn may lead to a more precise characterisation of the locomotor outcome. The additional transplantation of USSC in the combinatorial group did show a further increase in axonal regrowth and reduction in cavity formation. Hence, USSC seem to further contribute to an effective treatment for SCI recovery.

Based on these results, the design and the application of the mMS can be modified and expanded. The integrated channel system provides the opportunity not just for local drug application of, e.g., scar-suppressing treatments, growth factor cocktails, or immune modulating drugs with an osmotic mini-pump, but also over a longer/specific time period and even directly into the lesion centre. With a biodegradable version soon to be available and the possibility to adapt the mMS individually, as well as serving as a scaffold for matrix molecules, cellular implants, and support of directional growth it represents an ideal artificial substrate for bridging spinal cord lesions.

For future studies, it is important to consider methodical modification, such as a different anterograde tracing method, to further investigate the axonal regeneration. Moreover, different axonal spinal tracts should be investigated to gain more insight into what kind of axons are additionally involved in the functional recovery. As propriospinal interneurons did not show any involvement in locomotor function rostral to the lesion in this injury model, it may be interesting to study their involvement in functional recovery in other lesion models, where signals can bypass the injury site and sprout onto spared PNs. These other lesion models, especially contusions and compressions, are important as in human patients SCI is rarely a complete transection. Finally, a combinatorial treatment including the application of regenerative permitting drugs or neurotrophins via the integrated mMS channel system should be investigated to further promote axonal regrowth and their synaptic connections, which in turn may support the locomotor function.

Current modern single therapy approaches have not accomplished satisfactory results in treating spinal cord injury. As SCI consist not only of one event but provokes numerous consequences, a combination of interventions will be needed to obtain an effective therapeutic strategy. The first concern should be the prevention of secondary tissue loss through early neuroprotective, anti-inflammatory, or immunomodulatory interventions. Subsequently, approaches to reduce scar formation, overcoming additional inhibitory molecules, stimulating damaged nerve cells to regenerate axons, facilitating axonal growth across the injury site, and enabling the formation of new connections will be required in combination to promote axon regrowth and functional recovery. In conclusion, a combination of multiple therapies seems to be the best concept for an effective outcome in treating SCI.

6. Abbreviations

5-HT	5-hydroxytryptamine
AAV	Adeno-Associated Viral Vector
cAMP	Cyclic Adenosine Monophosphate
ch	Chicken
CNS	Central Nervous System
CPG	Central Pattern Generator
CST	Corticospinal Tract
DA	Dopamine
DMEM	Dulbecco's Modified Eagle Medium
DMSO	Dimethyl Sulfoxide
dpo	Days post operation
DPX	Distyrene, Plasticiser, Xylene (mounting medium)
DS	Donkey Serum
e.g.	for example
ECM	Extracellular Matrix
ED1	CD68 protein
EDTA	Ethylenediaminetetraacetic acid
ESC	Embryonic Stem Cells
etc.	et cetera
EtOH	Ethanol
FBS	Fetal Bovine Serum

FG	Fluorogold
GDNF	Glial Cell Line-derived Neurotrophic Factor
GFAP	Glial Fibrillary Acidic Protein
gpig	Guinea pig
gt	Goat
HGF	Hepatocyte Growth Factor
hNuc	human Nuclei
HSC	Hematopoietic Stem Cells
IHC	Immunohistochemistry
mBBB	Modified Basso-Beattie-Bresnahan Locomotor Score
mMS	Mechanical Microconnector System
ms	Mouse
MSC	Bone Marrow Stromal Cells
N_2O	Nitrous Oxide
NaCl	Sodium Chloride
NaOH	Sodium Hydroxide
NCAM	Neural cell adhesion molecule
NeuN	Neuronal Nuclear
NGS	Normal Goat Serum
NMDA	N-methyl-D, L-aspartate
NSC	Neural Stem Cells
O/N	Overnight

O_2	Oxygen
OPCs	Oligodendrocyte Progenitor Cells
PB	Phosphate Buffer
PBS	Phosphate Buffer Saline
PFA	Paraformaldehyde
PNs	Propriospinal Interneurons
PNS	Peripheral Nervous System
rb	Rabbit
RFP	Red Fluorescent Protein
ROI	Region of Interest
RT	Room Temperature
SB	Sudan Black
SC	Schwann Cell
SCI	Spinal Cord Injury
SDF-1	Stromal-derived Factor 1
Syn	Synaptophysin
TH	Tyrosine Hydroxylase
Th	Thoracic Segment
Tx	Complete Transection
USSC	Unrestricted Somatic Stem Cells
v.W.F.	Von Willebrand Faktor
VEGF	Vascular Endothelial Growth Factor
wpo	Week post operation

Metric System

°C	Degree Celsius
µm	Micrometre
cm	Centimetre
g	Gram
h	Hour
kg	Kilogram
M	Molar
m	Metre
mbar	Millibar
mg	Milligram
min	Minute
mm	Millimetre
pH	Potentia Hydrogenii
U	Units

7. Literature

1. Brazda, N., et al., *A mechanical microconnector system for restoration of tissue continuity and long-term drug application into the injured spinal cord.* Biomaterials, 2013. **34**(38): p. 10056-64.
2. Scholpa, N.E. and R.G. Schnellmann, *Mitochondrial-Based Therapeutics for the Treatment of Spinal Cord Injury: Mitochondrial Biogenesis as a Potential Pharmacological Target.* J Pharmacol Exp Ther, 2017. **363**(3): p. 303-313.
3. Kehl, T., *Combining a mechanical micro-connector device and human cord blood stem cells to enhance functional improvement after complete spinal cord injury.* Program No. 252.13. 2012 Neuroscience Meeting Planner. New Orleans, LA. **Society for Neuroscience, 2012**(Online).
4. Dietrich, W.D., *Protection and Repair After Spinal Cord Injury: Accomplishments and Future Directions.* Top Spinal Cord Inj Rehabil, 2015. **21**(2): p. 174-87.
5. Kawano, H., et al., *Role of the lesion scar in the response to damage and repair of the central nervous system.* Cell Tissue Res, 2012. **349**(1): p. 169-80.
6. *Querschnittslähmung.* http://www.wingsforlife.com/de/querschnittslaehmung/, 16.07.2018.
7. *International Perspectives on Spinal Cord Injury.* WHO Library Cataloguing-in-Publication Data, 2013. **ISBN 978 92 4 156466 3**.
8. Fu, S.Y. and T. Gordon, *The cellular and molecular basis of peripheral nerve regeneration.* Mol Neurobiol, 1997. **14**(1-2): p. 67-116.
9. Buss, A. and M.E. Schwab, *Sequential loss of myelin proteins during Wallerian degeneration in the rat spinal cord.* Glia, 2003. **42**(4): p. 424-32.
10. Ankeny, D.P. and P.G. Popovich, *Mechanisms and implications of adaptive immune responses after traumatic spinal cord injury.* Neuroscience, 2009. **158**(3): p. 1112-21.
11. Horky, L.L., et al., *Fate of endogenous stem/progenitor cells following spinal cord injury.* J Comp Neurol, 2006. **498**(4): p. 525-38.
12. Mothe, A.J. and C.H. Tator, *Proliferation, migration, and differentiation of endogenous ependymal region stem/progenitor cells following minimal spinal cord injury in the adult rat.* Neuroscience, 2005. **131**(1): p. 177-87.
13. Yamamoto, S., et al., *Proliferation of parenchymal neural progenitors in response to injury in the adult rat spinal cord.* Exp Neurol, 2001. **172**(1): p. 115-27.
14. Frisen, J., et al., *Rapid, widespread, and longlasting induction of nestin contributes to the generation of glial scar tissue after CNS injury.* J Cell Biol, 1995. **131**(2): p. 453-64.
15. Faulkner, J.R., et al., *Reactive astrocytes protect tissue and preserve function after spinal cord injury.* J Neurosci, 2004. **24**(9): p. 2143-55.
16. Silver, J. and J.H. Miller, *Regeneration beyond the glial scar.* Nat Rev Neurosci, 2004. **5**(2): p. 146-56.
17. Guo, L., et al., *Rescuing macrophage normal function in spinal cord injury with embryonic stem cell conditioned media.* Mol Brain, 2016. **9**(1): p. 48.
18. Jeon, S.B., et al., *Sulfatide, a major lipid component of myelin sheath, activates inflammatory responses as an endogenous stimulator in brain-resident immune cells.* J Immunol, 2008. **181**(11): p. 8077-87.
19. Toborek, M., et al., *Arachidonic acid-induced oxidative injury to cultured spinal cord neurons.* J Neurochem, 1999. **73**(2): p. 684-92.
20. Stys, P.K., *Anoxic and ischemic injury of myelinated axons in CNS white matter: from mechanistic concepts to therapeutics.* J Cereb Blood Flow Metab, 1998. **18**(1): p. 2-25.
21. Beattie, M.S., A.A. Farooqui, and J.C. Bresnahan, *Review of current evidence for apoptosis after spinal cord injury.* J Neurotrauma, 2000. **17**(10): p. 915-25.

22. Bareyre, F.M. and M.E. Schwab, *Inflammation, degeneration and regeneration in the injured spinal cord: insights from DNA microarrays.* Trends Neurosci, 2003. **26**(10): p. 555-63.
23. Tator, C.H., *Review of experimental spinal cord injury with emphasis on the local and systemic circulatory effects.* Neurochirurgie, 1991. **37**(5): p. 291-302.
24. Tator, C.H. and M.G. Fehlings, *Review of the secondary injury theory of acute spinal cord trauma with emphasis on vascular mechanisms.* J Neurosurg, 1991. **75**(1): p. 15-26.
25. Popovich, P.G., P. Wei, and B.T. Stokes, *Cellular inflammatory response after spinal cord injury in Sprague-Dawley and Lewis rats.* J Comp Neurol, 1997. **377**(3): p. 443-64.
26. Ramon y Cajal, S., *Degeneration and regeneration of the nervous system*. Degeneration and regeneration of the nervous system. 1928, Oxford, England: Clarendon Press.
27. Fawcett, J.W., *Astrocytic and neuronal factors affecting axon regeneration in the damaged central nervous system.* Cell Tissue Res, 1997. **290**(2): p. 371-7.
28. Asher, R.A., et al., *Versican is upregulated in CNS injury and is a product of oligodendrocyte lineage cells.* J Neurosci, 2002. **22**(6): p. 2225-36.
29. Asher, R.A., et al., *Neurocan is upregulated in injured brain and in cytokine-treated astrocytes.* J Neurosci, 2000. **20**(7): p. 2427-38.
30. Brook, G.A., et al., *Attempted endogenous tissue repair following experimental spinal cord injury in the rat: involvement of cell adhesion molecules L1 and NCAM?* Eur J Neurosci, 2000. **12**(9): p. 3224-38.
31. Huber, A.B. and M.E. Schwab, *Nogo-A, a potent inhibitor of neurite outgrowth and regeneration.* Biol Chem, 2000. **381**(5-6): p. 407-19.
32. Chen, M.S., et al., *Nogo-A is a myelin-associated neurite outgrowth inhibitor and an antigen for monoclonal antibody IN-1.* Nature, 2000. **403**(6768): p. 434-9.
33. Stichel, C.C. and H.W. Muller, *Experimental strategies to promote axonal regeneration after traumatic central nervous system injury.* Prog Neurobiol, 1998. **56**(2): p. 119-48.
34. Shearer, M.C. and J.W. Fawcett, *The astrocyte/meningeal cell interface--a barrier to successful nerve regeneration?* Cell Tissue Res, 2001. **305**(2): p. 267-73.
35. Stichel, C.C., et al., *Inhibition of collagen IV deposition promotes regeneration of injured CNS axons.* Eur J Neurosci, 1999. **11**(2): p. 632-46.
36. Stichel, C.C. and H.W. Muller, *The CNS lesion scar: new vistas on an old regeneration barrier.* Cell Tissue Res, 1998. **294**(1): p. 1-9.
37. Stichel, C.C., et al., *Basal membrane-depleted scar in lesioned CNS: characteristics and relationships with regenerating axons.* Neuroscience, 1999. **93**(1): p. 321-33.
38. David, S. and A.J. Aguayo, *Axonal elongation into peripheral nervous system "bridges" after central nervous system injury in adult rats.* Science, 1981. **214**(4523): p. 931-3.
39. George, R. and J.W. Griffin, *Delayed macrophage responses and myelin clearance during Wallerian degeneration in the central nervous system: the dorsal radiculotomy model.* Exp Neurol, 1994. **129**(2): p. 225-36.
40. Coumans, J.V., et al., *Axonal regeneration and functional recovery after complete spinal cord transection in rats by delayed treatment with transplants and neurotrophins.* J Neurosci, 2001. **21**(23): p. 9334-44.
41. Silver, J., M.E. Schwab, and P.G. Popovich, *Central nervous system regenerative failure: role of oligodendrocytes, astrocytes, and microglia.* Cold Spring Harb Perspect Biol, 2014. **7**(3): p. a020602.
42. Fitch, M.T. and J. Silver, *CNS injury, glial scars, and inflammation: Inhibitory extracellular matrices and regeneration failure.* Exp Neurol, 2008. **209**(2): p. 294-301.

43. Cizkova, D., et al., *Correction: Cizkova, D., et al. Localized Intrathecal Delivery of Mesenchymal Stromal Cells Conditioned Media Improves Functional Recovery in A Rat Model of Contusive Spinal Cord Injury. Int. J. Mol. Sci. 2018, 19, 870.* Int J Mol Sci, 2018. **19**(7).
44. Koenig, B., *Biochemical and pharmacological modulation of scarring, axon regeneration, and long-term functional improvement after spinal cord injury in rat.* Dissertation, 2014. **HHU Düsseldorf**.
45. Fan, W.L., et al., *Transplantation of hypoxic preconditioned neural stem cells benefits functional recovery via enhancing neurotrophic secretion after spinal cord injury in rats.* J Cell Biochem, 2018. **119**(6): p. 4339-4351.
46. Keirstead, H.S., et al., *Human embryonic stem cell-derived oligodendrocyte progenitor cell transplants remyelinate and restore locomotion after spinal cord injury.* J Neurosci, 2005. **25**(19): p. 4694-705.
47. Majczynski, H. and U. Slawinska, *Locomotor recovery after thoracic spinal cord lesions in cats, rats and humans.* Acta Neurobiol Exp (Wars), 2007. **67**(3): p. 235-57.
48. Rossignol, S. and A. Frigon, *Recovery of locomotion after spinal cord injury: some facts and mechanisms.* Annu Rev Neurosci, 2011. **34**: p. 413-40.
49. Cazalets, J.R., Y. Sqalli-Houssaini, and F. Clarac, *Activation of the central pattern generators for locomotion by serotonin and excitatory amino acids in neonatal rat.* J Physiol, 1992. **455**: p. 187-204.
50. Feraboli-Lohnherr, D., J.Y. Barthe, and D. Orsal, *Serotonin-induced activation of the network for locomotion in adult spinal rats.* J Neurosci Res, 1999. **55**(1): p. 87-98.
51. Fawcett, J.W., *Spinal cord repair: from experimental models to human application.* Spinal Cord, 1998. **36**(12): p. 811-7.
52. Aguayo, A.J., S. David, and G.M. Bray, *Influences of the glial environment on the elongation of axons after injury: transplantation studies in adult rodents.* J Exp Biol, 1981. **95**: p. 231-40.
53. Buchli, A.D. and M.E. Schwab, *Inhibition of Nogo: a key strategy to increase regeneration, plasticity and functional recovery of the lesioned central nervous system.* Ann Med, 2005. **37**(8): p. 556-67.
54. Kastin, A.J. and W. Pan, *Targeting neurite growth inhibitors to induce CNS regeneration.* Curr Pharm Des, 2005. **11**(10): p. 1247-53.
55. McKerracher, L., *Spinal cord repair: strategies to promote axon regeneration.* Neurobiol Dis, 2001. **8**(1): p. 11-8.
56. Rowland, J.W., et al., *Current status of acute spinal cord injury pathophysiology and emerging therapies: promise on the horizon.* Neurosurg Focus, 2008. **25**(5): p. E2.
57. Klapka, N., et al., *Suppression of fibrous scarring in spinal cord injury of rat promotes long-distance regeneration of corticospinal tract axons, rescue of primary motoneurons in somatosensory cortex and significant functional recovery.* Eur J Neurosci, 2005. **22**(12): p. 3047-58.
58. Schiwy, N., N. Brazda, and H.W. Muller, *Enhanced regenerative axon growth of multiple fibre populations in traumatic spinal cord injury following scar-suppressing treatment.* Eur J Neurosci, 2009. **30**(8): p. 1544-53.
59. Barritt, A.W., et al., *Chondroitinase ABC promotes sprouting of intact and injured spinal systems after spinal cord injury.* J Neurosci, 2006. **26**(42): p. 10856-67.
60. Bradbury, E.J., et al., *Chondroitinase ABC promotes functional recovery after spinal cord injury.* Nature, 2002. **416**(6881): p. 636-40.
61. Garcia-Alias, G., et al., *Therapeutic time window for the application of chondroitinase ABC after spinal cord injury.* Exp Neurol, 2008. **210**(2): p. 331-8.

62. Tester, N.J. and D.R. Howland, *Chondroitinase ABC improves basic and skilled locomotion in spinal cord injured cats.* Exp Neurol, 2008. **209**(2): p. 483-96.
63. Burdick, J.A., et al., *Stimulation of neurite outgrowth by neurotrophins delivered from degradable hydrogels.* Biomaterials, 2006. **27**(3): p. 452-9.
64. Houle, J.D. and M.K. Ziegler, *Bridging a complete transection lesion of adult rat spinal cord with growth factor-treated nitrocellulose implants.* J Neural Transplant Plast, 1994. **5**(2): p. 115-24.
65. Jones, L.L., et al., *Neurotrophic factors, cellular bridges and gene therapy for spinal cord injury.* J Physiol, 2001. **533**(Pt 1): p. 83-9.
66. Lu, P. and M.H. Tuszynski, *Growth factors and combinatorial therapies for CNS regeneration.* Exp Neurol, 2008. **209**(2): p. 313-20.
67. Plunet, W., B.K. Kwon, and W. Tetzlaff, *Promoting axonal regeneration in the central nervous system by enhancing the cell body response to axotomy.* J Neurosci Res, 2002. **68**(1): p. 1-6.
68. Tuszynski, M.H., et al., *NT-3 gene delivery elicits growth of chronically injured corticospinal axons and modestly improves functional deficits after chronic scar resection.* Exp Neurol, 2003. **181**(1): p. 47-56.
69. Yang, Y., et al., *Neurotrophin releasing single and multiple lumen nerve conduits.* J Control Release, 2005. **104**(3): p. 433-46.
70. Ye, J.H. and J.D. Houle, *Treatment of the chronically injured spinal cord with neurotrophic factors can promote axonal regeneration from supraspinal neurons.* Exp Neurol, 1997. **143**(1): p. 70-81.
71. Houle, J.D. and A. Tessler, *Repair of chronic spinal cord injury.* Exp Neurol, 2003. **182**(2): p. 247-60.
72. Hou, S., et al., *The repair of brain lesion by implantation of hyaluronic acid hydrogels modified with laminin.* J Neurosci Methods, 2005. **148**(1): p. 60-70.
73. Ozgenel, G.Y., *Effects of hyaluronic acid on peripheral nerve scarring and regeneration in rats.* Microsurgery, 2003. **23**(6): p. 575-81.
74. Burd, D.A., et al., *Hyaluronan and wound healing: a new perspective.* Br J Plast Surg, 1991. **44**(8): p. 579-84.
75. Vacanti, C.A. and J.P. Vacanti, *The science of tissue engineering.* Orthop Clin North Am, 2000. **31**(3): p. 351-6.
76. Estrada, V., et al., *Long-lasting significant functional improvement in chronic severe spinal cord injury following scar resection and polyethylene glycol implantation.* Neurobiol Dis, 2014. **67**: p. 165-79.
77. Cholas, R.H., H.P. Hsu, and M. Spector, *The reparative response to cross-linked collagen-based scaffolds in a rat spinal cord gap model.* Biomaterials, 2012. **33**(7): p. 2050-9.
78. Prang, P., et al., *The promotion of oriented axonal regrowth in the injured spinal cord by alginate-based anisotropic capillary hydrogels.* Biomaterials, 2006. **27**(19): p. 3560-9.
79. Estrada, V., *Low-pressure micro-mechanical re-adaptation device sustainably and effectively improves locomotor recovery from complete spinal cord.* in revision, 2018.
80. Park, D.-H., et al., *Transplantation of Umbilical Cord Blood Stem Cells for Treating Spinal Cord Injury.* Stem Cell Reviews and Reports, 2011. **7**(1): p. 181-194.
81. Tetzlaff, W., et al., *A systematic review of cellular transplantation therapies for spinal cord injury.* J Neurotrauma, 2011. **28**(8): p. 1611-82.
82. Sahni, V. and J.A. Kessler, *Stem cell therapies for spinal cord injury.* Nat Rev Neurol, 2010. **6**(7): p. 363-72.
83. Mezey, E., et al., *Turning blood into brain: cells bearing neuronal antigens generated in vivo from bone marrow.* Science, 2000. **290**(5497): p. 1779-82.

84. Eglitis, M.A. and E. Mezey, *Hematopoietic cells differentiate into both microglia and macroglia in the brains of adult mice.* Proc Natl Acad Sci U S A, 1997. **94**(8): p. 4080-5.
85. Koshizuka, S., et al., *Transplanted hematopoietic stem cells from bone marrow differentiate into neural lineage cells and promote functional recovery after spinal cord injury in mice.* J Neuropathol Exp Neurol, 2004. **63**(1): p. 64-72.
86. Thuret, S., L.D. Moon, and F.H. Gage, *Therapeutic interventions after spinal cord injury.* Nat Rev Neurosci, 2006. **7**(8): p. 628-43.
87. Friedenstein, A.J., et al., *Heterotopic of bone marrow. Analysis of precursor cells for osteogenic and hematopoietic tissues.* Transplantation, 1968. **6**(2): p. 230-47.
88. Wright, K.T., et al., *Concise review: Bone marrow for the treatment of spinal cord injury: mechanisms and clinical applications.* Stem Cells, 2011. **29**(2): p. 169-78.
89. Vawda, R. and M.G. Fehlings, *Mesenchymal cells in the treatment of spinal cord injury: current & future perspectives.* Curr Stem Cell Res Ther, 2013. **8**(1): p. 25-38.
90. Vaquero, J. and M. Zurita, *Bone marrow stromal cells for spinal cord repair: a challenge for contemporary neurobiology.* Histol Histopathol, 2009. **24**(1): p. 107-16.
91. Parr, A.M., I. Kulbatski, and C.H. Tator, *Transplantation of adult rat spinal cord stem/progenitor cells for spinal cord injury.* J Neurotrauma, 2007. **24**(5): p. 835-45.
92. Picard-Riera, N., B. Nait-Oumesmar, and A. Baron-Van Evercooren, *Endogenous adult neural stem cells: limits and potential to repair the injured central nervous system.* J Neurosci Res, 2004. **76**(2): p. 223-31.
93. Olson, H.E., et al., *Neural stem cell- and Schwann cell-loaded biodegradable polymer scaffolds support axonal regeneration in the transected spinal cord.* Tissue Eng Part A, 2009. **15**(7): p. 1797-805.
94. Mothe, A.J. and C.H. Tator, *Advances in stem cell therapy for spinal cord injury.* J Clin Invest, 2012. **122**(11): p. 3824-34.
95. Weiss, M.L., et al., *Human umbilical cord matrix stem cells: preliminary characterization and effect of transplantation in a rodent model of Parkinson's disease.* Stem Cells, 2006. **24**(3): p. 781-92.
96. Kogler, G., et al., *A new human somatic stem cell from placental cord blood with intrinsic pluripotent differentiation potential.* J Exp Med, 2004. **200**(2): p. 123-35.
97. Kluth, S.M., et al., *DLK-1 as a marker to distinguish unrestricted somatic stem cells and mesenchymal stromal cells in cord blood.* Stem Cells Dev, 2010. **19**(10): p. 1471-83.
98. Liedtke, S., et al., *The HOX Code as a "biological fingerprint" to distinguish functionally distinct stem cell populations derived from cord blood.* Stem Cell Res, 2010. **5**(1): p. 40-50.
99. Schira, J., et al., *Characterization of Regenerative Phenotype of Unrestricted Somatic Stem Cells (USSC) from Human Umbilical Cord Blood (hUCB) by Functional Secretome Analysis.* Mol Cell Proteomics, 2015. **14**(10): p. 2630-43.
100. Schira, J., et al., *Significant clinical, neuropathological and behavioural recovery from acute spinal cord trauma by transplantation of a well-defined somatic stem cell from human umbilical cord blood.* Brain, 2012. **135**(Pt 2): p. 431-46.
101. Aktas, M., et al., *Good manufacturing practice-grade production of unrestricted somatic stem cell from fresh cord blood.* Cytotherapy, 2010. **12**(3): p. 338-48.
102. Aach, M., et al., *Voluntary driven exoskeleton as a new tool for rehabilitation in chronic spinal cord injury: a pilot study.* Spine J, 2014. **14**(12): p. 2847-53.
103. Aach, M., et al., *The primary stability of pelvic reconstruction after partial supraacetabular pelvic resection due to malignant tumours of the human pelvis: a biomechanical in vitro study.* Med Eng Phys, 2013. **35**(12): p. 1731-5.

104. Wall, A., J. Borg, and S. Palmcrantz, *Clinical application of the Hybrid Assistive Limb (HAL) for gait training-a systematic review.* Front Syst Neurosci, 2015. **9**: p. 48.
105. Kwakkel, G., et al., *Effects of augmented exercise therapy time after stroke: a meta-analysis.* Stroke, 2004. **35**(11): p. 2529-39.
106. Langhorne, P., F. Coupar, and A. Pollock, *Motor recovery after stroke: a systematic review.* Lancet Neurol, 2009. **8**(8): p. 741-54.
107. Langhorne, P., J. Bernhardt, and G. Kwakkel, *Stroke rehabilitation.* Lancet, 2011. **377**(9778): p. 1693-702.
108. Peurala, S.H., et al., *Evidence for the effectiveness of walking training on walking and self-care after stroke: a systematic review and meta-analysis of randomized controlled trials.* J Rehabil Med, 2014. **46**(5): p. 387-99.
109. Sczesny-Kaiser, M., et al., *HAL(R) exoskeleton training improves walking parameters and normalizes cortical excitability in primary somatosensory cortex in spinal cord injury patients.* J Neuroeng Rehabil, 2015. **12**: p. 68.
110. Ying, Z., et al., *Exercise restores levels of neurotrophins and synaptic plasticity following spinal cord injury.* Exp Neurol, 2005. **193**(2): p. 411-9.
111. Fong, A.J., et al., *Spinal cord-transected mice learn to step in response to quipazine treatment and robotic training.* J Neurosci, 2005. **25**(50): p. 11738-47.
112. Goldshmit, Y., et al., *Treadmill training after spinal cord hemisection in mice promotes axonal sprouting and synapse formation and improves motor recovery.* J Neurotrauma, 2008. **25**(5): p. 449-65.
113. Silva, N.A., et al., *From basics to clinical: a comprehensive review on spinal cord injury.* Prog Neurobiol, 2014. **114**: p. 25-57.
114. Kwon, B.K., T.R. Oxland, and W. Tetzlaff, *Animal models used in spinal cord regeneration research.* Spine (Phila Pa 1976), 2002. **27**(14): p. 1504-10.
115. Zhang, N., et al., *Evaluation of spinal cord injury animal models.* Neural Regen Res, 2014. **9**(22): p. 2008-12.
116. Akhtar, A.Z., J.J. Pippin, and C.B. Sandusky, *Animal models in spinal cord injury: a review.* Rev Neurosci, 2008. **19**(1): p. 47-60.
117. Hodgetts, S.P., G.; Harvey A., *Chapter 14 - Spinal Cord Injury: experimental animal models and relation to human therapy*. The Spinal Cord, ed. G.P. in Charles Watson, Gulgun Kayalioglu (eds). 2009: First edition. Amsterdam ; Boston : Elsevier/Academic Press, 2009.
118. Rosenzweig, E.S. and J.W. McDonald, *Rodent models for treatment of spinal cord injury: research trends and progress toward useful repair.* Curr Opin Neurol, 2004. **17**(2): p. 121-31.
119. Stokes, B.T. and L.B. Jakeman, *Experimental modelling of human spinal cord injury: a model that crosses the species barrier and mimics the spectrum of human cytopathology.* Spinal Cord, 2002. **40**(3): p. 101-9.
120. Tuszynski, M.H. and O. Steward, *Concepts and methods for the study of axonal regeneration in the CNS.* Neuron, 2012. **74**(5): p. 777-91.
121. Steward, O., B. Zheng, and M. Tessier-Lavigne, *False resurrections: distinguishing regenerated from spared axons in the injured central nervous system.* J Comp Neurol, 2003. **459**(1): p. 1-8.
122. Talac, R., et al., *Animal models of spinal cord injury for evaluation of tissue engineering treatment strategies.* Biomaterials, 2004. **25**(9): p. 1505-10.
123. Rasouli, A., et al., *Resection of glial scar following spinal cord injury.* J Orthop Res, 2009. **27**(7): p. 931-6.
124. Cote, M.P., et al., *Plasticity in ascending long propriospinal and descending supraspinal pathways in chronic cervical spinal cord injured rats.* Front Physiol, 2012. **3**: p. 330.

125. Bareyre, F.M., et al., *The injured spinal cord spontaneously forms a new intraspinal circuit in adult rats.* Nat Neurosci, 2004. **7**(3): p. 269-77.
126. Sherrington, C.S., *The integrative action of the nervous system.* New Haven, CTYale University Press, 1906.
127. Rosenzweig, E.S., et al., *Extensive spontaneous plasticity of corticospinal projections after primate spinal cord injury.* Nat Neurosci, 2010. **13**(12): p. 1505-10.
128. Purves, D., *Neuroscience*. 5th ed. 2012, Sunderland, Mass.: Sinauer Associates.
129. Vavrek, R., et al., *BDNF promotes connections of corticospinal neurons onto spared descending interneurons in spinal cord injured rats.* Brain, 2006. **129**(Pt 6): p. 1534-45.
130. Flynn, J.R., et al., *The role of propriospinal interneurons in recovery from spinal cord injury.* Neuropharmacology, 2011. **60**(5): p. 809-22.
131. Courtine, G., et al., *Recovery of supraspinal control of stepping via indirect propriospinal relay connections after spinal cord injury.* Nat Med, 2008. **14**(1): p. 69-74.
132. Lu, P., et al., *Long-distance growth and connectivity of neural stem cells after severe spinal cord injury.* Cell, 2012. **150**(6): p. 1264-73.
133. Adler, A.F., et al., *Comprehensive Monosynaptic Rabies Virus Mapping of Host Connectivity with Neural Progenitor Grafts after Spinal Cord Injury.* Stem Cell Reports, 2017. **8**(6): p. 1525-1533.
134. Estrada, V., et al., *Low-pressure micro-mechanical re-adaptation device sustainably and effectively improves locomotor recovery from complete spinal cord injury.* Commun Biol, 2018. **1**: p. 205.
135. Kehl, T., *Combining a mechanical micro-connector device and human umbilical cord blood stem cells to enhance functional improvement after complete spinal cord injury.* Dissertation, 2017. **HHU Düsseldorf**.
136. Schmued, L.C. and J.H. Fallon, *Fluoro-Gold: a new fluorescent retrograde axonal tracer with numerous unique properties.* Brain Res, 1986. **377**(1): p. 147-54.
137. Wang, M., et al., *Bioengineered scaffolds for spinal cord repair.* Tissue Eng Part B Rev, 2011. **17**(3): p. 177-94.
138. Yang, Y., et al., *Multiple channel bridges for spinal cord injury: cellular characterization of host response.* Tissue Eng Part A, 2009. **15**(11): p. 3283-95.
139. Basso, D.M., M.S. Beattie, and J.C. Bresnahan, *A sensitive and reliable locomotor rating scale for open field testing in rats.* J Neurotrauma, 1995. **12**(1): p. 1-21.
140. Oudega, M., *Molecular and cellular mechanisms underlying the role of blood vessels in spinal cord injury and repair.* Cell Tissue Res, 2012. **349**(1): p. 269-88.
141. Barbeau, H. and S. Rossignol, *Initiation and modulation of the locomotor pattern in the adult chronic spinal cat by noradrenergic, serotonergic and dopaminergic drugs.* Brain Res, 1991. **546**(2): p. 250-60.
142. Pearse, D.D., et al., *cAMP and Schwann cells promote axonal growth and functional recovery after spinal cord injury.* Nat Med, 2004. **10**(6): p. 610-6.
143. Ramon-Cueto, A., et al., *Functional recovery of paraplegic rats and motor axon regeneration in their spinal cords by olfactory ensheathing glia.* Neuron, 2000. **25**(2): p. 425-35.
144. Donnelly, D.J. and P.G. Popovich, *Inflammation and its role in neuroprotection, axonal regeneration and functional recovery after spinal cord injury.* Exp Neurol, 2008. **209**(2): p. 378-88.
145. Haines, D.M. and B.J. Chelack, *Technical considerations for developing enzyme immunohistochemical staining procedures on formalin-fixed paraffin-embedded tissues for diagnostic pathology.* J Vet Diagn Invest, 1991. **3**(1): p. 101-12.

146. Hoedemakers, R.M., et al., *Heterogeneity in secretory responses of rat liver macrophages of different size.* Liver, 1995. **15**(6): p. 313-9.
147. Johansson, A., et al., *Functional, morphological, and phenotypical differences between rat alveolar and interstitial macrophages.* Am J Respir Cell Mol Biol, 1997. **16**(5): p. 582-8.
148. Pallini, R., E. Fernandez, and A. Sbriccoli, *Retrograde degeneration of corticospinal axons following transection of the spinal cord in rats. A quantitative study with anterogradely transported horseradish peroxidase.* J Neurosurg, 1988. **68**(1): p. 124-8.
149. Balentine, J.D., *Pathology of experimental spinal cord trauma. II. Ultrastructure of axons and myelin.* Lab Invest, 1978. **39**(3): p. 254-66.
150. Balentine, J.D., *Pathology of experimental spinal cord trauma. I. The necrotic lesion as a function of vascular injury.* Lab Invest, 1978. **39**(3): p. 236-53.
151. Bresnahan, J.C., *An electron-microscopic analysis of axonal alterations following blunt contusion of the spinal cord of the rhesus monkey (Macaca mulatta).* J Neurol Sci, 1978. **37**(1-2): p. 59-82.
152. Bunge, M.B., et al., *Characterization of photochemically induced spinal cord injury in the rat by light and electron microscopy.* Exp Neurol, 1994. **127**(1): p. 76-93.
153. Noble, L.J. and J.R. Wrathall, *Spinal cord contusion in the rat: morphometric analyses of alterations in the spinal cord.* Exp Neurol, 1985. **88**(1): p. 135-49.
154. Noble, L.J. and J.R. Wrathall, *Correlative analyses of lesion development and functional status after graded spinal cord contusive injuries in the rat.* Exp Neurol, 1989. **103**(1): p. 34-40.
155. Beattie, M.S., et al., *Endogenous repair after spinal cord contusion injuries in the rat.* Exp Neurol, 1997. **148**(2): p. 453-63.
156. Fitch, M.T., et al., *Cellular and molecular mechanisms of glial scarring and progressive cavitation: in vivo and in vitro analysis of inflammation-induced secondary injury after CNS trauma.* J Neurosci, 1999. **19**(19): p. 8182-98.
157. Kjell, J., et al., *Rat substrains differ in the magnitude of spontaneous locomotor recovery and in the development of mechanical hypersensitivity after experimental spinal cord injury.* J Neurotrauma, 2013. **30**(21): p. 1805-11.
158. Butovsky, O., E. Hauben, and M. Schwartz, *Morphological aspects of spinal cord autoimmune neuroprotection: colocalization of T cells with B7--2 (CD86) and prevention of cyst formation.* FASEB J, 2001. **15**(6): p. 1065-7.
159. Nakajima, H., et al., *Transplantation of mesenchymal stem cells promotes an alternative pathway of macrophage activation and functional recovery after spinal cord injury.* J Neurotrauma, 2012. **29**(8): p. 1614-25.
160. Sharp, J., et al., *Human embryonic stem cell-derived oligodendrocyte progenitor cell transplants improve recovery after cervical spinal cord injury.* Stem Cells, 2010. **28**(1): p. 152-63.
161. Widenfalk, J., et al., *Vascular endothelial growth factor improves functional outcome and decreases secondary degeneration in experimental spinal cord contusion injury.* Neuroscience, 2003. **120**(4): p. 951-60.
162. Krombach, F., et al., *Cell size of alveolar macrophages: an interspecies comparison.* Environ Health Perspect, 1997. **105 Suppl 5**: p. 1261-3.
163. Paino, C.L. and M.B. Bunge, *Induction of axon growth into Schwann cell implants grafted into lesioned adult rat spinal cord.* Exp Neurol, 1991. **114**(2): p. 254-7.
164. Kogler, G., et al., *Cytokine production and hematopoiesis supporting activity of cord blood-derived unrestricted somatic stem cells.* Exp Hematol, 2005. **33**(5): p. 573-83.
165. Nomura, H., C.H. Tator, and M.S. Shoichet, *Bioengineered strategies for spinal cord repair.* J Neurotrauma, 2006. **23**(3-4): p. 496-507.

166. Assuncao-Silva, R.C., et al., *Hydrogels and Cell Based Therapies in Spinal Cord Injury Regeneration.* Stem Cells Int, 2015. **2015**: p. 948040.
167. Friedman, J.A., et al., *Biodegradable polymer grafts for surgical repair of the injured spinal cord.* Neurosurgery, 2002. **51**(3): p. 742-51; discussion 751-2.
168. Teng, Y.D., et al., *Functional recovery following traumatic spinal cord injury mediated by a unique polymer scaffold seeded with neural stem cells.* Proc Natl Acad Sci U S A, 2002. **99**(5): p. 3024-9.
169. Lu, P., et al., *Combinatorial therapy with neurotrophins and cAMP promotes axonal regeneration beyond sites of spinal cord injury.* J Neurosci, 2004. **24**(28): p. 6402-9.
170. Tuszynski, M.H., et al., *Nerve growth factor delivery by gene transfer induces differential outgrowth of sensory, motor, and noradrenergic neurites after adult spinal cord injury.* Exp Neurol, 1996. **137**(1): p. 157-73.
171. Liu, Y., et al., *Transplants of fibroblasts genetically modified to express BDNF promote regeneration of adult rat rubrospinal axons and recovery of forelimb function.* J Neurosci, 1999. **19**(11): p. 4370-87.
172. McKerracher, L., et al., *Identification of myelin-associated glycoprotein as a major myelin-derived inhibitor of neurite growth.* Neuron, 1994. **13**(4): p. 805-11.
173. Schwab, M.E. and D. Bartholdi, *Degeneration and regeneration of axons in the lesioned spinal cord.* Physiol Rev, 1996. **76**(2): p. 319-70.
174. Filbin, M.T., *Myelin-associated inhibitors of axonal regeneration in the adult mammalian CNS.* Nat Rev Neurosci, 2003. **4**(9): p. 703-13.
175. Fitch, M.T. and J. Silver, *Beyond the glial scar. In: CNS regeneration: basic science and clinical aspects.* Tuszynski MH, Kordower JA, eds, 1999. **San Diego: Academic**: p. pp 55–81.
176. Jones, L.L., et al., *NG2 is a major chondroitin sulfate proteoglycan produced after spinal cord injury and is expressed by macrophages and oligodendrocyte progenitors.* J Neurosci, 2002. **22**(7): p. 2792-803.
177. Jones, L.L., D. Sajed, and M.H. Tuszynski, *Axonal regeneration through regions of chondroitin sulfate proteoglycan deposition after spinal cord injury: a balance of permissiveness and inhibition.* J Neurosci, 2003. **23**(28): p. 9276-88.
178. Bomze, H.M., et al., *Spinal axon regeneration evoked by replacing two growth cone proteins in adult neurons.* Nat Neurosci, 2001. **4**(1): p. 38-43.
179. Ankeny, D.P., D.M. McTigue, and L.B. Jakeman, *Bone marrow transplants provide tissue protection and directional guidance for axons after contusive spinal cord injury in rats.* Exp Neurol, 2004. **190**(1): p. 17-31.
180. Neuhuber, B., et al., *Axon growth and recovery of function supported by human bone marrow stromal cells in the injured spinal cord exhibit donor variations.* Brain Res, 2005. **1035**(1): p. 73-85.
181. Lu, J., et al., *Olfactory ensheathing cells promote locomotor recovery after delayed transplantation into transected spinal cord.* Brain, 2002. **125**(Pt 1): p. 14-21.
182. Lu, J., et al., *Transplantation of nasal olfactory tissue promotes partial recovery in paraplegic adult rats.* Brain Res, 2001. **889**(1-2): p. 344-57.
183. Stokols, S. and M.H. Tuszynski, *Freeze-dried agarose scaffolds with uniaxial channels stimulate and guide linear axonal growth following spinal cord injury.* Biomaterials, 2006. **27**(3): p. 443-51.
184. Bittner, G.D., T. Schallert, and J.D. Peduzzi, *Degeneration, Trophic Interactions, and Repair of Severed Axons: A Reconsideration of Some Common Assumptions.* The Neuroscientist, 2000. **6**(2): p. 88-109.

185. Kuscha, V., et al., *Plasticity of tyrosine hydroxylase and serotonergic systems in the regenerating spinal cord of adult zebrafish.* J Comp Neurol, 2012. **520**(5): p. 933-51.
186. Guest, J.D., et al., *Influence of IN-1 antibody and acidic FGF-fibrin glue on the response of injured corticospinal tract axons to human Schwann cell grafts.* J Neurosci Res, 1997. **50**(5): p. 888-905.
187. Kanno, H., et al., *Combination of engineered Schwann cell grafts to secrete neurotrophin and chondroitinase promotes axonal regeneration and locomotion after spinal cord injury.* J Neurosci, 2014. **34**(5): p. 1838-55.
188. Schnell, L., et al., *Neurotrophin-3 enhances sprouting of corticospinal tract during development and after adult spinal cord lesion.* Nature, 1994. **367**(6459): p. 170-3.
189. Schnell, L. and M.E. Schwab, *Sprouting and regeneration of lesioned corticospinal tract fibres in the adult rat spinal cord.* Eur J Neurosci, 1993. **5**(9): p. 1156-71.
190. Brosamle, C. and M.E. Schwab, *Ipsilateral, ventral corticospinal tract of the adult rat: ultrastructure, myelination and synaptic connections.* J Neurocytol, 2000. **29**(7): p. 499-507.
191. Steward, O., et al., *The dorsolateral corticospinal tract in mice: an alternative route for corticospinal input to caudal segments following dorsal column lesions.* J Comp Neurol, 2004. **472**(4): p. 463-77.
192. Seif, G.I., H. Nomura, and C.H. Tator, *Retrograde axonal degeneration "dieback" in the corticospinal tract after transection injury of the rat spinal cord: a confocal microscopy study.* J Neurotrauma, 2007. **24**(9): p. 1513-28.
193. Challagundla, M., *AAV-based gene therapy for axonal regeneration in a rat model of rubrospinal tract lesion.* Dissertation, 2014. **Georg-August-Universität-Göttingen**.
194. Castellanos, D.A., et al., *TrkC overexpression enhances survival and migration of neural stem cell transplants in the rat spinal cord.* Cell Transplant, 2002. **11**(3): p. 297-307.
195. Xu, X.M., et al., *Regrowth of axons into the distal spinal cord through a Schwann-cell-seeded mini-channel implanted into hemisected adult rat spinal cord.* Eur J Neurosci, 1999. **11**(5): p. 1723-40.
196. Chung, K. and R.E. Coggeshall, *Propriospinal fibers in the rat.* J Comp Neurol, 1983. **217**(1): p. 47-53.
197. Chung, K., et al., *An estimate of the ratio of propriospinal to long tract neurons in the sacral spinal cord of the rat.* Neurosci Lett, 1984. **44**(2): p. 173-7.
198. Alstermark, B. and S. Sasaki, *Integration in descending motor pathways controlling the forelimb in the cat. 14. Differential projection to fast and slow motoneurones from excitatory C3-C4 propriospinal neurones.* Exp Brain Res, 1986. **63**(3): p. 530-42.
199. Alstermark, B. and S. Sasaki, *Integration in descending motor pathways controlling the forelimb in the cat. 15. Comparison of the projection from excitatory C3-C4 propriospinal neurones to different species of forelimb motoneurones.* Exp Brain Res, 1986. **63**(3): p. 543-56.
200. Alstermark, B., et al., *Branching and termination of C3-C4 propriospinal neurones in the cervical spinal cord of the cat.* Neurosci Lett, 1987. **74**(3): p. 291-6.
201. Pierrot-Deseilligny, E., *Propriospinal transmission of part of the corticospinal excitation in humans.* Muscle Nerve, 2002. **26**(2): p. 155-72.
202. Kostyuk, P.G., D.A. Vasilenko, and E. Lang, *Propriospinal pathways in the dorsolateral funiculus and their effects on lumbosacral motoneuronal pools.* Brain Res, 1971. **28**(2): p. 233-49.
203. Kostyuk, P.G. and V.A. Maisky, *Propriospinal projections in the lumbar spinal cord of the cat.* Brain Res, 1972. **39**(2): p. 530-5.

204. Gerasimenko, Y.P., A.N. Makarovskii, and O.A. Nikitin, *Control of locomotor activity in humans and animals in the absence of supraspinal influences.* Neurosci Behav Physiol, 2002. **32**(4): p. 417-23.
205. Jordan, L.M. and B.J. Schmidt, *Propriospinal neurons involved in the control of locomotion: potential targets for repair strategies?* Prog Brain Res, 2002. **137**: p. 125-39.
206. Honda, C.N. and C.L. Lee, *Immunohistochemistry of synaptic input and functional characterizations of neurons near the spinal central canal.* Brain Res, 1985. **343**(1): p. 120-8.
207. Matsushita, M., *Ascending propriospinal afferents to area X (substantia grisea centralis) of the spinal cord in the rat.* Exp Brain Res, 1998. **119**(3): p. 356-66.
208. Juvin, L., J. Simmers, and D. Morin, *Propriospinal circuitry underlying interlimb coordination in mammalian quadrupedal locomotion.* J Neurosci, 2005. **25**(25): p. 6025-35.
209. Steeves, J.D., et al., *Effect of noradrenaline and 5-hydroxytryptamine depletion on locomotion in the cat.* Brain Res, 1980. **185**(2): p. 349-62.
210. Schmidt, B.J. and L.M. Jordan, *The role of serotonin in reflex modulation and locomotor rhythm production in the mammalian spinal cord.* Brain Res Bull, 2000. **53**(5): p. 689-710.
211. Anderson, M.A., et al., *Required growth facilitators propel axon regeneration across complete spinal cord injury.* Nature, 2018. **561**(7723): p. 396-400.
212. van den Brand, R., et al., *Restoring voluntary control of locomotion after paralyzing spinal cord injury.* Science, 2012. **336**(6085): p. 1182-5.
213. Asboth, L., et al., *Cortico-reticulo-spinal circuit reorganization enables functional recovery after severe spinal cord contusion.* Nat Neurosci, 2018. **21**(4): p. 576-588.
214. Caudle, K.L., et al., *Hindlimb stretching alters locomotor function after spinal cord injury in the adult rat.* Neurorehabil Neural Repair, 2015. **29**(3): p. 268-77.
215. Keller, A.V., et al., *Disruption of Locomotion in Response to Hindlimb Muscle Stretch at Acute and Chronic Time Points after a Spinal Cord Injury in Rats.* J Neurotrauma, 2017. **34**(3): p. 661-670.
216. Cheng, H., Y. Cao, and L. Olson, *Spinal cord repair in adult paraplegic rats: partial restoration of hind limb function.* Science, 1996. **273**(5274): p. 510-3.
217. Buford, J.A. and A.G. Davidson, *Movement-related and preparatory activity in the reticulospinal system of the monkey.* Exp Brain Res, 2004. **159**(3): p. 284-300.
218. Deumens, R., G.C. Koopmans, and E.A. Joosten, *Regeneration of descending axon tracts after spinal cord injury.* Prog Neurobiol, 2005. **77**(1-2): p. 57-89.
219. Tracey, D., *Ascending and Descending Pathways in the Spinal Cord. The Rat Nervous System.* 3rd Edition, 2004. **Paxinos, G. (ED)**.
220. Chen, A., et al., *Methylprednisolone administration improves axonal regeneration into Schwann cell grafts in transected adult rat thoracic spinal cord.* Exp Neurol, 1996. **138**(2): p. 261-76.
221. Guest, J.D., et al., *The ability of human Schwann cell grafts to promote regeneration in the transected nude rat spinal cord.* Exp Neurol, 1997. **148**(2): p. 502-22.
222. Menei, P., et al., *Schwann cells genetically modified to secrete human BDNF promote enhanced axonal regrowth across transected adult rat spinal cord.* Eur J Neurosci, 1998. **10**(2): p. 607-21.
223. Xu, X.M., et al., *A combination of BDNF and NT-3 promotes supraspinal axonal regeneration into Schwann cell grafts in adult rat thoracic spinal cord.* Exp Neurol, 1995. **134**(2): p. 261-72.
224. Xu, X.M., et al., *Axonal regeneration into Schwann cell-seeded guidance channels grafted into transected adult rat spinal cord.* J Comp Neurol, 1995. **351**(1): p. 145-60.
225. Pompeiano, O., *Spinovestibular relations: anatomical and physiological aspects.* Prog Brain Res, 1972. **37**: p. 263-96.

226. Kim, J.E., et al., *Nogo-66 receptor prevents raphespinal and rubrospinal axon regeneration and limits functional recovery from spinal cord injury.* Neuron, 2004. **44**(3): p. 439-51.
227. Bregman, B.S., et al., *Recovery from spinal cord injury mediated by antibodies to neurite growth inhibitors.* Nature, 1995. **378**(6556): p. 498-501.
228. Park, J., et al., *Nerve regeneration following spinal cord injury using matrix metalloproteinase-sensitive, hyaluronic acid-based biomimetic hydrogel scaffold containing brain-derived neurotrophic factor.* J Biomed Mater Res A, 2010. **93**(3): p. 1091-9.
229. Perrier, J.F. and R. Delgado-Lezama, *Synaptic release of serotonin induced by stimulation of the raphe nucleus promotes plateau potentials in spinal motoneurons of the adult turtle.* J Neurosci, 2005. **25**(35): p. 7993-9.
230. Hounsgaard, J., et al., *Bistability of alpha-motoneurones in the decerebrate cat and in the acute spinal cat after intravenous 5-hydroxytryptophan.* J Physiol, 1988. **405**: p. 345-67.
231. Muir, G.D. and I.Q. Whishaw, *Complete locomotor recovery following corticospinal tract lesions: measurement of ground reaction forces during overground locomotion in rats.* Behav Brain Res, 1999. **103**(1): p. 45-53.

Eidesstattliche Versicherung / Statutory Declaration

Ich versichere an Eides statt, dass die Dissertation selbständig und ohne unzulässige fremde Hilfe unter Beachtung der „Grundsätze zur Sicherung guter wissenschaftlicher Praxis an der Heinrich-Heine-Universität Düsseldorf“ erstellt und die hier vorgelegte Dissertation nicht von einer anderen mathematisch-naturwissenschaftlichen Fakultät abgelehnt worden ist.

I hereby declare that I have developed and written the enclosed thesis completely by myself, and have not used sources or means without declaration in the text. Any thoughts from others or literal quotations are clearly marked.

I am aware that the thesis in digital form can be examined for the use of unauthorized aid and in order to determine whether the thesis as a whole or parts incorporated in it may be deemed as plagiarism. For the comparison of my work with existing sources I agree that it shall be entered in a database where it shall also remain after examination, to enable comparison with future theses submitted. Further rights of reproduction and usage, however, are not granted here.

This paper was not previously presented to another examination board and has not been published.

Ort, Datum	Jennifer Illgen

Danksagung

An dieser Stelle möchte ich meinen besonderen Dank nachstehenden Personen entgegenbringen, ohne deren Mithilfe die Anfertigung dieser Promotionsschrift niemals zustande gekommen wäre:

Mein Dank gilt zuallererst meinem Doktorvater, Prof. Dr. Hans Werner Müller, und Dr. Veronica Estrada, für die Zeit der Betreuung, für die konstruktive Kritik und dafür, dass sie an meine Arbeit und meinen Fähigkeiten geglaubt haben. Des Weiteren möchte ich Prof. Dr. Dieter Willbold danken, der meine Doktorarbeit als zweiter Gutachter betreut hat.

Danken möchte ich außerdem Marion Hendricks und Dr. Jessica Schira-Heinen, die es ermöglicht haben Stammzellarbeiten durchzuführen. Ohne meine Büronachbarin Nicole Kaminski wäre die Arbeit nur halb so effizient gewesen, vielen Dank für die spontanen und konstruktiven Diskussionen.

All diesen Personen, sowie der gesamten Belegschaft des Labors für molekulare Neurobiologie danke ich für die Unterstützung und vielen lieben Worte während der Erarbeitung meiner Dissertation.

Im Rahmen der finanziellen Unterstützung gilt mein spezieller Dank der Manchot Stiftung, die mir ein dreijähriges Stipendium zur Bearbeitung der Doktorarbeit ermöglicht haben.

Ein besonderer Dank gilt neben vielen Freuden meiner Familie, insbesondere meiner Mutter Marion und meiner Schwester Jessica, die mich auf meinem Weg durch die Promotion begleitet, aufgebaut und unterstützt haben.